Nucleon-nucleon scattering on the basis of Wilsonian renormalization group analysis in nuclear effective field theory

榮田, 達也

https://doi.org/10.15017/1398272

出版情報：九州大学, 2013, 博士（理学）, 課程博士
バージョン：

Nucleon-nucleon scattering on the basis of Wilsonian renormalization group analysis in nuclear effective field theory

Tatsuya Sakaeda

Abstract

We consider the nuclear effective field theory including pions using a power counting determined by a Wilsonian renormalization group analysis in the two nucleon sector in the S waves. Our power counting is very close to the one proposed by Kaplan, Savage, and Wise (KSW) and independently by van Kolck, but emphasizes the separation of the pion exchange into its long distance part (L-OPE) and its short distance part (S-OPE). In order to implement the idea of the separation in practicable calculations, we adopt a hybrid regularization. In the hybrid regularization, the diagrams including only nucleons and/or S-OPEs are regularized by the power divergence subtraction (PDS) which is a kind of dimensional regularization, and the diagrams containing L-OPEs are regularized by introducing a Gaussian damping factor(GDF) each of them. We calculate nucleon-nucleon scattering phase shifts up to and including next-to-next-to-leading order (NNLO), fit them to Nijmegen partial wave analysis data, and show that the calculation of the phase shifts converge. We discuss naturalness of the values of the coupling constants of the contact interactions that are obtained by fitting.

Contents

Chapter 1

Introduction

The fundamental theory of all strong interactions is Quantum Chromodynamics(QCD), which is an SU(3) gauge theory of quarks and gluons. Because of chiral symmetry breaking and color confinement, QCD at low energies is very difficult to solve. Properties of hadrons, observed bound states of quarks and gluons, are calculated by large scale lattice simulations using fastest super computers, but it is still beyond the reach to calculate the hadronic scattering accurately.

Historically, the nuclear physics is based on accurately determined potential models which describes nucleon-nucleon scattering at low energies. There are several precise potentials in the energy scales in which pions contribute to nucleon-nucleon scatterings, for example, CD-Bonn [1,2], Argonne V_{18} [3], and Nijmegen [4] etc..

Although there are precise analyses of hadronic phenomena with potential models, it is impossible to improve the description in a systematic way in the sense that the size of the errors cannot be evaluated theoretically. The effective field theory (EFT) description of nucleon systems emerges as an alternative which allows such an error estimate [5]. Once symmetries and degrees of freedom are decided, an unique Lagrangian can be constructed. It is however necessary to decide power counting to calculate the magnitude of interactions, because there are an infinite number of interactions in a low energy EFT.

The EFT description of low energy hadronic interactions incorporate the chiral symmetry which is one of the most important features of QCD at low energies. The interactions between nucleons and pions are determined so as to respect the symmetry. The link to QCD through chiral symmetry is missing in the potential model approach, and makes the EFT description special.

Application of EFT to physics involving more than one nucleon was first considered by Weinberg in his seminal articles [6, 7], the EFT for nuclear physics is called nuclear effective field theory(NEFT). NEFT has chiral symmetry. In a low-energy effective field theory, only a relevant degrees of freedom are considered. In the NEFT, we consider nucleons, and, for higher energies, pions as explicit degrees of freedom

Weinberg proposed a power counting based on naive dimensional analysis in constructing the effective potential, and use it in the Lippmann-Schwinger equation [5–7]. The applications of NEFT with the Weinberg's power counting have achieved a great success, but there is a problem in renormalization. Namely, higher order operators are needed to renormalize cutoff dependence which arises from loop diagrams. It implies that there is inconsistency in the Weinberg's power counting scheme.

To solve the inconsistency problem in Weinberg power counting scheme, Kaplan, Savage and Wise [8,9] (and independently van Kolck [10]) proposed a new power counting scheme, called the KSW power counting. In the KSW power counting, only a contact operator that doesn't include derivatives, is a relevant operator. Other contact operators and pion exchange are treated as irrelevant. With the KSW power counting, there doesn't exist inconsistency problem.

It turned out, however, that the KSW power counting is not without defeats. Fleming, Mehen, and Stewart [11] analyzed nucleon-nucleon scattering including pions up to NNLO in the NEFT based on the KSW power counting. They found that in the $^1S_0$ channel convergent result is obtained, but in the $^3S_1$ channel, the KSW expansion does not converge at the NNLO. It is because the tensor force in the $^3S_1$ channel is too singular in the high energy region.

A power counting is the counting the powers of Λ_0 which is the scale of the theory. To know the power of Λ_0 we need to analyze renormalization group equation and determined anomalous dimensions of operators in the vicinity of a fixed point. To find anomalous dimensions in NEFT including pions, Harada, Kubo, and Yamamoto [12] analyzed Wilsonian renormalization group equation(RGE). They showed that in the S waves of nucleon-nucleon scattering, there is only one relevant operator and other operators are irrelevant. Note that, although in this aspect it is very similar to the KSW power counting, the treatment of pion contribution is different from that of the KSW scheme. A part of the contributions from short-range exchange of pions is included in the relevant operator.

Our approach is very similar to that by Beane, Kaplan, and Vuorinen [13](BKV) in the respect that a separation scale is introduced. There are however important differences: (i) We use the same regularization both for the $^1S_0$ and $^3S_1$ channels, though BKV introduce the separation scale only for the $^3S_1$ channel. (ii) We use a GDF to regularize the pion potential, while BKV use a Pauli-Villars type regulator, which we find insufficient to render several diagrams convergent. (iii) We interpret the separation scale as an analog of the floating cutoff in the Wilsonian RG analysis so that it does not exceed the physical cutoff $\Lambda_0 \sim 400$ MeV above which the effective field theory description does not hold, while BKV consider a rather large value in the range 600 MeV $\leq \lambda \leq$ 1000 MeV, although it is considered as a low-momentum scale of $\mathcal{O}(Q)$. (iv) We interpret the "renormalization scale" μ appeared in the PDS as the separation scale too so that we relate μ to λ through the relation $\mu = \lambda/\sqrt{\pi}$. (v) In our formulation, the separation scale λ is smaller than or equal to the physical cutoff Λ_0, but otherwise arbitrary. On the other hand, BKV tune the value of λ to optimize the perturbation expansion.

In this thesis, we provide a systematic way of understanding of nucleon-nucleon scattering including pions, by calculating the scattering phase shifts employing a hybrid regularization which enables us to divide pion contributions into two parts, S-OPE and L-OPE, in accordance with the power counting which is determined by the Wilsonian RGE.

Finally, we obtain cutoff independent phase shifts of the S waves in nucleon-nucleon scattering and naturalness of coupling constants is realized as results of fitting. It is a very important thing because it implies that there is inconsistency in power counting if naturalness is not kept.

This thesis is organized as follows. In Chapter 2, we give a brief introduction to EFT and power counting. In Chapter 3, we explain the basic idea of power counting for nucleon systems and renormalization and show the examples of power countings, the Weinberg power counting and the KSW power counting. In Chapter 4, we give a review of the NEFT and analysis of nucleon-nucleon scattering in NEFT in $^1S_0$ channel and $^3S_1$ channel by Fleming et al. [11, 14] and explain why the KSW power counting breaks down. In Chapter 5, we explain how to determine power counting on the basis of the Wilsonian RGE analysis in NEFT in cases without and with pions and show that the power counting determined by RGE analysis is very similar to the KSW power counting but different in pion contribution. In Chapter 6, the results of our research are explained. First of all we explain how to divide pion contributions into S-OPE and L-OPE parts. Next, we expand the phase shifts order by order. Finally, we show our result of the $^1S_0$ and $^3S_1$ phase shift for nucleon-nucleon scattering. In Chapter 7, we summarize the thesis. In Appendix A, we explain how to calculate some of integrals and collect useful formulae. In Appendix B, we give a Wilsonian RG analysis for the P waves.

Chapter 2

Effective field theory

In this chapter we explain some of the basic ideas in effective field theory.

2.1 General ideas

The method of EFT seems to be the most powerful alternative to the potential model to understand long distance physics, which is based on a familiar idea that long distance physics is insensitive to the details of short distance physics. We can construct a theory which is valid only up to certain physical energy scale. This energy scale is called a physical cutoff of EFT. By giving up the range of applicability, we are able to describe what happens at low energy without knowing high energy physics.

2.2 Lagrangian

To construct an EFT Lagrangian, we must decide the relevant degrees of freedom and the symmetry of the system at the energy scale of interest. It does not matter how the heavier particles interact at higher energies than we are interested, as long as the relevant degrees of freedom are identified. Once we decide the relevant degrees of freedom and the symmetry, the EFT Lagrangian contains all the operators, in general an infinite number of operators, allowed by the symmetry. We must not drop any operators without any reason.

2.3 Power counting and naturalness

Because an EFT Lagrangian has an infinite number of operators in general, there are infinite kinds of divergences. But it is not a problem because there are corresponding operators to absorb the divergences. In order for EFT to be useful, we must order the operators by the magnitude of contributions. The ordering is called power counting.

The basic idea of power counting is the order of magnitude estimate based on dimensional analysis. The EFT expansion is effective when the hierarchy relation of scales is given by $p \ll \Lambda_0$ where p is the typcal energy scale of the process which we consider and Λ_0 is the cutoff scale of the EFT. In this case, p/Λ_0 is a good expansion parameter.

If we don't know anything about the parameters of EFT, we usually consider the power counting based on naturalness assumptions. If a coupling constant G has mass dimension d then dimensionless coupling constant g may be defined as $g = G/\Lambda_0^d$. Naturalness means that the dimensionless coupling g should be of order one.

From the assumption of naturalness, we can obtain useful expansion. An operator like $G_d p^d$ may be expressed using the dimensionless coupling as $G_d p^d = g_d p^d/\Lambda_0^d$. Because we consider an expansion based on naturalness, if we include all the operators of dimension d, then errors of the calculation are expected to be smaller than $\mathcal{O}\left(Q^d/\Lambda_0^d\right)$, where Q is a typical magnitude of the momentum p. We can improve the accuracy of the predictions to the desired order by taking into account contributions of appropriate higher dimensional operators.

Chapter 3

Power counting and Renormalization for NEFT

In this chapter we explain two types of power countings, which are called Weinberg power counting and the KSW power counting. The power counting scheme is a necessary ingredient for an EFT to know the order of diagrams.

3.1 Weinberg power counting

The power counting for nucleon-nucleon system was first proposed by Weinberg [6, 7].

First of all, we distinguish scattering amplitude into two types of diagrams, reducible diagrams and irreducible diagrams. Two-nucleon reducible diagrams are defined to contain pure two nucleon states in the intermediate states and the rest of the diagrams are defined as irreducible diagrams, because nucleon propagator $S(q) = i/(q_0 - \mathbf{q}^2/2M)$ scales like $1/Q$ if q_0 scales like m or external three-momentum, while $S(q) \sim M/Q^2$ if q_0 scales like an external kinetic energy. Similarly, in loops $\int dq_0$ can scale like Q or Q^2/M depending on which type of pole is picked up, where Q is the typical momentum of the process of interest and M is the mass of nucleon. Then one can solve the Lippmann-Schwinger equation with the sum of irreducible diagrams as effective potential.

3.2 Inconsistency in Weinberg power counting

Although the Weinberg power counting scheme has achieved great success as in Ref. [15], there are problems. To see them, let us consider the contribution shown in Fig.3.1. When it is calculated using dimensional regularization, it gives,

$$-\frac{1}{\epsilon}\frac{g_A^2 m_\pi^2}{128\pi^2 f^2}C_0^2, \tag{3.1}$$

where ϵ is a parameter defined by $\epsilon = (4-D)/2$, with D being the dimension of spacetime. This diagram contribute to LO amplitude but the counter term that is required to absorb the divergence is $m_\pi^2 D_2$. In the Weinberg power counting scheme, such an operator is of higher order term.

To solve the problem, a new power counting scheme has proposed by Kaplan, Savage, and Wise [8, 9], known as KSW power counting.

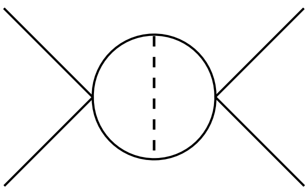

Figure 3.1: The diagram that causes the inconsistency problem in Weinberg power counting that described in the text. Solid lines are nucleon propagator and dotted line is pion propagator.

3.3 KSW power counting

To explain KSW power counting, let consider the calculation for the diagram shown in Fig.3.2, which appear in the calculations of nucleon-nucleon scattering, including only nucleon. One must evaluate the integral I_n:

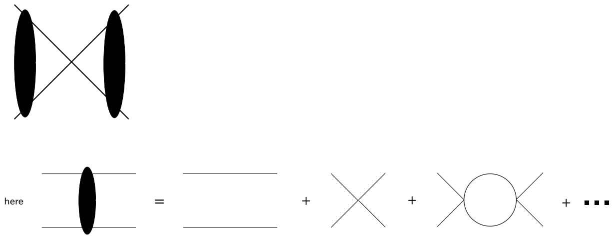

Figure 3.2: The LO amplitude in the pionless theory. Solid lines are nucleon propagator. In this section, we consider pionless diagrams. A black bulb is the sum of all bubble diagrams.

$$
\begin{aligned}
I_n = & - i \left(\frac{\mu}{2}\right)^{4-D} \int \frac{d^D q}{(2\pi)^D} \mathbf{q}^{2n} \frac{i}{E - q^0 - \frac{\mathbf{q}^2}{2M} + i\epsilon} \frac{i}{E + q^0 - \frac{\mathbf{q}^2}{2M} + i\epsilon} \\
= & - M(ME)^n (-ME - i\epsilon)^{\frac{D-3}{2}} \Gamma\left(\frac{3-D}{2}\right) \frac{\left(\frac{\mu}{2}\right)^{4-D}}{(4\pi)^{\frac{D-1}{2}}},
\end{aligned} \tag{3.2}
$$

where D is the spacetime dimension which is eventually set to 4, and E is the total energy of the system. The parameter μ of mass dimension is introduced to make the dimension of I_n $n+2$ irrespective to D. I_n does not have a pole at $D = 4$, but it has a pole at $D = 3$, corresponding to the power(linear in the case of $n = 0$) divergence of the original integral at $D = 4$. It is the power divergence subtraction (PDS) regularization to subtract the poles at $D = 3$ as well as poles at $D = 4$. The counter term is

$$
\delta I_n = -\frac{M(ME)^n \mu}{4\pi(D-3)}, \tag{3.3}
$$

and subtracted integral I_n^{PDS} is defined as

$$
I_n^{PDS} = \lim_{D \to 4} (I_n + \delta I_n) = -(ME)^n \left(\frac{M}{4\pi}\right)(\mu + ip). \tag{3.4}
$$

To obtain scattering amplitude at LO, one needs to sum all bubble diagrams in Fig.3.2:

$$
i\mathcal{A}_{LO} = \frac{-iC_0}{1 + \frac{MC_0}{4\pi}(\mu + ip)}. \tag{3.5}
$$

One can get renormalization group equations by requiring that the physical scattering amplitude is independent of μ:

$$\mu \frac{\partial}{\partial \mu} i\mathcal{A}_{LO} = 0. \tag{3.6}$$

It is only possible when the coupling constant C_0 depends on μ according to the following renormalization group equation:

$$\mu \frac{\partial}{\partial \mu} C_0 = \frac{M\mu}{4\pi} C_0^2. \tag{3.7}$$

Solving this equation, we obtain

$$C_0(\mu) = \frac{4\pi}{M} \frac{1}{-\mu + \frac{1}{a}}. \tag{3.8}$$

When a is natural size($\sim \Lambda$), naive dimensional counting can be adopted to know the magnitude of coupling constants. In this case, it is convenient to take $\mu = 0$.

In case of $a \leq 1$ and $\mu \to 0$, the coupling constants are very large; $C_{2n} \sim (4\pi a^{n+1})/(M\Lambda^n)$. This difficulty can be avoided to take μ nonzero value in which case the coefficients may not be large; $C_{2n} \sim 4\pi/(M\Lambda^n \mu^{n+1})$.

Chapter 4

Nuclear Effective Field Theory

In this chapter we will show brief review about nuclear effective field theory(NEFT) and phase shift analysis based on the EFT shown in the literature. NEFT is low energy effective theory of nucleons based on symmetries of QCD and the freedoms of this theory is nucleons and pions.

4.1 Formalism

In this thesis, we will follow the notation in [14, 16, 17].

The Lagrangian for a nucleon system including pions is

$$\begin{aligned}\mathcal{L} =& \frac{f_\pi^2}{8}\mathrm{Tr}\left(\partial^\mu\Sigma\partial_\mu\Sigma^\dagger\right) + \frac{f_\pi^2\omega}{8}\mathrm{Tr}\left(m_q\Sigma + m_q\Sigma^\dagger\right) + N^\dagger\left(i\vec{D}_0 + \frac{D^2}{2M}\right)N \\ &+ \frac{ig_A}{2}N^\dagger\sigma_i\left(\xi\partial_i\xi^\dagger - \xi^\dagger\partial_i\xi\right) - C_0^{(s)}\mathcal{O}_0^{(s)} + \frac{C_2^{(s)}}{8}\mathcal{O}_2^{(s)} - D_2^{(s)}\omega\mathrm{Tr}(m^\xi)\mathcal{O}_0^{(s)} \\ &- \frac{C_4^{(s)}}{64}\mathcal{O}_4^{(s)} + \frac{E_4^{(s)}}{8}\omega\mathrm{Tr}(m^\xi)\mathcal{O}_2^{(s)} - \frac{D_4^{(s)}}{2}\omega^2\left\{\mathrm{Tr}^2(m^\xi) + 2\mathrm{Tr}\left[(m^\xi)^2\right]\right\}\mathcal{O}_0^{(s)} \\ &- C_2^{(SD)}\mathcal{O}_2^{(SD)} + \cdots\,. \end{aligned} \tag{4.1}$$

Here $g_A = 1.25$ is the nucleon axial-vector coupling, and $f_\pi = 131$ MeV is the pion-decay constant.

$$\begin{aligned}\Sigma =&\xi^2 = \exp\left(2i\frac{\Pi}{f_\pi}\right),\\ \text{where,} \qquad \Pi =& \begin{pmatrix} \frac{\pi^0}{\sqrt{2}} & \pi^+ \\ \pi^- & -\frac{\pi^0}{\sqrt{2}} \end{pmatrix},\end{aligned} \tag{4.2}$$

in which $\pi^{0,\pm}$ are pion fields. The chiral covariant derivative is $D_\mu = \partial_\mu + \frac{1}{2}\left(\xi\partial_i\xi^\dagger + \xi^\dagger\partial_i\xi\right)$ and $m^\xi = \frac{1}{2}\left(\xi m_q\xi^\dagger + \xi^\dagger m_q\xi\right)$ and $m_q = \text{diag}\left(m_u, m_d\right)$ is the quark mass matrix, $\omega\text{Tr}(m^\xi) = m_\pi^2 = (137\text{MeV})^2$. The theory has a global (chiral) symmetry, $SU(2)_L \times SU(2)_R$ which is spontaneously broken to the vector subgroup $SU(2)_V$. $\Sigma(x) \to L\Sigma(x)R^\dagger$. The nucleon field transforms as

$$N(x) \to U(x)N(x), \tag{4.3}$$

where $U(x)$ is defined as

$$\xi(x) \to L\xi(x)U(x)^\dagger = U(x)\xi(x)R^\dagger. \tag{4.4}$$

Two nucleon operators for ${}^1S_0$ and ${}^3S_1$ waves which appear in eq.(4.1) are defined as,

$$\begin{aligned}
\mathcal{O}_0^{(s)} &= \left(N^T P_i^{(s)} N\right)^\dagger \left(N^T P_i^{(s)} N\right),\\
\mathcal{O}_2^{(s)} &= \left(N^T P_i^{(s)} N\right)^\dagger \left(N^T P_i^{(s)} \nabla^2 N\right) + h.c,\\
\mathcal{O}_4^{(s)} &= \left(N^T P_i^{(s)} N\right)^\dagger \left(N^T P_i^{(s)} \nabla^4 N\right) + h.c + 2\left(N^T P_i^{(s)} \nabla^2 N\right)^\dagger \left(N^T P_i^{(s)} \nabla^2 N\right),\\
\mathcal{O}_4^{(s)} &= \left(N^T P_i^{({}^3S_1)} N\right)^\dagger \left(N^T P_i^{({}^3D_1)} N\right) + h.c.
\end{aligned} \tag{4.5}$$

where $P_i^{(s)}$ are the projection matrices with s specifying partial wave;

$$\begin{aligned}
P_i^{({}^1S_0)} =& \frac{(i\sigma_2)(i\tau_2\tau_i)}{2\sqrt{2}},\\
P_i^{({}^1S_0)} =& \frac{(i\sigma_2\sigma_i)(i\tau_2)}{2\sqrt{2}}.
\end{aligned} \tag{4.6}$$

4.2 Amplitudes obtained by Fleming et al.

First of all, we show the result for the $^1S_0$ channel obtained by Fleming et.al [11]. In this paper, LO, NLO, and NNLO amplitudes are written $\mathcal{A}_{-1}$, $\mathcal{A}_0$, and $\mathcal{A}_1$ respectively:

$$
\begin{aligned}
\mathcal{A}_{-1} &= -\frac{4\pi}{M}\frac{1}{\gamma+ip}\,, \\
\mathcal{A}_0 &= -\mathcal{A}_{-1}^2(\zeta_1\,p^2+\zeta_2\,m_\pi^2) \\
&\quad +\frac{g_A^2}{2f^2}\mathcal{A}_{-1}^2\Big(\frac{Mm_\pi}{4\pi}\Big)^2\left[\frac{(\gamma^2-p^2)}{4p^2}\ln\Big(1+\frac{4p^2}{m_\pi^2}\Big)-\frac{\gamma}{p}\tan^{-1}\left(\frac{2p}{m_\pi}\right)\right], \\
\mathcal{A}_1 &= \frac{\mathcal{A}_0^2}{\mathcal{A}_{-1}}-\mathcal{A}_{-1}^2\Big(\zeta_3\,m_\pi^2+\zeta_4\,p^2+\zeta_5\frac{p^4}{m_\pi^2}\Big)+\mathcal{A}_0\frac{Mg_A^2}{8\pi f^2}\,\frac{m_\pi^2}{p}\left[\frac{\gamma}{2p}\ln\Big(1+\frac{4p^2}{m_\pi^2}\Big)\right. \\
&\quad \left.-\tan^{-1}\Big(\frac{2p}{m_\pi}\Big)\right]+\frac{M\mathcal{A}_{-1}^2}{4\pi}\Big(\frac{Mg_A^2}{8\pi f^2}\Big)^2\frac{m_\pi^4}{4p^3}\left\{2(\gamma^2-p^2)\,\mathrm{Im}\,\mathrm{Li}_2\Big(\frac{-m_\pi}{m_\pi-2ip}\Big)\right. \\
&\quad -4\gamma\,p\,\mathrm{Re}\,\mathrm{Li}_2\Big(\frac{-m_\pi}{m_\pi-2ip}\Big)-\frac{\gamma\,p\,\pi^2}{3}-(\gamma^2+p^2)\left[\mathrm{Im}\,\mathrm{Li}_2\Big(\frac{m_\pi+2ip}{-m_\pi+2ip}\Big)\right. \\
&\quad \left.\left.+\frac{\gamma}{4p}\ln^2\left(1+\frac{4p^2}{m_\pi^2}\right)-\tan^{-1}\left(\frac{2p}{m_\pi}\right)\ln\left(1+\frac{4p^2}{m_\pi^2}\right)\right]\right\}.
\end{aligned}
\tag{4.7}
$$

where,

$$
\begin{aligned}
\gamma &= \frac{4\pi}{MC_0} + \mu \ , \qquad\qquad \zeta_1 = \left[\frac{C_2}{(C_0)^2}\right] , \\
\zeta_2 &= \left[\frac{D_2}{(C_0)^2} - \frac{g_A^2}{4f^2}\Big(\frac{M}{4\pi}\Big)^2 \ln\Big(\frac{\mu^2}{m_\pi^2}\Big)\right] + \frac{1}{m_\pi^2}\left[\frac{C_0^{(0)}}{(C_0)^2} + \frac{g_A^2}{2f^2}\Big(\frac{M}{4\pi}\Big)^2 (\gamma^2 - \mu^2)\right] , \\
\zeta_3 &= -\frac{g_A^2}{2f^2}\frac{Mm_\pi}{4\pi}\left[\frac{C_2}{(C_0)^2}\right] + \frac{1}{m_\pi^2}\left[\frac{C_0^{(1)}}{(C_0)^2} - \frac{(C_0^{(0)})^2}{(C_0)^3} - \left(\frac{g_A^2}{2f^2}\right)^2\left(\frac{M}{4\pi}\right)^3 (\mu^3 - \gamma^3)\right] \\
&\quad - \frac{2\gamma}{m_\pi^2}\frac{Mg_A^2}{8\pi f^2}\left[\frac{C_0^{(0)}}{(C_0)^2} + \frac{g_A^2}{2f^2}\left(\frac{M}{4\pi}\right)^2 (-\mu^2 + \gamma^2)\right] - 2\frac{M\gamma}{4\pi}\Big(\frac{Mg_A^2}{8\pi f^2}\Big)^2\Big(\ln 2 - \frac{3}{2}\Big) \\
&\quad + m_\pi^2\left\{\frac{D_4}{(C_0)^2} - \frac{D_2^2}{(C_0)^3}\right\} + \left[\frac{D_2^{(-1)}}{(C_0)^2} - \frac{2D_2C_0^{(0)}}{(C_0)^3} - \frac{g_A^2}{f^2}\frac{M\gamma}{4\pi}\frac{D_2}{(C_0)^2}\right] + \zeta_3^{rad} , \\
\zeta_4 &= \left[\frac{C_2^{(-1)}}{(C_0)^2} - \frac{2\,C_2\,C_0^{(0)}}{(C_0)^3} - \frac{g_A^2}{f^2}\frac{M\gamma}{4\pi}\frac{C_2}{(C_0)^2}\right] + m_\pi^2 \left\{\frac{E_4}{(C_0)^2} - \frac{2\,C_2\,D_2}{(C_0)^3}\right\} , \\
\zeta_5 &= m_\pi^2 \left\{\frac{C_4}{(C_0)^2} - \frac{(C_2)^2}{(C_0)^3}\right\} .
\end{aligned} \tag{4.8}
$$

The parameters $\zeta_1 \sim \zeta_5$ are dimensionless constants. Because of renormalization equation, quantities in square and curly brackets are separately μ independent.

To fit the phase shift to partial wave analysis data, they used the so-called good fit conditions. For the leading order operator C_0, it is

$$
-\frac{1}{a} + \frac{r_0}{2}(p^*)^2 - ip^* = 0 \, . \tag{4.9}
$$

This decide determines $\gamma = -7.88$MeV. For NLO, the condition is

$$
\zeta_2 = \frac{\gamma^2}{m_\pi^2}\,\zeta_1 - \frac{M}{4\pi}\,\frac{g_A^2 M}{8\pi f^2}\log\left(1 + \frac{2\gamma}{m_\pi}\right) , \tag{4.10}
$$

At NNLO, $\zeta_5 = 0$ and the ranges $p = 7 \sim 80$ MeV and $p = 7 \sim 200$MeV were used for the fitting at NLO and NNLO respectively, with low momentum weighted more heavily.

$$
\begin{aligned}
&\text{NLO}: \qquad \zeta_1 = 0.216; \qquad \zeta_2 = 0.0318; \\
&\text{NNLO}: \qquad \zeta_1 = 0.0777; \qquad \zeta_2 = 0.0313; \qquad \zeta_3 = 0.1831; \qquad \zeta_4 = 0.245.
\end{aligned} \tag{4.11}
$$

Note that the value of ζ_1 changes significantly from NLO to NNLO.

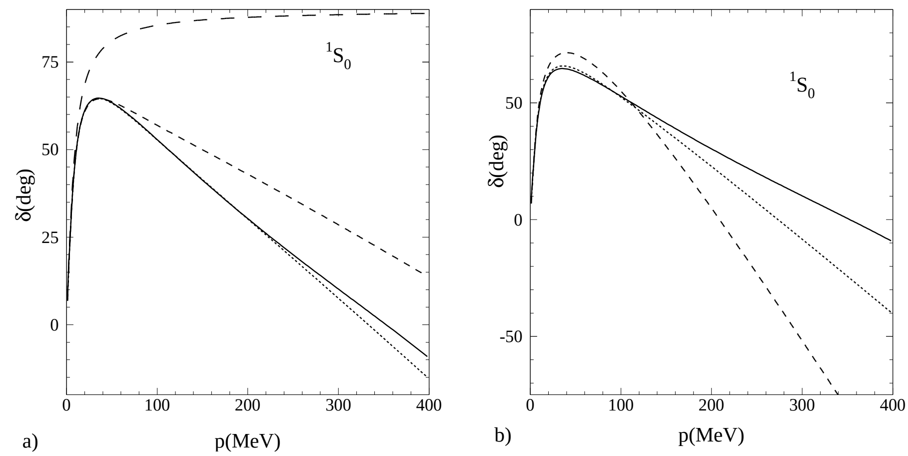

Figure 4.1: Fit to the $^1S_0$ phase shift δ from Ref. [11]. The solid line is the Nijmegen fit [18] to the data. In a), the long dashed, short dashed, and dotted lines are the LO, NLO, and NNLO results respectively. In b) we show two other NNLO fits with a different choice of parameters.

The solid line is the Nijmegen phase shift analysis in each graph. The coupling constants given above are in Fig.4.1(a). At the LO fit, the error is about 48%, at the NLO, the error is 17%, and at the NNLO, the error is less than 1%. The KSW expansion gives improvement at this channel. In Fig4.1(b), the phase shift is fitted in constraints that the value of ζ_1 is close to its NLO value and $\zeta_4 \leq \zeta_1$.

Let us move on the $^3S_1$ channel. In this channel, there is a mixing with the $^3D_1$ channel.

The phase shift is expanded perturbatively.

$$\bar{\delta}_0 = \bar{\delta}_0^{(0)} + \bar{\delta}_0^{(1)} + \bar{\delta}_0^{(2)} + \cdots . \tag{4.12}$$

The phase shift at each order is given by

$$\begin{aligned}
\bar{\delta}_0^{(0)} &= \frac{1}{2i} \ln\left(1 + \frac{ipM}{2\pi}\mathcal{A}_{-1}^{SS}\right), \qquad \bar{\delta}_0^{(1)} = \frac{pM}{4\pi}\frac{\mathcal{A}_0^{SS}}{1+\frac{ipM}{2\pi}\mathcal{A}_{-1}^{SS}}, \\
\bar{\delta}_0^{(2)} &= \frac{pM}{4\pi}\frac{\mathcal{A}_1^{SS}}{1+\frac{ipM}{2\pi}\mathcal{A}_{-1}^{SS}} - i\left(\frac{pM}{4\pi}\right)^2\left[\left(\frac{\mathcal{A}_0^{SS}}{1+\frac{ipM}{2\pi}\mathcal{A}_{-1}^{SS}}\right)^2 + \frac{(\mathcal{A}_0^{SD})^2}{1+\frac{ipM}{2\pi}\mathcal{A}_{-1}^{SS}}\right].
\end{aligned} \tag{4.13}$$

where the S-D mixing amplitude becomes ,

$$\mathcal{A}_0^{SD} = \sqrt{2}\frac{Mg_A^2}{8\pi f^2}\mathcal{A}_{-1}^{SS}\left\{ -\frac{3m_\pi^3}{4p^2} + \left(\frac{m_\pi^2}{2p} + \frac{3m_\pi^4}{8p^3}\right)\tan^{-1}\left(\frac{2p}{m_\pi}\right) + \frac{3\gamma m_\pi^2}{4p^2} - \frac{\gamma}{2} \right.$$
$$\left. -\left(\frac{\gamma m_\pi^2}{4p^2} + \frac{3\gamma m_\pi^4}{16p^4}\right)\ln\left(1 + \frac{4p^2}{m_\pi^2}\right)\right\}. \quad (4.14)$$

$$
\begin{aligned}
\mathcal{A}_{-1}^{SS} =& -\frac{4\pi}{M}\frac{1}{\gamma+ip},\\
\mathcal{A}_{0}^{SS} =& -\left[\mathcal{A}_{-1}^{SS}\right]^2(\zeta_1 p^2+\zeta_2 m_\pi^2)\\
&+\left[\mathcal{A}_{-1}^{SS}\right]^2\frac{g_A^2}{2f^2}\Big(\frac{Mm_\pi}{4\pi}\Big)^2\left[\frac{(\gamma^2-p^2)}{4p^2}\log\left(1+\frac{4p^2}{m_\pi^2}\right)-\frac{\gamma}{p}\tan^{-1}\left(\frac{2p}{m_\pi}\right)\right],\\
\mathcal{A}_{1}^{SS} =& \frac{[\mathcal{A}_0^{SS}]^2}{\mathcal{A}_{-1}^{SS}}+\frac{ipM}{4\pi}\left[\mathcal{A}_0^{SD}\right]^2+\mathcal{A}_0^{SS}\frac{Mg_A^2}{8\pi f^2}\frac{m_\pi^2}{p}\left[\frac{\gamma}{2p}\log\left(1+\frac{4p^2}{m_\pi^2}\right)-\tan^{-1}\Big(\frac{2p}{m_\pi}\Big)\right]\\
&-\left[\mathcal{A}_{-1}^{SS}\right]^2\left(\zeta_3 m_\pi^2+\zeta_4 p^2+\zeta_5\frac{p^4}{m_\pi^2}\right)\\
&+\left[\mathcal{A}_{-1}^{SS}\right]^2\frac{M}{4\pi}\Big(\frac{Mg_A^2}{8\pi f^2}\Big)^2\left[\frac{-6\gamma^2 m_\pi^3+9\gamma m_\pi^4-3m_\pi^5}{4p^2}\right.\\
&+\log 2\Big(\frac{9\gamma m_\pi^6}{4p^4}+\frac{3\gamma m_\pi^4}{2p^2}-\frac{9m_\pi^7}{4p^4}-\frac{3m_\pi^5}{p^2}\Big)\\
&+\left(6p^2+6m_\pi^2-\frac{3m_\pi^4}{4p^2}-\frac{9m_\pi^6}{8p^4}\right)\left[\frac{p^2-\gamma^2}{p}\tan^{-1}\left(\frac{p}{m_\pi}\right)-\gamma\log\left(1+\frac{p^2}{m_\pi^2}\right)\right]\\
&-\left(\frac{3m_\pi^5}{p^3}+\frac{9m_\pi^7}{4p^5}\right)\left[\gamma\tan^{-1}\left(\frac{p}{m_\pi}\right)-\frac{(\gamma^2-p^2)}{4p}\log\left(1+\frac{p^2}{m_\pi^2}\right)\right]\\
&+\left(\frac{9m_\pi^7}{8p^5}+\frac{3m_\pi^5}{2p^3}-\frac{9\gamma m_\pi^6}{8p^5}-\frac{3\gamma m_\pi^4}{4p^3}+\frac{\gamma m_\pi^2}{p}\right)\\
&\times\left[\gamma\tan^{-1}\left(\frac{2p}{m_\pi}\right)+\frac{p}{2}\log\left(1+\frac{4p^2}{m_\pi^2}\right)\right]\\
&+\left(\frac{9m_\pi^8}{32p^7}+\frac{3m_\pi^6}{4p^5}+\frac{3m_\pi^4}{4p^3}\right)\left\{2(\gamma^2-p^2)\mathrm{Im}\,\mathrm{Li}_2\Big(\frac{-m_\pi}{m_\pi-2ip}\Big)\right.\\
&-4\gamma p\mathrm{Re}\,\mathrm{Li}_2\Big(\frac{-m_\pi}{m_\pi-2ip}\Big)-\frac{\gamma p\pi^2}{3}-(\gamma^2+p^2)\left[\mathrm{Im}\,\mathrm{LI}_2\Big(\frac{m_\pi+2ip}{-m_\pi+2ip}\Big)\right.\\
&\left.\left.+\frac{\gamma}{4p}\log^2\left(1+\frac{4p^2}{m_\pi^2}\right)-\tan^{-1}\left(\frac{2p}{m_\pi}\right)\log\left(1+\frac{4p^2}{m_\pi^2}\right)\right]\right\}\\
&\left.+\gamma\left(\frac{9m_\pi^8}{32p^6}+\frac{3m_\pi^6}{4p^4}+\frac{m_\pi^4}{2p^2}\right)\left[\tan^{-1}\left(\frac{2p}{m_\pi}\right)-\frac{\gamma}{2p}\log\left(1+\frac{4p^2}{m_\pi^2}\right)\right]^2\right].
\end{aligned}
\tag{4.15}
$$

We have introduced the notations:

$$\begin{aligned}
\gamma =& \frac{4\pi}{MC_0} + \mu, \qquad\qquad \zeta_1 = \left[\frac{C_2}{(C_0)^2}\right], \\
\zeta_2 =& \left[\frac{D_2}{(C_0)^2} - \frac{g_A^2}{4f^2}\Big(\frac{M}{4\pi}\Big)^2 \log\Big(\frac{\mu^2}{m_\pi^2}\Big)\right] + \frac{1}{m_\pi^2}\left[\frac{C_0^{(0)}}{(C_0)^2} + \frac{g_A^2}{2f^2}\Big(\frac{M}{4\pi}\Big)^2(\gamma^2-\mu^2)\right], \\
\zeta_3 =& -\frac{g_A^2}{2f^2}\frac{Mm_\pi}{4\pi}\left[\frac{C_2}{(C_0)^2}\right] - \frac{1}{m_\pi^2}\frac{M}{4\pi}\Big(\frac{Mg_A^2}{8\pi f^2}\Big)^2\Big(\gamma^3 - 6m_\pi\gamma^2 - \frac{7}{2}m_\pi^2\gamma + 4m_\pi^3\Big) \\
& + \frac{1}{m_\pi^2}\left[\frac{C_0^{(1)}}{(C_0)^2} - \frac{(C_0^{(0)})^2}{(C_0)^3} - \frac{g_A^2}{f^2}\frac{M\gamma}{4\pi}\frac{C_0^{(0)}}{(C_0)^2} - \frac{M}{4\pi}\Big(\frac{Mg_A^2}{8\pi f^2}\Big)^2\Big(4\mu\gamma^2 - 6\gamma\mu^2 + \frac{4}{3}\mu^3\Big)\right] \\
& + m_\pi^2\left\{\frac{D_4}{(C_0)^2} - \frac{(D_2)^2}{(C_0)^3}\right\} \\
& + \left[\frac{D_2^{(-1)}}{(C_0)^2} - \frac{2D_2C_0^{(0)}}{(C_0)^3} - \frac{g_A^2}{f^2}\frac{M\gamma}{4\pi}\frac{D_2}{(C_0)^2} - 5\frac{M\gamma}{4\pi}\Big(\frac{Mg_A^2}{8\pi f^2}\Big)^2 \ln\Big(\frac{\mu^2}{m_\pi^2}\Big)\right] \\
& + \zeta_3^{rad}, \\
\zeta_4 =& \left[\frac{C_2^{(-1)}}{(C_0)^2} - \frac{2C_2C_0^{(0)}}{(C_0)^3} - 6\frac{M\gamma}{4\pi}\Big(\frac{Mg_A^2}{8\pi f^2}\Big)^2 \ln\Big(\frac{\mu^2}{m_\pi^2}\Big)\right] + m_\pi^2\left\{\frac{E_4}{(C_0)^2} - \frac{2C_2D_2}{(C_0)^3}\right\}, \\
& - \frac{g_A^2}{f^2}\frac{M\gamma}{4\pi}\left[\frac{C_2}{(C_0)^2}\right] - \frac{M}{4\pi}\Big(\frac{Mg_A^2}{8\pi f^2}\Big)^2\Big(-3\gamma + 6m_\pi\Big), \\
\zeta_5 =& m_\pi^2\left\{\frac{C_4}{(C_0)^2} - \frac{(C_2)^2}{(C_0)^3}\right\}.
\end{aligned} \tag{4.16}$$

By fitting to the data, they obtained the following values for these parameters,

$$\begin{aligned}
&\text{NLO}: && \zeta_1 = 0.327; && \zeta_2 = -0.0936; && && \qquad (4.17)\\
&\text{NNLO}: && \zeta_1 = 0.432; && \zeta_2 = -0.0818; && \zeta_3 = 0.165; && \zeta_4 = 0.399.
\end{aligned}$$

At LO, the phase shift has no free parameters. At NLO there is one free parameter ξ_1, and the fit to the data is very good. However, at NNLO the fit of the phase shift to the data becomes worse at the momentum region more than $p \simeq 50$ MeV.

In the ${}^3S_1$ channel, the term expressed below appear in the scattering

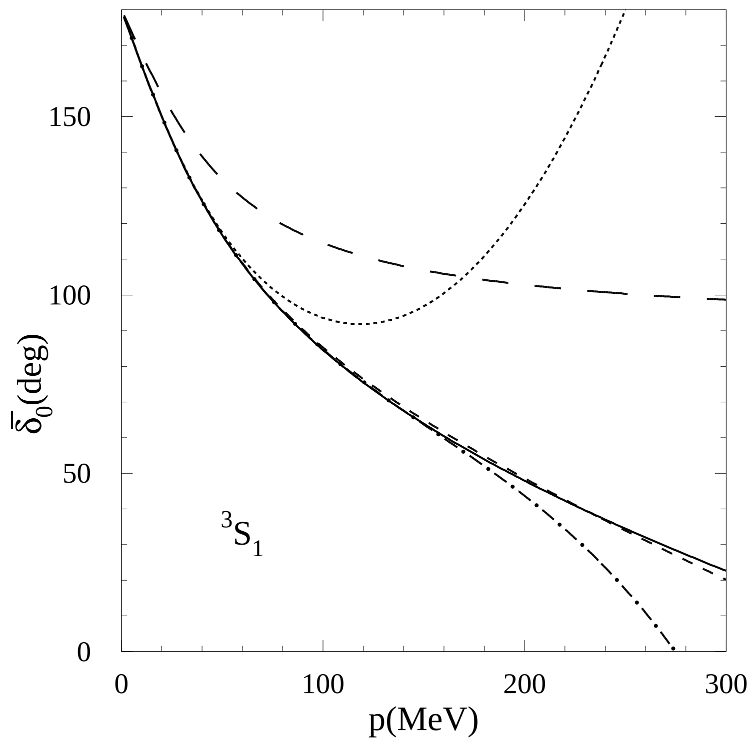

Figure 4.2: The $^3S_1$ phase shift for NN scattering from Ref [11]. The solid line is the Nijmegen multi-energy fit [18], the long dashed line is the LO effective field theory result, the short dashed line is the NLO result, and the dotted line is the NNLO result. The dash-dotted line shows the result of including the parameter ζ_5 which is higher order in the power counting.

amplitude,

$$\mathcal{A}_1^{SS} \simeq 6\,[\mathcal{A}_{-1}^{SS}]^2\,\frac{M}{4\pi}\left(\frac{Mg_A^2}{8\pi f^2}\right)^2 p^3\tan^{-1}\left(\frac{p}{m_\pi}\right)\,. \tag{4.18}$$

For the momentum region $p \gg m_\pi$, this term grows linearly with p. This is the source of the failure of the KSW power counting at NNLO in the ${}^3S_1$ channel. It is considered that such a term comes from the singularity of the tensor force near the origin, $r = 0$ in the coordinate space.

Chapter 5

Wilsonian renormalization group analysis

In this chapter we review Wilsonian renormalization group analysis in the NEFT.

5.1 Scaling dimensions

Let us consider the interaction Lagrangian $\mathcal{L} = \Sigma G_i \mathcal{O}_i$ where G_i is coupling constant and $\mathcal{O}_i$ is corresponding operator. It is useful to consider the RG equations written in terms of dimensionless coupling constants defined as,

$$G_i(\Lambda) \equiv \frac{g_i(\Lambda)}{\Lambda^{d_i - D}}, \tag{5.1}$$

where Λ is the floating cutoff, D is the dimension of spacetime, and d_i is the canonical dimension of the operator $\mathcal{O}_i$. The RG equation of coupling g_i may be written as

$$\frac{dg_i}{dt} = \beta_i(g), \qquad t \equiv \log\left(\frac{\Lambda_0}{\Lambda}\right). \tag{5.2}$$

We are interested in the behavior of the coupling constants near the fixed point, so we substitute $g_i = g_i^* + \delta g_i$ to the RG equation, where g_i^* is value of the coupling constant on the fixed point, $\beta(g^*) = 0$, and δg_i is small deviation from fixed point,

$$\frac{d}{dt}\delta g_i = \left.\frac{\partial \beta_i}{\partial g_j}\right|_g^* \equiv A_{ij}(g^*)\delta g_j. \tag{5.3}$$

By diagonalizing A_{ij}, we get

$$\frac{d\mathbf{u}_i}{dt} = \nu_i \mathbf{u}_i, \tag{5.4}$$

where $\nu_i's$ are the eigenvalues and $\mathbf{u}_i's$ are the corresponding eigenvectors. This RG equation may be integrated as,

$$\mathbf{u}_i(\Lambda) = \mathbf{u}_i(\Lambda_0) \left(\frac{\Lambda}{\Lambda_0}\right)^{-\nu_i}. \tag{5.5}$$

The coupling are called irrelevant, marginal, and relevant when $\nu_i < 0$, $\nu_i = 0$, and $\nu_i > 0$ respectively.

Suppose that coupling constant $g_i(\Lambda)$ is written as

$$g_i(\Lambda) \sim g_i^* + \Sigma_k c_{ik} \left(\frac{\Lambda}{\Lambda_0}\right)^{-\nu_k}, \tag{5.6}$$

so dimensionful coupling constant becomes

$$G_i(\Lambda) \sim \frac{g_i^*}{\Lambda^{d_i - D}} + \Sigma_k c_{ik} \frac{\Lambda_0^{\nu_k}}{\Lambda^{d_i - D + \nu_k}}. \tag{5.7}$$

Counting powers of Λ_0 is the correct power counting.

5.2 Renormalization group equations

The Wilsonian RGEs for NEFT including pions are obtained in [19]

$$
\begin{aligned}
\frac{dx}{dt} &= -x - \left[x^2 + 2xy + y^2 + 2xz + 2yz + z^2\right] \\
&\quad -2(x+y+z)\gamma - \gamma^2, &(5.8)\\
\frac{dy}{dt} &= -3y - \left[\frac{1}{2}x^2 + 2xy + \frac{3}{2}y^2 + yz - \frac{1}{2}z^2\right] \\
&\quad -(x+2y)\gamma - \frac{1}{2}\gamma^2, &(5.9)\\
\frac{dz}{dt} &= -3z + \left[\frac{1}{2}x^2 + xy + \frac{1}{2}y^2 - xz - yz - \frac{3}{2}z^2\right] \\
&\quad +(x+y-z)\gamma + \frac{1}{2}\gamma^2, &(5.10)\\
\frac{du}{dt} &= -3u - 2(x+y+z)(u-\gamma) - 2u\gamma + 2\gamma^2, &(5.11)
\end{aligned}
$$

and for γ,

$$\frac{d\gamma}{dt} = -\gamma. \tag{5.12}$$

Here, we have introduced of dimensionless coupling constants,

$$x \equiv \frac{M\Lambda}{2\pi^2}C_0^{(S)}, \quad y \equiv \frac{M\Lambda^3}{2\pi^2}4C_2^{(S)}, \quad z \equiv \frac{\Lambda^3}{2\pi^2}B^{(S)}, \quad u \equiv \frac{M\Lambda^3}{2\pi^2}D_2^{(S)}, \quad u' \equiv \frac{M\Lambda^3}{2\pi^2}D_2^{(T)}. \tag{5.13}$$

The nontrivial fixed point of the above RGEs relevant to the real two-nucleon system is found to be,

$$(x^\star, y^\star, z^\star, u^\star, \gamma^\star) = \left(-1, -\frac{1}{2}, \frac{1}{2}, 0, 0\right), \tag{5.14}$$

which is identified with that found in the pionless NEFT given in Ref. [20].

The eigenvalues and corresponding eigenvectors are,

$$
\begin{aligned}
\nu_1 &= +1: \; u_1 = \begin{pmatrix} 1 \\ 1 \\ -1 \\ 0 \\ 0 \end{pmatrix}, \quad \nu_2 = -1: \; u_2 = \begin{pmatrix} 0 \\ -1 \\ 1 \\ 0 \\ 0 \end{pmatrix}, \\
\nu_3 &= -2: \; u_3 = \begin{pmatrix} 2 \\ -1 \\ -2 \\ 0 \\ 0 \end{pmatrix}, \quad \nu_4 = -1: \; u_4 = \begin{pmatrix} 0 \\ 0 \\ 0 \\ 1 \\ 0 \end{pmatrix}.
\end{aligned}
\tag{5.15}
$$

This is only one operator with positive eigenvalue which corresponds to a relevant operator explained in the previous section. All the other operators are irrelevant. This aspect is very similar to KSW power counting in which only the contact interaction without derivatives is a relevant operator, and other operators are irrelevant, but pion contributions are different. In the KSW power counting, pion contributions are perturbative but the Wilsonian RGEs analysis implies that short-distance contributions of pions are included into contact interactions. Furthermore one of the contact interaction is relevant, so a part of short-distance pion contributions have to be treated as relevant. The long-distance contributions of pions are irrelevant so one can treat them as perturbations.

Chapter 6

Computation of phase shifts of nucleon-nucleon scattering

In this chapter, we show the computation of nucleon-nucleon scattering phase shifts in NEFT based on the power counting found in [19].

6.1 Hybrid regularization

From the Wilsonian RG analysis described in the previous chapter, we think that it is necessary to make a decomposition of pion exchange contributions into its short-distance part and long-distance part. We first notice that the pion exchange can be written as

$$\frac{\mathbf{k}^2}{\mathbf{k}^2 + m_\pi^2} \to 1 - \frac{m_\pi^2}{\mathbf{k}^2 + m_\pi^2}. \tag{6.1}$$

The first term may be viewed as the short-distance part, while the second term, which has a milder short-distance behavior, may be viewed as the long-distance part. It however still has a large contribution for short-distance, we therefore introduce a Gaussian damping factor, $e^{-\mathbf{k}^2/\lambda^2}$, which suppresses the short-distance contributions,

$$-\frac{m_\pi^2}{\mathbf{k}^2 + m_\pi^2} \to -\frac{m_\pi^2}{\mathbf{k}^2 + m_\pi^2} e^{-\frac{\mathbf{k}^2}{\lambda^2}}, \tag{6.2}$$

where λ is the cutoff scale, which is an analog of the floating cutoff in the Wilsonian RG analysis. All diagrams including pions are calculated with this damping factor.

Of course, another dumping factor may be used. For example a Lorentzian damping factor such as,

$$\frac{m_\pi^2}{\mathbf{k}^2+m_\pi^2} \to \frac{m_\pi^2}{\mathbf{k}^2+m_\pi^2}\left(\frac{\lambda^2}{\mathbf{k}^2+\lambda^2}\right)^n, \tag{6.3}$$

may be used, as Beane, Kaplan, and Vourinen [13] did, where n is a positive integer. It would be good if the $n=1$ case regularizes all the diagrams but it turns out that the convergence of multi-loop diagrams requires $n \geq 2$. On the other hand the same GDF can be used for all the diagrams, so we adopted the GDF regularization.

A very nontrivial point with the GDF regularization of the pion exchange is that the pion exchange coupling constant should be defined independent of the cutoff, so that an extra factor $e^{-m_\pi^2/\lambda^2}$ is necessary. Including the coupling constant, the pion exchange may be written as

$$-i\frac{g_A^2}{2f^2}e^{-\frac{m_\pi^2}{\lambda^2}}. \tag{6.4}$$

It turns out that this definition of the coupling constant has several favorable features: (i) The coupling constant defined by the residue of the Yukawa pole is independent of the separation scale λ. (ii) The results of loop integrals including pion propagators with GDFs contain the factor $e^{m_\pi^2/\lambda^2}$, which produces (disastrous) non-local contributions to higher orders when expanded in powers of m_π^2/λ^2. This extra factor cancels all such terms. (iii) One might wonder why this factor is necessary even for the S-OPE (the first term). It actually cancels the NNLO contribution of the tree L-OPE. Note that $e^{-m_\pi^2/\lambda^2}\left[1-\left(m_\pi^2/\left(\mathbf{k}^2+m_\pi^2\right)\right)\right]$ converges faster than $\left[1-\left(m_\pi^2/\left(\mathbf{k}^2+m_\pi^2\right)\right)\right]$ to $\mathbf{k}^2/\left(\mathbf{k}^2+m_\pi^2\right)$ as $\left(\mathbf{k}^2,m_\pi^2\right)/\lambda^2 \to 0$.

6.2 Perturbative expansion of phase shifts

The phase shift δ is related to the scattering amplitude as,

$$S-1=e^{2i\delta}-1=i\left(\frac{pM}{2\pi}\right)\mathcal{A}. \tag{6.5}$$

At low energies, it is convenient to consider $p\cot\delta$, as the effective range expansion teaches us.

In ${}^1S_0$ channel, $p\cot\delta$ may be written as,

$$p\cot\delta = ip + \frac{4\pi}{M\mathcal{A}}. \tag{6.6}$$

We divide scattering amplitude each of order, $\mathcal{A}_{\rm LO}, \mathcal{A}_{\rm NLO}, \mathcal{A}_{\rm NNLO}$, the leading order(LO), the next to the leading order(NLO), and the next to next to the leading order(NNLO) amplitudes respectively. The magnitudes of these amplitudes are expected to satisfy $\mathcal{A}_{\rm LO} > \mathcal{A}_{\rm NLO} > \mathcal{A}_{\rm NNLO}$, so we can expand phase shift perturbatively,

$$\begin{aligned}
\delta_{\rm LO} &= \frac{1}{2i}\log\left(1+\frac{ipM}{2\pi}\mathcal{A}_{\rm LO}\right), \\
\delta_{\rm NLO} &= \frac{pM}{4\pi}\frac{\mathcal{A}_{NLO}}{1+\frac{ipM}{2\pi}\mathcal{A}_{\rm LO}}, \\
\delta_{\rm NNLO} &= \frac{pM}{4\pi}\frac{\mathcal{A}_{NNLO}}{1+\frac{ipM}{2\pi}\mathcal{A}_{\rm LO}} - i\left(\frac{pM}{4\pi}\right)^2\left(\frac{\mathcal{A}_{NLO}}{1+\frac{ipM}{2\pi}\mathcal{A}_{\rm LO}}\right)^2,
\end{aligned} \tag{6.7}$$

where $\delta_{\rm LO}, \delta_{\rm NLO}, \delta_{\rm NNLO}$, are the LO, the NLO, and the NNLO phase shifts, respectively.

In the case of ${}^3S_1$ channel, there is a mixing with the ${}^3D_1$ channel, so that the S matrix becomes a 2×2 matrix,

$$S = \mathbf{1} + \frac{iMp}{2\pi}\begin{pmatrix}\mathcal{A}^{SS} & \mathcal{A}^{SD} \\ \mathcal{A}^{SD} & \mathcal{A}^{DD}\end{pmatrix} = \begin{pmatrix} e^{2i\bar\delta_{(0)}}\cos 2\bar\epsilon_1 & ie^{i\bar\delta_{(0)}+i\bar\delta_{(2)}}\sin 2\bar\epsilon_1 \\ ie^{i\bar\delta_{(0)}+i\bar\delta_{(2)}}\sin 2\bar\epsilon_1 & e^{2i\bar\delta_{(2)}}\cos 2\bar\epsilon_1\end{pmatrix}. \tag{6.8}$$

Expanding the phase shift perturbatively, we obtain,

$$\begin{aligned}
\delta_{\rm LO} =& \frac{1}{2i}\log\left(1+\frac{ipM}{2\pi}\mathcal{A}_{\rm LO}\right), \\
\delta_{\rm NLO} =& \frac{pM}{4\pi}\frac{\mathcal{A}_{NLO}}{1+\frac{ipM}{2\pi}\mathcal{A}_{\rm LO}}, \\
\delta_{\rm NNLO} =& \frac{pM}{4\pi}\frac{\mathcal{A}^{(SS)}_{NNLO}}{1+\frac{ipM}{2\pi}\mathcal{A}^{(SS)}_{\rm LO}} - i\left(\frac{pM}{4\pi}\right)^2\left[\left(\frac{\mathcal{A}^{(SS)}_{NLO}}{1+\frac{ipM}{2\pi}\mathcal{A}^{(SS)}_{\rm LO}}\right)^2 + \frac{\left(\mathcal{A}^{(SD)}_{NLO}\right)^2}{1+\frac{ipM}{2\pi}\mathcal{A}^{(SS)}_{\rm LO}}\right].
\end{aligned} \tag{6.9}$$

6.3 Spin singlet

In the literature, the expansion with the KSW power counting converges very well up to NNLO [11]. We can check that the hybrid regularization works effectively by analyzing the ${}^1S_0$ channel.

The diagrams are drawn in Fig.6.1.

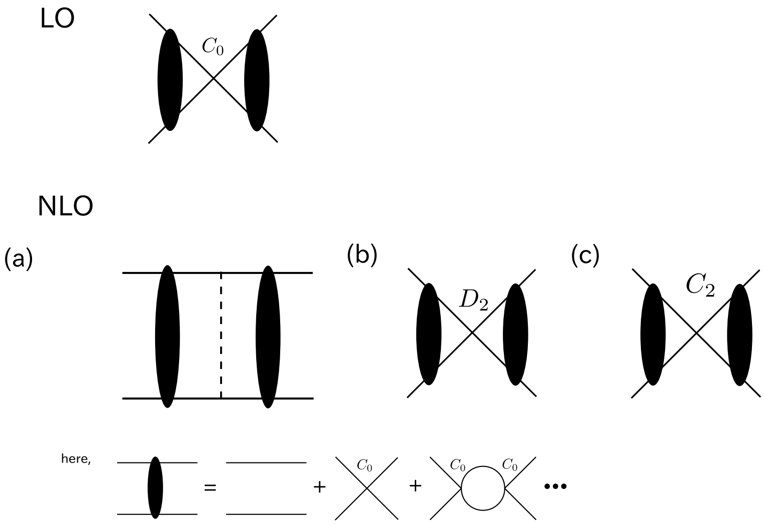

Figure 6.1: The LO and the NLO diagrams are shown above. First diagram is the LO diagram, which include only relevant operator with the coupling constant C_0. In the NLO, diagram (a) includes pion contributions. Two additional contact interactions appear in diagram (b) and (c).

6.3.1 LO analysis

The LO amplitude is given by

$$\mathcal{A}_{\mathrm{LO}} = -\frac{C_0}{1 + \frac{C_0 M}{4\pi}(\mu + ip)}. \tag{6.10}$$

It is same as that in Ref. [11]

6.3.2 NLO amplitude

The NLO amplitude is given by,

$$
\begin{aligned}
\mathcal{A}_{\rm NLO} =& -\frac{\mathcal{A}_{\rm LO}^2}{C_0^2} C_2 p^2 - \frac{\mathcal{A}_{\rm LO}^2}{C_0^2} D_2 m_\pi^2 + \frac{g^2}{2f^2}\frac{m_\pi^2}{4p^2} \log\left(1+\frac{4p^2}{m_\pi^2}\right) \\
&+ m_\pi^2 \frac{g^2}{f_0^2}\frac{M\mathcal{A}_{\rm LO}}{4\pi} Z_1 + m_\pi^2 \frac{g^2}{2f_0^2}\left(\frac{M\mathcal{A}_{\rm LO}}{4\pi}\right)^2 Z_2,
\end{aligned}
\tag{6.11}
$$

where Z_is are written below,

$$
\begin{aligned}
Z_1 =& \frac{i}{2p}\log\left(1-\frac{2ip}{m_\pi}\right) - \frac{2}{\sqrt{\pi}\lambda} - \frac{ip}{\lambda^2} + \mathcal{O}(\lambda^{-2}), \\
Z_2 =& -\left[\log\left(\frac{m_\pi - 2ip}{\lambda}\right) + \frac{\gamma_E}{2}\right] - \frac{4ip}{\sqrt{\pi}\lambda} + \frac{m_\pi^2 + 4p^2}{2\lambda^2} + \mathcal{O}(\lambda^{-2}), \\
Z_3 =& \frac{\lambda}{\sqrt{\pi}} - m_\pi + \frac{m_\pi^2}{\sqrt{\pi}\lambda} + \mathcal{O}(\lambda^{-2}).
\end{aligned}
\tag{6.12}
$$

The dependence on λ first appears at this order in the second term of Z_1.

6.3.3 NLO renormalization equations

We require that amplitudes are independent of the cutoff scale at each order:

$$
\mu\frac{\partial}{\partial\mu}\mathcal{A}_{\rm LO} = 0, \qquad \lambda\frac{\partial}{\partial\lambda}\mathcal{A}_{\rm LO} = 0, \tag{6.13}
$$

$$
\mu\frac{\partial}{\partial\mu}\left(\mathcal{A}_{\rm LO} + \mathcal{A}_{\rm NLO}\right) = 0, \qquad \lambda\frac{\partial}{\partial\lambda}\left(\mathcal{A}_{\rm LO} + \mathcal{A}_{\rm NLO}\right) = 0. \tag{6.14}
$$

From eq.(6.13), the RGEs for C_0 with respect to λ and μ are obtained as,

$$
\mu\frac{\partial}{\partial\mu}C_0 = \frac{M\mu}{4\pi}C_0^2, \qquad \lambda\frac{\partial}{\partial\lambda}C_0 = 0. \tag{6.15}
$$

At the NLO, the RGE for the coupling constant C_0 is not different from that of the LO. The RGEs for the other coupling constants, C_2 and D_2, with respect to μ are,

$$\mu\frac{\partial}{\partial\mu}C_2 = \frac{M\mu}{2\pi}C_0C_2, \tag{6.16}$$

$$\mu\frac{\partial}{\partial\mu}D_2 = \frac{M\mu}{2\pi}C_0D_2. \tag{6.17}$$

We obtain the derivatives of Z_is with respect to λ as follows:

$$\begin{aligned}
\lambda\frac{\partial}{\partial\lambda}Z_1 =& \frac{2}{\sqrt{\pi}\lambda} + \frac{2ip}{\lambda^2}, \\
\lambda\frac{\partial}{\partial\lambda}Z_2 =& 1 + \frac{4ip}{\sqrt{\pi}\lambda} - \frac{m_\pi^2 + 4p^2}{\lambda^2}, \\
\lambda\frac{\partial}{\partial\lambda}Z_3 =& \frac{\lambda}{\sqrt{\pi}} - \frac{m_\pi^2}{\sqrt{\pi}\lambda},
\end{aligned} \tag{6.18}$$

so that the RGEs for C_2 and D_2 with respect to λ are,

$$\lambda\frac{\partial}{\partial\lambda}C_2 = 0, \tag{6.19}$$

$$\lambda\frac{\partial}{\partial\lambda}D_2 = \frac{g^2}{2f^2}\left(\frac{M}{4\pi}\right)^2 C_0^2 - \frac{Mg^2}{8\pi f^2}C_0\left(1 + \frac{MC_0}{4\pi}\mu\right)\frac{4}{\sqrt{\pi}\lambda}. \tag{6.20}$$

6.3.4 NNLO

Diagrams that contribute to the NNLO amplitude are shown in Fig.6.2. In Figs.(a)∼(c), the diagrams containing a two-pion exchange are shown. We call the contribution of each diagram B_1, B_2, and B_3 respectively. In Figs.6.2(d)∼(f) the diagrams containing two one-pion exchanges are shown. We call the sum of the contributions of these diagrams B_4. In Fig.6.2(g), the diagrams containing a D_2 and containing a one-pion exchange are shown. We call the sum of the contributions of these diagrams B_5. In Fig.6.2(h), the diagrams containing C_2 vertex and a one-pion exchange are shown. We call the sum of the contributions of these diagrams B_6. The diagrams shown in Fig.6.2(i)∼(n) contain only nucleons. We call the sum of the contributions of these diagrams B_7. Including Fig.6.2(o) is equivalent to renormalize g_A^2/f^2 as explained above. The NNLO amplitude is given as the sum of all B_i's,

$$\mathcal{A}_{\mathrm{NNLO}} = \sum_{i=1}^{8} B_i. \tag{6.21}$$

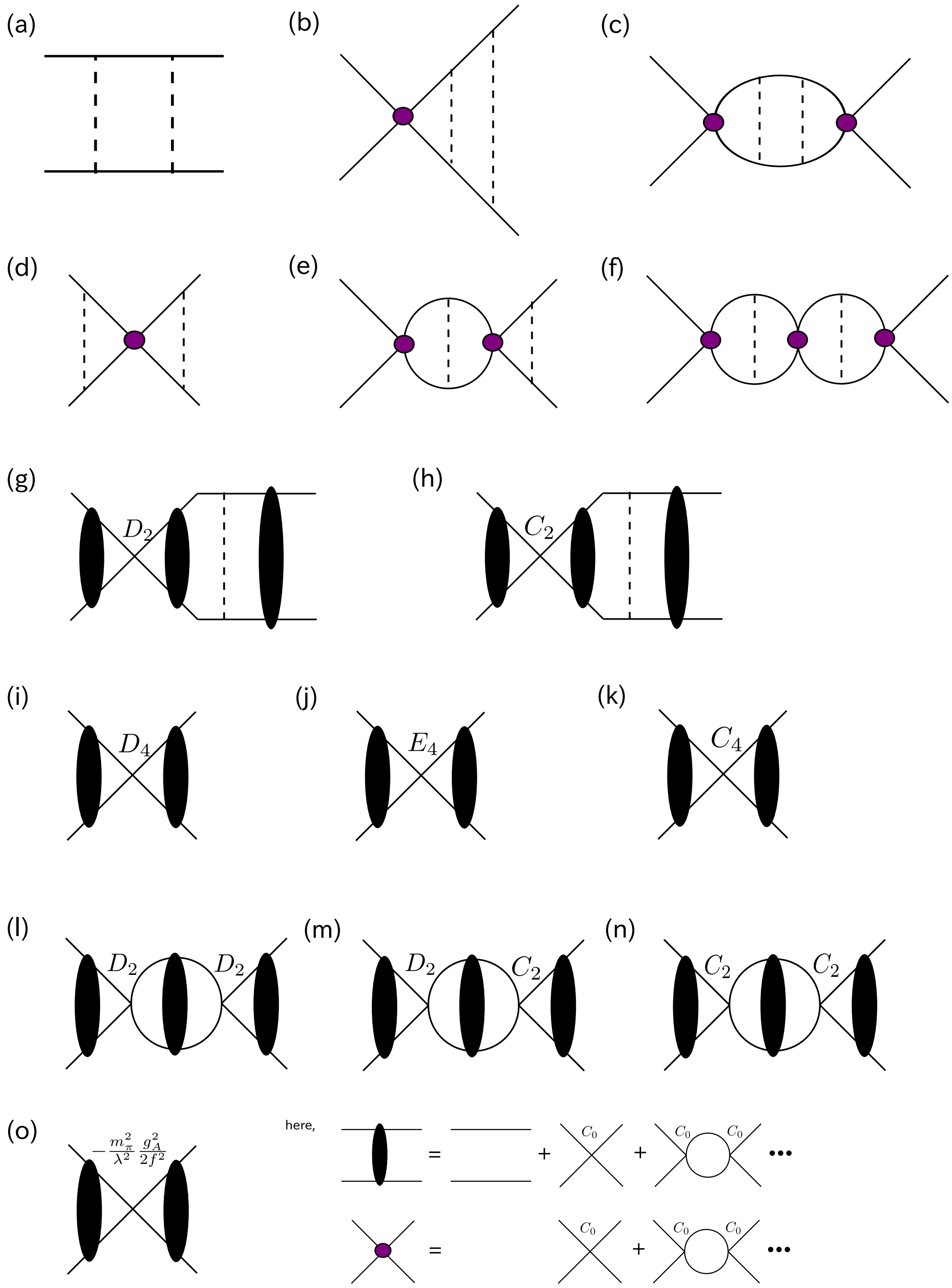

Figure 6.2: The NNLO diagrams are shown. Solid lines represent nucleons, and dashed lines pion exchanges.The coupling constants of the contact interaction is shown at each vertex.

We obtained the analytic expressions for B_i's to $\mathcal{O}\left(m/\lambda\right)$ or $\mathcal{O}\left(p/\lambda\right)$

$$
\begin{aligned}
B_1 =& \frac{M}{4\pi}\left(\frac{g^2}{2f^2}\right)^2 \frac{m_\pi^4}{4p^3} \\
& \times \left[\frac{i}{4}\log^2\left(1+\frac{4p^2}{m_\pi^2}\right) + \mathrm{ImLi}_2\left(\frac{im_\pi p - 2p^2}{m_\pi^2}\right) + \mathrm{ImLi}_2\left(\frac{2p^2 - im_\pi p}{m_\pi^2 + 4p^2}\right)\right], \\
B_2 =& -2\mathcal{A}_{\mathrm{LO}}\left(\frac{Mg^2}{8\pi f^2}\right)^2 \frac{m_\pi^4}{4p^2}\left[\frac{3}{2}\log^2\left(1-\frac{2ip}{m_\pi}\right) + 2\mathrm{Li}_2\left(-\frac{m_\pi - 2ip}{m_\pi}\right)\right. \\
& \left. +\mathrm{Li}_2\left(-\frac{m_\pi + 2ip}{m_\pi - 2ip}\right) + \frac{\pi^2}{4} + \frac{4ip}{\sqrt{\pi}\lambda}\log\left(1-\frac{2ip}{m_\pi}\right)\right], \\
B_3 =& i{\mathcal{A}_{\mathrm{LO}}}^2\frac{M}{4\pi}\left(\frac{Mg^2}{8\pi f^2}\right)^2 \frac{m_\pi^4}{p}\left\{\mathrm{Li}_2\left(-\frac{m_\pi}{m_\pi - 2ip}\right) + \frac{\pi^2}{12}\right. \\
& \left. + \frac{4ip}{\sqrt{\pi}\lambda}\left[-\frac{\gamma}{2} - \log\left(\frac{m_\pi}{\lambda}\right) - \log\left(1-\frac{2ip}{m_\pi}\right) + \left(\sqrt{2} - \sinh^{-1}(1)\right)\right]\right\}, \\
\\
B_4 =& m_\pi^4\mathcal{A}_{\mathrm{LO}}\left(\frac{Mg^2}{8\pi f^2}\right)^2\left(Z_1 + \frac{M\mathcal{A}_{\mathrm{LO}}}{4\pi}Z_2\right)^2, \\
B_5 =& -2m_\pi^4{\mathcal{A}_{\mathrm{LO}}}^2\frac{Mg^2}{8\pi f^2}\frac{D_2}{C_0^2}\left(Z_1 + \frac{M\mathcal{A}_{\mathrm{LO}}}{4\pi}Z_2\right), \\
B_6 =& -2p^2m_\pi^2{\mathcal{A}_{\mathrm{LO}}}^2\frac{Mg^2}{8\pi f^2}\frac{C_2}{C_0^2}\left(Z_1 + \frac{M\mathcal{A}_{\mathrm{LO}}}{4\pi}Z_2\right) - m_\pi^2{\mathcal{A}_{\mathrm{LO}}}^2\frac{Mg^2}{8\pi f^2}\frac{C_2}{C_0^2}Z_3, \\
B_7 =& -{\mathcal{A}_{\mathrm{LO}}}^2\frac{D_4}{C_0^2}m_\pi^4 - {\mathcal{A}_{\mathrm{LO}}}^2\frac{E_4}{C_0^2}p^2m_\pi^2 - {\mathcal{A}_{\mathrm{LO}}}^2\frac{C_4}{C_0^2}p^4, \\
& -{\mathcal{A}_{\mathrm{LO}}}^3\frac{M}{4\pi}(ip+\mu)\frac{\left(D_2m_\pi^2 + C_2p^2\right)^2}{C_0^3} \\
B_8 =& \frac{{\mathcal{A}_{\mathrm{LO}}}^2}{C_0^2}\frac{m_\pi^2}{\lambda^2}\frac{g^2}{2f^2}.
\end{aligned}
\tag{6.22}
$$

Note that the scattering amplitude for the $^3S_1$ channel is the same as the amplitude given above except for B_1, B_2, B_3 and the contribution from the S-D mixing amplitudes.

6.3.5 NNLO renormalization equations

We require that scattering amplitude is independent of the cutoff scale;

$$\mu\frac{\partial}{\partial\mu}\left(\mathcal{A}_{\rm LO}+\mathcal{A}_{\rm NLO}+\mathcal{A}_{\rm NNLO}\right)=0,\quad \lambda\frac{\partial}{\partial\lambda}\left(\mathcal{A}_{\rm LO}+\mathcal{A}_{\rm NLO}+\mathcal{A}_{\rm NNLO}\right)=0 \tag{6.23}$$

The RGEs for C_0, C_2 and D_2 with respect to μ are the same as those obtained at NLO. The RGEs for C_4, E_4 and D_4 with respect to μ are given by

$$\begin{aligned}\mu\frac{\partial}{\partial\mu}C_4 =&\frac{M\mu}{2\pi}C_0C_4+\frac{M\mu}{4\pi}C_2^2,\\ \mu\frac{\partial}{\partial\mu}E_4 =&\frac{M\mu}{2\pi}C_0E_4+\frac{M\mu}{2\pi}C_2D_2,\\ \mu\frac{\partial}{\partial\mu}D_4 =&\frac{M\mu}{2\pi}C_0D_4+\frac{M\mu}{4\pi}D_2^2.\end{aligned} \tag{6.24}$$

The RGEs for C_0,C_2 with respect to λ are also the same as those obtained at NLO, while the RGEs for D_2,C_4, E_4 and D_4 with respect to λ are

$$\begin{aligned}\lambda\frac{\partial}{\partial\lambda}D_2 =&\frac{g^2}{2f^2}\left(\frac{M}{4\pi}\right)^2C_0^2-\frac{Mg^2}{8\pi f^2}C_0\left(1+\frac{MC_0}{4\pi}\mu\right)\left(\frac{4}{\sqrt{\pi}\lambda}-\frac{4\mu}{\lambda^2}\right)\\ &-\frac{g^2}{f^2}\left(\frac{M}{4\pi}\right)^2\frac{\mu^2}{\lambda^2}C_0^2-\frac{Mg^2}{8\pi f^2}\frac{\lambda}{\sqrt{\pi}}C_2,\\ \lambda\frac{\partial}{\partial\lambda}C_4 =&0,\\ \lambda\frac{\partial}{\partial\lambda}E_4 =&\frac{g^2}{f^2}\left(\frac{M}{4\pi}\right)^2C_0C_2-\frac{Mg^2}{8\pi f^2}\frac{4C_2}{\sqrt{\pi}\lambda}\left(1+2\frac{MC_0}{4\pi}\mu\right)-\frac{g^2}{2f^2}\left(\frac{M}{4\pi}\right)^2\frac{C_0^2}{\lambda^2},\\ \lambda\frac{\partial}{\partial\lambda}D_4 =&\frac{g^2}{f^2}\left(\frac{M}{4\pi}\right)^2C_0D_2+\frac{M}{4\pi}\left(\frac{Mg^2}{8\pi f^2}\right)^2\frac{4C_0^2}{\sqrt{\pi}\lambda}\left(\sqrt{2}-\sinh^{-1}(1)\right)\\ &-\frac{Mg^2}{8\pi f^2}\frac{4}{\sqrt{\pi}\lambda}\left(1+2\frac{MC_0}{4\pi}\mu\right)D_2-\frac{g^2}{2f^2}\left(\frac{M}{4\pi}\right)^2\frac{C_0^2}{\lambda^2}+\frac{Mg^2}{8\pi f^2}\frac{C_2}{\sqrt{\pi}\lambda}.\end{aligned} \tag{6.25}$$

Note that, the second term of RGE of D_2 vanishes in the case of $\mu=\lambda/\sqrt{\pi}$.

6.3.6 Phase shift fitting for $^1S_0$

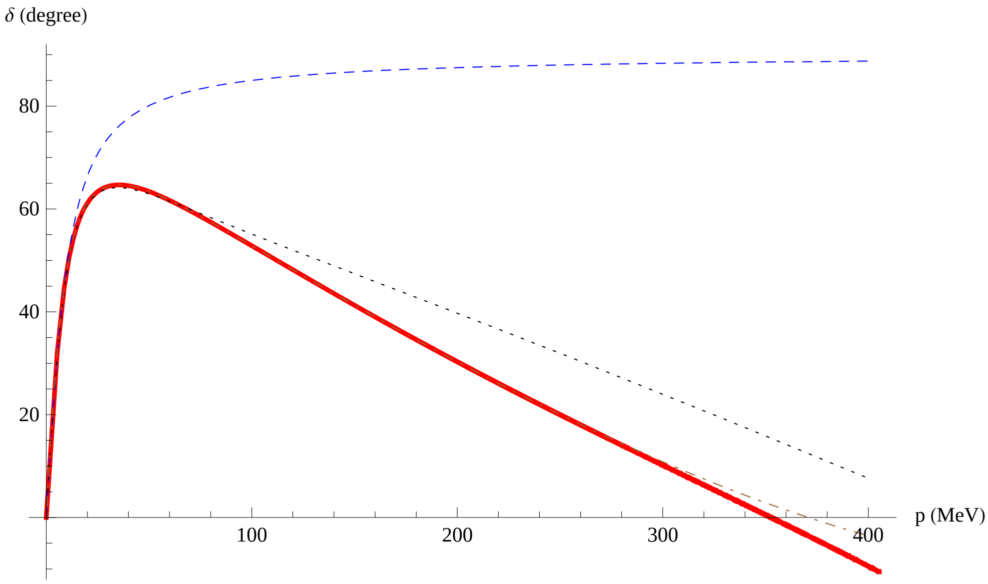

Figure 6.3: Our result of the $^1S_0$ phase shift for NN scattering. Solid line is the Nijmegen data for np scattering.The dashed, dotted, and dashed-dotted lines are the LO, the NLO, and the NNLO results respectively.

The results for $^1S_0$ phase shifts are shown in Fig.6.3. The fitted values of the dimensionless coupling constants are given below:

$$\begin{aligned}
\text{LO}: &\quad \hat{C}_0 = -0.963; && && \quad (6.26)\\
\text{NLO}: &\quad \hat{C}_0 = -0.957; &\hat{C}_2 = 0.744; &&\hat{D}_2 = 0.639; \quad (6.27)\\
\text{NNLO}: &\quad \hat{C}_0 = -0.957; &\hat{C}_2 = 0.454; &&\hat{D}_2 = 0.676; \quad (6.28)\\
&\quad \hat{C}_4 = -0.273; &\hat{E}_4 = 0.166; &&\hat{D}_4 = 0.695..
\end{aligned}$$

Here dimensionless couplings are defined as,

$$\begin{aligned}
\hat{C}_0 &= \frac{M\mu}{4\pi} C_0, \qquad \hat{C}_2 = \frac{M\mu^3}{4\pi} C_2, \qquad \hat{D}_2 = \frac{M\mu^3}{4\pi} D_2,\\
\hat{C}_4 &= \frac{M\mu^5}{4\pi} C_4, \qquad \hat{E}_4 = \frac{M\mu^5}{4\pi} E_4, \qquad \hat{D}_4 = \frac{M\mu^5}{4\pi} D_4. \qquad (6.29)
\end{aligned}$$

Note that the sizes of all dimensionless couplings are natural. Note also that the values do not change very much as higher order contributions are included. These facts are important because it implies that the power counting is consistent. Because the power counting tells us that NLO couplings are smaller than the LO coupling, it is clear that there are inconsistency if NLO couplings are bigger than LO coupling. Furthermore it is needed for a systematic calculation that the variation of coupling constants that arise when we consider the higher order has to be small.

6.4 Spin triplet

In this section, we show the calculation of the $^3S_1$ phase shifts. Because the tensor type contributions are included in this channel, we need to know corresponding S-OPE.

6.4.1 Calculation of amplitudes

The LO and NLO amplitudes are the same as in case of singlet so they can be written as in eqs.(6.10) and (6.11) respectively. The scalar part of the NNLO contributions is the same as in the $^3S_1$ channel.

Tensor contributions are included in the diagrams Fig.6.2(a)∼(c). The sum of their contributions is written as

$$\begin{aligned}\mathcal{A}^{tensor}_{\mathrm{NNLO}} =& 6M\left(\frac{g_A^2}{2f^2}\right)^2(\mathrm{Box}_1+\mathrm{Box}_2)\\&+24\mathcal{A}_{\mathrm{LO}}\left(\frac{Mg_A^2}{2f^2}\right)^2B_2^T+12\mathcal{A}_{\mathrm{LO}}^2M\left(\frac{Mg_A^2}{2f^2}\right)^2B_3^T,\end{aligned} \tag{6.30}$$

where Box_1, Box_2, B_2^T, and B_3^T are given in eqs(A.66), (A.67), (A.38), and (A.39) respectively.

6.5 Phase shift fitting for $^3S_1$

We show the calculation of the scattering phase shifts by using the fitted values of the coupling constants for the $^3S_1$ channel. There is a problem that the calculated phase shift is not real, so we fit the real part of phase shift.

The coupling constants obtained by fitting the calculated phase shift to the data are,

$$\begin{aligned}
\mathrm{LO}: &\quad \hat{C}_0=-1.19; && && (6.31)\\
\mathrm{NLO}: &\quad \hat{C}_0=-1.26; &\quad \hat{C}_2=1.71; &\quad \hat{D}_2=0.891; && (6.32)\\
\mathrm{NNLO}: &\quad \hat{C}_0=-1.50; &\quad \hat{C}_2=3.13; &\quad \hat{D}_2=0.195; && (6.33)\\
&\quad \hat{C}_4=-26.6; &\quad \hat{E}_4=-1.25; &\quad \hat{D}_4=23.9;.
\end{aligned}$$

The sizes of two of coupling constants are not natural. It may be because of existence of imaginary part in phase shift. This problem comes from the

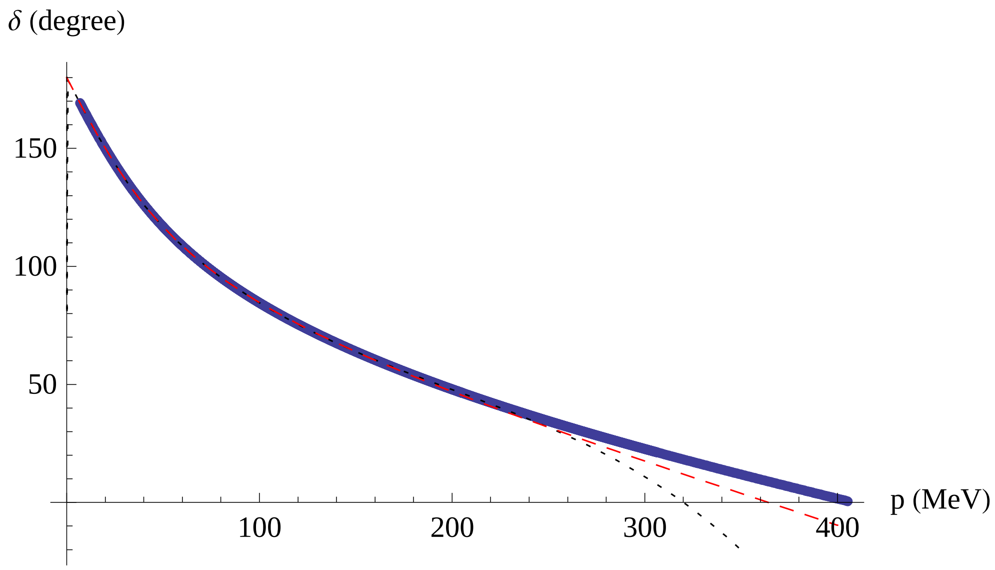

Figure 6.4: Our result for the $^3S_1$ phase shift for NN scattering. Solid line is the Nijmegen data for np scattering.The dashed, dotted, and dashed-dotted lines are the LO, the NLO, and the NNLO results respectively.

fact that we are still not able to consistently extract the S-OPE part in our calculation. This reflects the large change of the coupling constant $\tilde{C}_0$. Our present calculation however implies that the separation of the S-OPE from L-OPE works at least in the real part, as shown in Fig.(6.4), where the breakdown shown by Fleming et al. does not arise. In the NNLO calculation by Fleming et al., there is a linearly rising contribution $p\ \tan^{-1}(2p/m_\pi)$ for large p which comes from the tensor part of the two-pion-exchange box diagram in the $^3S_1$ channel. The term is also present in our calculation. but we have an additional term so that only the combination $p\ \tan^{-1}(2p/m_\pi) - 4p^2/(\sqrt{\pi}\lambda))$ appears. This additional term suppresses the linear increase for large p.

Chapter 7

Summary

In this thesis, we analyze the nucleon-nucleon scattering in the S-waves at low energies based on the power counting which is determined by a Wilsonian RGE analysis [19]. We show that the phase shift of the ${}^3S_1$ channel converges at NNLO to the contrary to the previous calculation done by Fleming et al. with the KSW power counting [8,9], despite the fact that our power counting is very similar to the KSW power counting.

The difference between the analysis by Fleming et al. and ours lies in treatment of pion contributions. In their calculations, pion contribution are perturbative. In our analysis, on the other hand, pion contributions are divided into two parts, S-OPE and L-OPE. A part of S-OPE is treated as non-perturbative while the L-OPE is perturbative.

The separation of pion contributions into S-OPE and L-OPE is done by introducing a separation scale. We employ a hybrid regularization: diagrams without pion exchanges are regularized with PDS, while diagrams containing pion exchanges are regularized with a Gaussian damping factor. The scales μ in PDS and λ in the regularization with GDF play essentially the same role of the separation scale.

In the ${}^1S_0$ channel, we got similar results to those obtained by Fleming et al. [11]. We obtain the result that all the coupling constants has natural size. At this channel, we success in calculation of phase shift.

In the ${}^3S_1$ channel, our calculation has an unitarity problem: the phase shift has relatively large imaginary part which can not be explained by numerical error. This probably reflects that our procedure of extracting the S-OPE for the tensor part is not sufficient. We however expect that the absence of the linearly rising contribution in the real part is a general feature in the hybrid regularization.

By introducing two schemes to integrate loop diagrams, we can derives convergent expansion for the phase shift in the ${}^3S_1$ channel relatively simply.

We can get natural size of values of coupling constants and they do not change very much when higher order terms are included. It is very important. If the power counting is correct, our ordering of the contributions is correct, that is, the higher order terms one includes the smaller the effects one gets. If the power counting is not correct, the best fitted values of the coupling constants for wrongly ordered operators would be very small or very large to compensate the wrong ordering. In addition, when higher order contributions are added, they change drastically because they do not need to compensate any more. Our results about the best fitted values of coupling constants implies that our power counting is actually correct.

We have not yet obtained the RGEs for the ${}^3S_1$ channel. It is very important to obtain them and solve them to check the consistency of the approach. It is left as a future work.

Acknowledgment

The author would like to thank Koji Harada, Hirofumi Kubo, and Yuki Yamamoto for helpful discussion.

Appendix A

Integral formulae

A.1 Integral of box diagram

In this subsection, I explain a series of the most complicated integrals. These are appear in the box diagram.

First of all, we consider the integral,

$$
\begin{aligned}
&\int d\left(\cos\theta\right)\int \frac{d^3k}{(2\pi)^3}\frac{1}{\left(k^2+2\mathbf{k}\cdot\mathbf{p}\right)\left(k^2+m_\pi^2\right)\left(\left(\mathbf{k}-\mathbf{q}\right)^2+m_\pi^2\right)}\\
=&\frac{1}{8\pi p^3}\\
&\times\left[\frac{i}{4}\log^2\left(1+\frac{4p^2}{m_\pi^2}\right)+\mathrm{Im}\ \mathrm{Li}_2\left(\frac{2p^2-ipm_\pi}{m_\pi^2+4p^2}\right)+\mathrm{Im}\ \mathrm{Li}_2\left(\frac{-2p^2+ipm_\pi}{m_\pi^2}\right)\right].
\end{aligned}
\tag{A.1}
$$

Here,

$$
\begin{aligned}
\mathbf{q}=&\mathbf{p}'-\mathbf{p},\\
\mathbf{p}^2=\mathbf{p}'^2=p^2,&\quad \mathbf{p}\cdot\mathbf{p}'=p^2\cos\theta,\\
\mathbf{q}^2=2p^2(1-\cos\theta),&\quad \mathbf{p}\cdot\mathbf{q}=-p^2(1-\cos\theta).
\end{aligned}
\tag{A.2}
$$

We define

$$
I\left(\cos\theta\right)=\int\frac{d^3k}{(2\pi)^3}\frac{1}{\left(k^2+2\mathbf{k}\cdot\mathbf{p}\right)\left(k^2+m_\pi^2\right)\left(\left(\mathbf{k}-\mathbf{q}\right)^2+m_\pi^2\right)},\tag{A.3}
$$

$$
\begin{aligned}
a =& |\mathbf{p} + \mathbf{q}x| \ , \\
\alpha =& (\mathbf{p} + \mathbf{q}x)^2 - p^2 \, , \\
\beta =& q^2 x(1-x) + m_\pi^2 \, .
\end{aligned} \tag{A.4}
$$

They satisfy the following relations,

$$
\begin{aligned}
\alpha + \beta =& m_\pi^2 \, , \\
a^2 - \alpha =& p^2 \, .
\end{aligned} \tag{A.5}
$$

So $I(\cos\theta)$ may be calculated as

$$
\begin{aligned}
I(\cos\theta) =& \int_0^1 dx \int \frac{d^3k}{(2\pi)^3} \frac{1}{(k^2 + 2\mathbf{k}\cdot\mathbf{p})\,(k^2 - 2\mathbf{k}\cdot\mathbf{p}x + q^2x + m_\pi^2)} \\
=& \int_0^1 dx \int \frac{d^3k}{(2\pi)^3} \frac{1}{\left[(\mathbf{k} + \mathbf{p} + \mathbf{q}x)^2 - p^2\right] [k^2 + q^2x(1-x) + m_\pi^2]^2} \\
=& \int_0^1 dx \int \frac{d^3k}{(2\pi)^3} \frac{1}{(k^2 + 2ak\cos\theta_k + \alpha)\,(k^2 + \beta^2)^2} \\
=& \frac{1}{4\pi^2} \int_0^1 dx \int_0^\infty dk \int_{-1}^1 d\left(\cos\theta_k\right) \frac{k^2}{(k^2 + 2ak\cos\theta_k + \alpha)\,(k^2 + \beta^2)^2} \\
=& \frac{1}{8\pi^2} \int_0^1 dx \int_0^\infty dk \frac{k}{a\,(k^2 + \beta^2)^2} \log\left(\frac{k^2 + 2ak + \alpha}{k^2 - 2ak + \alpha}\right) \\
=& -\frac{1}{16\pi^2} \int_0^1 dx \frac{1}{a} \int_0^\infty dk \left[\frac{d}{dk}\left(\frac{1}{k^2 + \beta^2}\right)\right] \log\left(\frac{k^2 + 2ak + \alpha}{k^2 - 2ak + \alpha}\right) \\
=& \frac{1}{8\pi^2} \int_0^1 dx \frac{1}{a} \int_0^\infty dk \frac{1}{k^2 + \beta^2} \left(\frac{k + a}{k^2 + 2ak + \alpha} - \frac{k - a}{k^2 - 2ak + \alpha}\right) \\
=& -\frac{1}{4\pi^2} \int_0^1 dx \frac{1}{a} \int_0^\infty dk \frac{k^2 - \alpha}{(k^2 + \beta^2)\,(k^2 + 2ak + \alpha)\,(k^2 - 2ak + \alpha)} \\
=& -\frac{1}{8\pi^2} \int_0^1 dx \frac{1}{a} \int_{-\infty}^\infty dk \frac{k^2 - \alpha}{(k^2 + \beta^2)\,(k^2 + 2ak + \alpha)\,(k^2 - 2ak + \alpha)} .
\end{aligned} \tag{A.6}
$$

The integrand has six poles in the complex k plane,

$$\begin{aligned}
&\pm i\sqrt{\beta}\,,\\
&\lambda_1 = a + p + i\epsilon\,,\\
&\lambda_2 = a - p - i\epsilon\,,\\
&\lambda_3 = -a + p + i\epsilon\,,\\
&\lambda_4 = -a - p - i\epsilon\,.
\end{aligned} \tag{A.7}$$

Among them, $i\sqrt{\beta}, \lambda_1, \lambda_3$ are in the upper half plane. We perform the k-integral using the residue theorem and write $I\left(\cos\theta\right)$, $I_1\left(\cos\theta\right)$, $I_2\left(\cos\theta\right)$: $I(\cos\theta) = I_1(\cos\theta) + I_2(\cos\theta)$.

$$\begin{aligned}
I_1\left(\cos\theta\right) &= -\frac{i}{4\pi}\int_0^1 dx\left[\frac{\lambda_1^2-\alpha}{\left(\lambda_1^2+\beta\right)\left(\lambda_1-\lambda_2\right)\left(\lambda_1-\lambda_3\right)\left(\lambda_1-\lambda_4\right)}\right.\\
&\qquad\qquad\left.+\frac{\lambda_3^2-\alpha}{\left(\lambda_3^2+\beta\right)\left(\lambda_3-\lambda_1\right)\left(\lambda_3-\lambda_2\right)\left(\lambda_3-\lambda_4\right)}\right]\\
&= -\frac{i}{4\pi}\int_0^1 dx\frac{1}{4a}\left[\frac{1}{\left(a+p\right)^2+\beta}-\frac{1}{\left(a-p\right)^2+\beta}\right]\\
&= \frac{ip}{4\pi}\int_0^1 dx\frac{1}{\left[\left(a+p\right)^2+\beta\right]\left[\left(\left(a-p\right)^2+\beta\right]}\\
&= \frac{ip}{4\pi}\int_0^1 dx\frac{1}{\left(a^2+p^2+\beta\right)^2-4a^2p^2}\\
&= \frac{ip}{4\pi}\int_0^1 dx\frac{1}{\left(m_\pi^2+2p^2\right)^2-4\left[p^2-q^2x(1-x)\right]p^2}\\
&= \frac{ip}{4\pi}\int_0^1 dx\frac{1}{m_\pi^2\left(m_\pi^2+4p^2\right)+4p^2q^2x(1-x)}\\
&= \frac{i}{16\pi pq^2}\int_0^1 dx\frac{1}{b+x(1-x)}\\
&= \frac{i}{16\pi pq^2}\left[\frac{1}{\sqrt{1+4b}}\log\left|\frac{-2x+1-\sqrt{1+4b}}{-2x+1+\sqrt{1+4b}}\right|\right]_0^1\\
&= \frac{i}{8\pi pq^2\sqrt{1+4b}}\log\frac{\sqrt{1+4b}+1}{\sqrt{1+4b}-1}\\
&= \frac{i}{16\pi p^3(1-\cos\theta)\sqrt{1+4b}}\log\frac{\sqrt{1+4b}+1}{\sqrt{1+4b}-1}.
\end{aligned} \tag{A.8}$$

where b and c are introduced as

$$b = \frac{m_\pi^2 \left(m_\pi^2 + 4p^2\right)}{4p^2 q^2} = \frac{c}{4\left(1-\cos\theta\right)}, \tag{A.9}$$

$$c = \frac{m_\pi^2 \left(m_\pi^2 + 4p^2\right)}{2p^4}. \tag{A.10}$$

By making a change of variable

$$t = \frac{1}{\sqrt{1+4b}} = \frac{1}{\sqrt{1+\frac{c}{1-\cos\theta}}}, \tag{A.11}$$

we have

$$\begin{aligned}\int_{-1}^{1} d\left(\cos\theta\right) I_1(\cos\theta) =& \frac{i}{8\pi p^3}\int_0^{\frac{1}{1+\frac{c}{2}}} dt \frac{1}{1-t^2}\log\left(\frac{1+t}{1-t}\right) \\ =& \frac{i}{32\pi p^3}\log^2\left(1+\frac{4p^2}{m_\pi^2}\right).\end{aligned} \tag{A.12}$$

Next we calculate $I_2(\cos\theta)$

$$
\begin{aligned}
I_2\left(\cos\theta\right) =& \frac{1}{8\pi}\int_0^1 dx \frac{\alpha+\beta}{\sqrt{\beta}(\alpha-\beta+2i\alpha\sqrt{\beta})(\alpha-\beta-2i\alpha\sqrt{\beta})} \\
=& \frac{1}{8\pi}\int_0^1 dx \frac{\alpha+\beta}{\sqrt{\beta}\left(m_\pi^2+4p^2\beta\right)} \\
=& \frac{1}{8\pi}\int_0^1 \frac{m_\pi^2}{\sqrt{q^2x(1-x)+m_\pi^2}\left[m_\pi^4+4p^2(q^2x(1-x)+m_\pi^2)\right]} \\
=& \frac{m_\pi^2}{8\pi q}\int_{-1/f}^{1/f} \frac{1}{\sqrt{1-y^2}\left[m_\pi^4+4p^2q^2f^2(1-y^2)\right]} \\
=& \frac{m_\pi^2}{8\pi p^2q^3f^2}\int_0^{1/f} \frac{1}{\sqrt{1-y^2}\left(g^2-y^2\right)} \\
=& \frac{1}{4\pi q\sqrt{p^2(q^2+4m_\pi^2)+m_\pi^4}}\left(\frac{\pi}{2}-\arctan\frac{2\sqrt{p^2(q^2+4m_\pi^2)+m_\pi^4}}{mq}\right) \\
=& \frac{1}{4\pi pq^2\sqrt{1+4b}}\arctan\frac{m_\pi}{2p\sqrt{1+4b}} \\
=& \frac{1}{8\pi p^3(1-\cos\theta)\sqrt{1+4b}}\mathrm{Im}\ \ln\left(1+i\frac{m_\pi}{2p\sqrt{1+4b}}\right),
\end{aligned}
\tag{A.13}
$$

where we introduce x, f, and g as

$$
\begin{aligned}
x =& \frac{fy+1}{2}, \\
f =& \frac{\sqrt{q^2+4m_\pi^2}}{q} = \sqrt{1+\frac{4m_\pi^2}{q^2}} = \sqrt{1+\frac{2m_\pi^2}{p^2(1-\cos\theta)}}, \\
g =& \sqrt{1+\frac{m_\pi^2}{p^2q^2f^2}} = \sqrt{1+\frac{m_\pi^2}{p^2(q^2+4m_\pi^2)}}.
\end{aligned}
\tag{A.14}
$$

Integrating $I_2(\cos\theta)$ over $\cos\theta$, we get

$$
\begin{aligned}
&\int_{-1}^{1} d(\cos\theta) I_2(\cos\theta) \\
=&\frac{1}{4\pi p^3}\mathrm{Im}\int^{1/\sqrt{1+c/2}} dt \frac{1}{1-t^2}\log\left(1+i\frac{m_\pi}{2p}t\right) \\
=&\frac{1}{4\pi p^3}\mathrm{Im}\left[-\log(1+iv)\log(1-u)+\log(1-iv)\log(1+u)\right. \\
&\left.+\mathrm{Li}_2\left(\frac{1-u}{1+1/iv}\right)-\mathrm{Li}_2\left(\frac{iv}{1+iv}\right)-\mathrm{Li}_2\left(\frac{1-u}{1-1/iv}\right)+\mathrm{Li}_2\left(\frac{iv}{1-iv}\right)\right],
\end{aligned}
\tag{A.15}
$$

where the dilogarithm function, Li_2, is defined as

$$
\mathrm{Li}_2(z) = -\int_0^z dt\frac{\log(1-t)}{t}, \tag{A.16}
$$

and u and v are defined as,

$$
u = \frac{1}{1+c/2} = \frac{2p^2}{m_\pi^2+2p^2}, \quad v = \frac{m_\pi}{2p}. \tag{A.17}
$$

There are several useful formulae for the dilogarithm function. One of them is

$$
\begin{aligned}
\mathrm{Li}_2(1-z) =&\mathrm{Li}_2(z)+\frac{\pi^2}{6}-\log(1-z)\log(z)=\sum_{k=1}^{\infty}\frac{z^k}{k^2}, \\
\mathrm{Li}_2\left(\frac{1}{z}\right) =&-\mathrm{Li}_2(z)+\frac{\pi^2}{6}-\log(z)\log(1-z).
\end{aligned}
\tag{A.18}
$$

Let us explain other integrals. The first one involves $I_1(\cos\theta)$,

$$\int_{-1}^{1}(1-\cos\theta)^n I_1(\cos\theta) \equiv \frac{ic^n}{8\pi p^3}F_n \tag{A.19}$$

Integrating by parts, this can be written as

$$F_n = \frac{m_\pi^2+2p^2}{4np^2}\left(\frac{2}{c}\right)^n \log\left(1+\frac{4p^2}{m_\pi^2}\right) - \frac{2n-1}{2n}F_{n-1} - \frac{1}{n}G_n, \tag{A.20}$$

where

$$G_n = \int_0^{1/\sqrt{1+c/2}} dt \frac{t^{2n-1}}{(1-t^2)^{n+1}}. \tag{A.21}$$

We obtain a recursion relation for G_n,

$$G_n = \frac{(m_\pi^2+2p^2)^2}{8np^4}\left(\frac{2}{c}\right)^n - \frac{n-1}{n}G_{n-1}. \tag{A.22}$$

From eq.(), F_0 is obtained easily.

$$F_0 = \frac{1}{4}\log^2\left(1+\frac{4p^2}{m_\pi^2}\right). \tag{A.23}$$

For $n=1$, we have

$$G_1 = \frac{1}{c}. \tag{A.24}$$

The recursion relations determine all the F_n's and G_n's.

Next we consider the integral involving $I_2(\cos\theta)$ given below:

$$\int_{-1}^{1}(1-\cos\theta)^n I_2(\cos\theta) \equiv \frac{c^n}{4\pi p^3}X_n. \tag{A.25}$$

As in the case of F_n, we derive recursion relation,

$$\begin{aligned} X_n =& \mathrm{Im}\int_0^{1/\sqrt{1+c/2}} dt \frac{t^{2n}}{(1-t^2)^{n+1}} \log\left(1+\frac{it}{2v}\right) \\ =& \frac{m_\pi^2+2p^2}{4np^2}\left(\frac{2}{c}\right)^n \arctan\frac{pm}{m_\pi^2+2p^2} - \frac{2n-1}{2n}X_{n-1} - \frac{m_\pi}{4np}Y_n, \end{aligned} \tag{A.26}$$

where

$$Y_n = \mathrm{Im} \int_0^{1/\sqrt{1+c/2}} dt \frac{it^{2n-1}}{(1-t^2)^n(1+it/2v)}. \tag{A.27}$$

We also derive a recursion relation for Y_n,

$$Y_n = \frac{2m_\pi^2}{p^2 c} \left(G_{n-1} - Y_{n-1} \right). \tag{A.28}$$

We can calculate X_0 and Y_1 as follows,

$$\begin{aligned} X_0 =& \frac{1}{2} \mathrm{Im} \left[2 \log (1 - 2iv) \log \frac{1+2v^2+iv}{1+2v^2} \right. \\ & - \mathrm{Li}_2 \left(\frac{2v(1+2v^2+iv)}{(2v+i)(1+2v^2)} \right) + \mathrm{Li}_2 \left(\frac{2v(1+2v^2+iv)}{(2v-i)(1+2v^2)} \right) \\ & \left. + \mathrm{Li}_2 \left(\frac{2v}{2v+i} \right) - \mathrm{Li}_2 \left(\frac{2v}{2v-i} \right) \right], \end{aligned} \tag{A.29}$$

$$Y_1 = \frac{m_\pi^2}{p^2 c} \log \left(1 + \frac{p^2}{m_\pi^2} \right), \tag{A.30}$$

so that we can determine all the X_n's and Y_n's recursively.

The results in case of $n = 1$ and $n = 2$ as,

$$\int_{-1}^{1} d\cos\theta (1 - \cos\theta) I(\cos\theta) = \mathrm{Box}_1, \tag{A.31}$$

$$\int_{-1}^{1} d\cos\theta (1 - \cos\theta)^2 I(\cos\theta) = \mathrm{Box}_2, \tag{A.32}$$

are given in eqs.(A.66) and eqs.(A.67).

A.2 Method of decomposition of the tensor part

There are integrals including inner products in the integrand which appear in the calculations of the diagrams involving tensor forces. We need to express such integrals in terms of integrals which do not include inner products. To do so, we decompose them as partial fractions. The tensorial structure of the integrals are also important in rewriting them. For example, the result of the following integral is a second-rank symmetric tensor of l, and therefore may be written as a sum of δ_{ij} and $l_i l_j$,

$$\int \frac{d^3k}{(2\pi)^3} \frac{k_i k_j e^{-\frac{\mathbf{k}^2}{\lambda^2}}}{\left[(\mathbf{k}+\mathbf{l})^2 - p^2 - i\epsilon\right]\left(\mathbf{k}^2 + m_\pi^2\right)} = \delta_{ij} g'(\mathbf{l}, p) + l_i l_j h'(\mathbf{l}, p)\,. \tag{A.33}$$

Multiplying δ_{ij} and $l_i l_j$ both sides of the equation,

$$\begin{aligned} ng'(\mathbf{l}, p) + \mathbf{l}^2 h'(\mathbf{l}, p) &= \int \frac{d^3k}{(2\pi)^3} \frac{\mathbf{k}^2 e^{-\frac{\mathbf{k}^2}{\lambda^2}}}{\left[(\mathbf{k}+\mathbf{l})^2 - p^2 - i\epsilon\right]\left(\mathbf{k}^2 + m_\pi^2\right)} \\ &= H_0'(\mathbf{l}, p) - m_\pi^2 H_2(\mathbf{l}, p)\,, \end{aligned} \tag{A.34}$$

$$\begin{aligned} \mathbf{l}^2 g'(\mathbf{l}, p) + \mathbf{l}^4 h'(\mathbf{l}, p) &= \int \frac{d^3k}{(2\pi)^3} \frac{(\mathbf{k}\cdot\mathbf{l})^2 e^{-\frac{\mathbf{k}^2}{\lambda^2}}}{\left[(\mathbf{k}+\mathbf{l})^2 - p^2 - i\epsilon\right]\left(\mathbf{k}^2 + m_\pi^2\right)} \\ &= -\frac{1}{2} X_2' + \frac{\Delta}{4} X_1' + \frac{\Delta^2}{4} H_2(\mathbf{l}, p)\,, \end{aligned} \tag{A.35}$$

where the notation $\Delta = \mathbf{l}^2 - p^2 - m_\pi^2$ is introduced and the integrals which appear in the above equation are given by equation are

$$\begin{aligned} H_0'(\mathbf{l}, p) &= \int \frac{d^3k}{(2\pi)^3} \frac{e^{-\frac{\mathbf{k}^2}{\lambda^2}}}{(\mathbf{k}+\mathbf{l})^2 - p^2 - i\epsilon}, \\ X_1' &= \int \frac{d^3k}{(2\pi)^3} \left(\frac{1}{(\mathbf{k}+\mathbf{l})^2 - p^2 - i\epsilon} - \frac{1}{\mathbf{k}^2 + m_\pi^2} \right) e^{-\frac{\mathbf{k}^2}{\lambda^2}}, \\ X_2' &= \int \frac{d^3k}{(2\pi)^3} \frac{(\mathbf{k}\cdot\mathbf{l})\, e^{-\frac{\mathbf{k}^2}{\lambda^2}}}{(\mathbf{k}+\mathbf{l})^2 - p^2 - i\epsilon}, \\ H_2'(\mathbf{l}, p) &= \int \frac{d^3k}{(2\pi)^3} \frac{e^{-\frac{\mathbf{k}^2}{\lambda^2}}}{\left[(\mathbf{k}+\mathbf{l})^2 - p^2 - i\epsilon\right]\left(\mathbf{k}^2 + m_\pi^2\right)}. \end{aligned} \tag{A.36}$$

Solving eqs.(A.34) and (A.35), we obtain g' and h', in terms of the integrals which do not include inner products in the integrands,

$$
\begin{aligned}
g'(\mathbf{l}, p) =& \frac{1}{n-1}\left(H_0' - m_\pi^2 H_2(\mathbf{l}, p)\right) \\
&+ \frac{1}{2(n-1)\mathbf{l}^2}\left\{X_2' - \frac{\Delta}{2}\left[X_1 + \Delta H_2(\mathbf{l}, p)\right]\right\}, \\
h'(\mathbf{l}, p) =& -\frac{1}{(n-1)\mathbf{l}^2}\left(H_0' - m_\pi^2 H_2(\mathbf{l}, p)\right) \\
&- \frac{n}{2(n-1)\mathbf{l}^4}\left\{X_2' - \frac{\Delta}{2}\left[X_1 + \Delta H_2(\mathbf{l}, p)\right]\right\}.
\end{aligned}
\tag{A.37}
$$

Substituting g' and h' back into eq.(A.37), we obtain a decomposition of the tensor integral, eq.(A.33).

A.3 Tensor integrals

In this section, we show how to calculate the tensor part of the two-loop triangle diagram shown in Fig.6.2(b) and the three-loop diagram shown in Fig.6.2(c). Let us consider the integral corresponding the two-loop diagram first:

$$
\begin{aligned}
B_2^T =& \int \frac{d^3\mathbf{k}d^3\mathbf{l}}{(2\pi)^6} \frac{\left\{[(\mathbf{k}-\mathbf{l})\cdot(\mathbf{l}-\mathbf{p}')]^2 - \frac{1}{n}(\mathbf{k}-\mathbf{l})^2(\mathbf{l}-\mathbf{p}')^2\right\} e^{-\frac{(\mathbf{k}-\mathbf{l})^2}{\lambda^2}} e^{-\frac{(\mathbf{l}-\mathbf{p}')^2}{\lambda^2}}}{(\mathbf{k}^2-p^2-i\epsilon)(\mathbf{l}^2-p^2-i\epsilon)\left[(\mathbf{k}-\mathbf{l})^2+m_\pi^2\right]\left[(\mathbf{l}-\mathbf{p}')^2+m_\pi^2\right]} \\
=& \frac{(p^2+m_\pi^2)^2(-3nm_\pi^4+6m_\pi^2p^2(n-4)+10np^4)}{48(n-1)p^4}U_1 + \frac{m_\pi^4\left(nm_\pi^2+4p^2\right)^2}{16(n-1)np^4}V_7 \\
&+ \frac{2m_\pi^2(12-7n)-7np^2}{48(n-1)}U_3 - \frac{m_\pi^2\left(nm_\pi^2+4p^2\right)\left(nm_\pi^2+2(2-n)p^2\right)}{16(n-1)np^4}V_2' \\
&+ \frac{(m_\pi^2+p^2)(3nm_\pi^4+3m_\pi^2p^2(8-3n)+(12-13n)p^4)}{48(n-1)p^4}U_4' - \frac{n(X_1)'^2}{24(n-1)} \\
&+ \frac{3nm_\pi^4-6(n-2)m_\pi^2p^2+2(6-5n)p^4}{48(n-1)p^4}(U_9X_1)' + \frac{(p^2+m_\pi^2)}{4(n-1)p^2}(U_9H_0)' \\
&+ \frac{(m_\pi^2+p^2)^2}{4(n-1)p^2}(U_2H_0)' + \frac{(m_\pi^2+p^2)(3nm_\pi^4-3m_\pi^2p^2(n-4)-7np^4)}{48(n-1)p^4}(U_2X_1)' \\
&- \frac{m_\pi^2\left(nm_\pi^2+4p^2\right)}{4(n-1)np^2}(V_1H_0)' - \frac{m_\pi^4(nm_\pi^2+4p^2)}{16(n-1)p^4}(V_1X_1)' + \frac{1}{4}(H_0X_1)' \\
&- \frac{n-2}{4(n-1)}\xi X_1H_0 + \frac{n-4}{4n}H_0'^2 + \frac{nm_\pi^2-2(n-2)p^2}{8(n-1)p^4}\Delta\zeta_1(-ip) - \frac{n\zeta_2(0)}{8(n-1)} \\
&- \frac{nm_\pi^4+4m_\pi^2p^2}{8(n-1)p^4}\Delta\zeta_2(-ip) + \frac{n\left(p^2+m_\pi^2\right)}{8(n-1)p^2}\frac{\Delta\zeta_1(\omega)}{\omega^2} + \frac{n(m_\pi^2+p^2)^2}{8(n-1)p^2\omega^2}\frac{\Delta\zeta_2(\omega)}{\omega^2} \\
&- \frac{n\left(p^2+m_\pi^2\right)^2}{16(n-1)p^2}\int\frac{d^3l}{(2\pi)^3}\frac{e^{-\frac{(\mathbf{l}-\mathbf{p}')^2}{\lambda^2}}}{\mathbf{l}^4}\left\{X_1-\left(p^2+m_\pi^2\right)H_2(\mathbf{l},p)\right\}\left[1-\frac{(p^2+m_\pi^2)}{(\mathbf{l}-\mathbf{p}')^2+m_\pi^2}\right] \\
&+ \frac{nm_\pi^2+4p^2}{8(n-1)p^4}\Delta\zeta_3(-ip) - \frac{nm_\pi^4+4m_\pi^2p^2-np^4}{8(n-1)p^4}\Delta\zeta_4(-ip) - \frac{n}{8(n-1)}\zeta_4(-ip) \\
&+ \frac{n}{4(n-1)p^4}\Delta\zeta_5(-ip) - \frac{nm_\pi^2}{8(n-1)p^4}H_1\zeta_6(-ip) - \frac{n(p^2+m_\pi^2)}{8(n-1)p^2}\frac{\zeta_3(\omega)}{\omega^2} \\
&+ \frac{n(p^2+m_\pi^2)^2}{8(n-1)p^2\omega^2}\left[\zeta_4(\omega)-\zeta_4(0)\right] + \frac{n}{4(n-1)p^2}\frac{\Delta\zeta_5(\omega)}{\omega^2} - \frac{n(p^2+m_\pi^2)}{8(n-1)p^2}H_1\frac{\zeta_6(\omega)}{\omega^2}.
\end{aligned}
\tag{A.38}
$$

Next, we show the tensor part of three loop diagram,

$$
\begin{aligned}
B_3^T =& \int \frac{d^3\mathbf{k}d^3\mathbf{l}d^3\mathbf{q}}{(2\pi)^9}\frac{1}{\mathbf{k^2}-p^2-i\epsilon}\frac{1}{\mathbf{l^2}-p^2-i\epsilon}\frac{1}{\mathbf{q^2}-p^2-i\epsilon} \\
&\times \frac{e^{-\frac{(\mathbf{k}-\mathbf{l})^2}{\lambda^2}}e^{-\frac{(\mathbf{l}-\mathbf{q})^2}{\lambda^2}}}{[(\mathbf{k}-\mathbf{l})^2+m_\pi^2]\,[(\mathbf{l}-\mathbf{q})^2+m_\pi^2]}\left\{[(\mathbf{k}-\mathbf{l})\cdot(\mathbf{l}-\mathbf{q})]^2-\frac{1}{n}(\mathbf{k}-\mathbf{l})^2(\mathbf{l}-\mathbf{q})^2\right\} \\
=& -\frac{1}{n}H_0^3+\frac{1}{2(n-1)}H_0^3+\frac{m_\pi^4}{n(n-1)}V_8+\frac{1}{2(n-1)}\left(\frac{nm_\pi^8}{8p^4}+\frac{m_\pi^6}{p^2}\right)(V_8-J_2) \\
&+\frac{(19n-48)m_\pi^4+2(13n-12)p^2m_\pi^2+10np^4}{48(n-1)}J_2+\frac{2m_\pi^2(12-7n)-7np^2}{48(n-1)}J_3 \\
&+\frac{1}{2(n-1)}\left(\left[H_0^2X_1\right]_{(3A)}-\left[H_0^2X_1\right]_{(3B)}+\left(1+\frac{m_\pi^2}{p^2}\right)[H_0U_9X_1]\right) \\
&-\frac{1}{(n-1)}\left(\frac{nm_\pi^6}{8p^4}+\frac{m_\pi^4}{2p^2}\right)\left\{[V_2X_1]-[J_4X_1]\right\}-\frac{2(5n-6)m_\pi^2+7np^2}{24(n-1)}[J_4X_1] \\
&-\frac{2m_\pi^2}{n(n-1)}[H_0V_2]+\frac{(2m_\pi^2+p^2)}{2(n-1)}[H_0J_4]+\frac{m_\pi^4}{2(n-1)p^2}\Big([H_0J_4]-[H_0V_2]\Big) \\
&+\frac{nm_\pi^4}{16(n-1)p^4}\left[U_9X_1^2\right]+\frac{\Delta R_1(-ip)}{2(n-1)p^2}+\frac{nm_\pi^2}{8(n-1)p^4}[\Delta R_1(-ip)-\Delta R_2(-ip)] \\
&+\frac{n(p^4-m_\pi^4)-4m_\pi^2p^2}{8(n-1)p^4}\Delta R_3(-ip)+\frac{n}{16(n-1)p^4}\Delta R_4(-ip) \\
&+\frac{n}{48(n-1)}\Bigg[\Big(3W_1(-ip)+W_1(0)\Big)-4H_1^2\Delta H_4(-ip)-3\Delta W_1(-ip)+6\Delta W_5(-ip) \\
&-2H_1\Big(3H_6(-ip)+H_6(0)\Big)+2W_{10}-6W_{12}(-ip)+6H_3H_5(-ip)\Bigg] \\
&+\frac{n}{16(n-1)}\Bigg[\frac{2(p^2+m_\pi^2)}{p^2}\frac{\Delta R_1(\omega)-\Delta R_2(\omega)}{\omega^2}-\frac{2(p^2+m_\pi^2)^2}{p^2}\frac{\Delta R_3(\omega)}{\omega^2} \\
&+\frac{1}{p^2}\frac{\Delta R_4(\omega)}{\omega^2}+\frac{(p^2+m_\pi^2)^2}{p^2}\frac{1}{\omega^2}\Big(\Delta W_1(\omega)-2H_1\Delta H_6(\omega)+H_1^2\Delta H_4(\omega)\Big) \\
&+\frac{2(p^2+m_\pi^2)^3}{p^2}\frac{1}{\omega^2}\Big(-\Delta W_9(\omega)+H_1\Delta H_5(\omega)\Big)+\frac{(p^2+m_\pi^2)^4}{p^2}J_5\Bigg]\Bigg|_{\omega\to 0}. \qquad \text{(A.39)}
\end{aligned}
$$

Integrals appearing in the above equations shown above are defined as:

$$
\begin{aligned}
(V_1H_0)' =& \int \frac{d^3l d^3k}{(2\pi)^6} \frac{e^{-\frac{(\mathbf{l}-\mathbf{p}')^2}{\lambda^2}} e^{-\frac{\mathbf{k}^2}{\lambda^2}}}{(\mathbf{l}^2 - p^2 - i\epsilon)\left[(\mathbf{l}-\mathbf{p}')^2 + m_\pi^2\right]} \frac{1}{(\mathbf{k}+\mathbf{l})^2 - p^2 - i\epsilon} \\
=& \frac{e^{\frac{m_\pi^2}{\lambda^2}}}{(4\pi)^2} \left\{ \left(\frac{\lambda}{\sqrt{\pi}} + ip - \frac{8p^2}{3\sqrt{\pi}\lambda} \right) \frac{i}{2p} \log\left(1 - \frac{2ip}{m_\pi}\right) - \left(\frac{1}{2} - \frac{2m_\pi}{3\lambda\sqrt{\pi}}\right) \right. \\
& \left. - \left[\frac{1}{\pi} + \frac{ip}{\sqrt{\pi}\lambda}\left(2\sqrt{2}+1\right) \right] \right\},
\end{aligned}
$$

$$
\begin{aligned}
(V_1X_1)' =& \int \frac{d^3l d^3k}{(2\pi)^6} \frac{e^{-\frac{(\mathbf{l}-\mathbf{p}')^2}{\lambda^2}} e^{-\frac{\mathbf{k}^2}{\lambda^2}}}{(\mathbf{l}^2 - p^2 - i\epsilon)\left[(\mathbf{l}-\mathbf{p}')^2 + m_\pi^2\right]} \left[\frac{1}{(\mathbf{k}+\mathbf{l})^2 - p^2} - \frac{1}{\mathbf{k}^2 + m_\pi^2} \right] \\
=& \frac{e^{\frac{m_\pi^2}{\lambda^2}}}{(4\pi)^2} \left\{ \left(m_\pi + ip - \frac{2m_\pi^2}{\sqrt{\pi}\lambda} - \frac{8p^2}{3\sqrt{\pi}\lambda} \right) \frac{i}{2p} \log\left(1 - \frac{2ip}{m_\pi}\right) \right. \\
& \left. - \frac{1}{2}\left(1 + \frac{m_\pi}{\sqrt{\pi}\lambda}\right) + \left[\frac{1}{\pi} - \frac{ip}{\sqrt{\pi}\lambda}\left(2\sqrt{2}+1\right) \right] \right\},
\end{aligned}
$$

$$
\begin{aligned}
V_2' =& \int \frac{d^3l d^3k}{(2\pi)^6} \frac{e^{-\frac{(\mathbf{l}-\mathbf{p}')^2}{\lambda^2}} e^{-\frac{(\mathbf{k}-\mathbf{l})^2}{\lambda^2}}}{(\mathbf{l}^2 - p^2 - i\epsilon)(\mathbf{k}^2 - p^2 - i\epsilon)\left[(\mathbf{k}-\mathbf{l})^2 + m_\pi^2\right]} \\
=& \frac{e^{\frac{m_\pi^2}{\lambda^2}}}{(4\pi)^2} \left[-\log\left(\frac{m_\pi - 2ip}{\lambda}\right) - \frac{\gamma_E}{2} - \frac{2Catalan}{\pi} - \frac{2ip}{\lambda}\sqrt{\frac{2}{\pi}} + \frac{2(m_\pi - ip)}{\sqrt{\pi}\lambda} \right],
\end{aligned}
$$

$$
\begin{aligned}
V_7 =& \int \frac{d^3k}{(2\pi)^3} \int \frac{d^3l}{(2\pi)^3} \frac{1}{\mathbf{k}^2 - p^2 - i\epsilon} \frac{1}{\mathbf{l}^2 - p^2 - i\epsilon} \frac{e^{-\frac{(\mathbf{k}-\mathbf{l})^2}{\lambda^2}}}{(\mathbf{k}-\mathbf{l})^2 + m_\pi^2} \frac{e^{-\frac{(\mathbf{l}-\mathbf{p})^2}{\lambda^2}}}{(\mathbf{l}-\mathbf{p})^2 + m_\pi^2} \\
=& -\left(\frac{1}{4\pi}\right)^2 \frac{e^{\frac{2m_\pi^2}{\lambda^2}}}{4p^2} \left[\frac{3}{2}\log^2\left(1 - \frac{2ip}{m_\pi}\right) + 2\mathrm{Li}_2\left(\frac{2ip - m_\pi}{m_\pi}\right) \right. \\
& \left. + \mathrm{Li}_2\left(\frac{m_\pi + 2ip}{2ip - m_\pi}\right) + \frac{\pi^2}{4} + \frac{4ip}{\sqrt{\pi}\lambda}\log\left(1 - \frac{2ip}{m_\pi}\right) \right],
\end{aligned}
\tag{A.40}
$$

$$
\begin{aligned}
U_1 =& \int \frac{d^3k}{(2\pi)^3} \int \frac{d^3l}{(2\pi)^3} \frac{1}{\mathbf{l}^2} \frac{1}{\mathbf{k}^2 - p^2 - i\epsilon} \frac{e^{-\frac{(\mathbf{k}-\mathbf{l})^2}{\lambda^2}}}{(\mathbf{k}-\mathbf{l})^2 + m_\pi^2} \frac{e^{-\frac{(\mathbf{l}-\mathbf{p})^2}{\lambda^2}}}{(\mathbf{l}-\mathbf{p})^2 + m_\pi^2} \\
=& \left(\frac{1}{4\pi}\right)^2 \frac{e^{\frac{2m_\pi^2}{\lambda^2}}}{m_\pi^2 + p^2} \left[\log(2) - \frac{i(m_\pi - ip)}{2p} \log\left(1 - \frac{ip}{m_\pi}\right)\right. \\
& \left. - \frac{i(m_\pi + ip)}{2p} \log\left(1 + \frac{ip}{m_\pi}\right) + \frac{i\left(m_\pi^2 + p^2\right)}{\sqrt{\pi}\lambda p} \log\left(\frac{m_\pi + ip}{m_\pi - ip}\right)\right],
\end{aligned}
$$

$$
\begin{aligned}
(U_2 H_0)' =& \int \frac{d^3l d^3k}{(2\pi)^6} \frac{e^{-\frac{(\mathbf{l}-\mathbf{p}')^2}{\lambda^2}} e^{-\frac{\mathbf{k}^2}{\lambda^2}}}{\mathbf{l}^2 \left[(\mathbf{l}-\mathbf{p}')^2 + m_\pi^2\right]} \frac{1}{(\mathbf{k}+\mathbf{l})^2 - p^2 - i\epsilon} \\
=& \frac{e^{\frac{m_\pi^2}{\lambda^2}}}{(4\pi)^2} \left\{\left(\frac{\lambda}{\sqrt{\pi}} + ip - \frac{2p^2}{\sqrt{\pi}\lambda}\right) \frac{1}{2ip} \log\left(\frac{m_\pi + ip}{m_\pi - ip}\right) - \left(\frac{1}{2} - \frac{2m_\pi}{3\sqrt{\pi}\lambda}\right)\right. \\
& \left. - \left(\frac{1}{\pi} + \frac{4ip}{\sqrt{2\pi}\lambda}\right)\right\},
\end{aligned}
$$

$$
\begin{aligned}
(U_2 X_1)' =& \int \frac{d^3l d^3k}{(2\pi)^6} \frac{e^{-\frac{(\mathbf{l}-\mathbf{p}')^2}{\lambda^2}} e^{-\frac{\mathbf{k}^2}{\lambda^2}}}{\mathbf{l}^2 \left[(\mathbf{l}-\mathbf{p}')^2 + m_\pi^2\right]} \left[\frac{1}{(\mathbf{k}+\mathbf{l})^2 - p^2 - i\epsilon} - \frac{1}{\mathbf{k}^2 + m_\pi^2}\right] \\
=& \frac{e^{\frac{m_\pi^2}{\lambda^2}}}{(4\pi)^2} \left\{\left(m_\pi + ip - \frac{2m_\pi^2}{\sqrt{\pi}\lambda} - \frac{2p^2}{\sqrt{\pi}\lambda}\right) \frac{1}{2ip} \log\left(\frac{m_\pi + ip}{m_\pi - ip}\right)\right. \\
& \left. - \left(\frac{1}{2} + \frac{m_\pi}{2\sqrt{\pi}\lambda}\right) + \left(\frac{1}{\pi} - \frac{4ip}{\sqrt{2\pi}\lambda}\right)\right\},
\end{aligned}
$$

$$
\begin{aligned}
U_3 =& \int \frac{d^3k}{(2\pi)^3} \int \frac{d^3l}{(2\pi)^3} \frac{1}{\mathbf{k}^2 - p^2 - i\epsilon} \frac{e^{-\frac{(\mathbf{k}-\mathbf{l})^2}{\lambda^2}}}{(\mathbf{k}-\mathbf{l})^2 + m_\pi^2} \frac{e^{-\frac{(\mathbf{l}-\mathbf{p})^2}{\lambda^2}}}{(\mathbf{l}-\mathbf{p})^2 + m_\pi^2} \\
=& \left(\frac{1}{4\pi}\right)^2 e^{\frac{2m_\pi^2}{\lambda^2}} \left[\frac{m_\pi - ip}{ip} \log\left(\frac{m_\pi - ip}{m_\pi}\right) - \log\left(\frac{m_\pi}{\lambda}\right)\right. \\
& \left. + \left(1 + \frac{8R_4}{\pi}\right) + \frac{4}{\sqrt{\pi}} \frac{m_\pi}{\lambda} - i\frac{2\sqrt{2}}{\sqrt{\pi}} \frac{p}{\lambda}\right],
\end{aligned}
\tag{A.41}
$$

$$R_4 = \int_0^\infty dx e^{-x^2} Er(x)\log(x) = -\frac{\pi}{16}\gamma_E + \frac{1}{8}(-2Catalan - \pi\log(2)),$$

$$Catalan = -\int_0^{\frac{\pi}{4}} dx \log\left[\tan(x)\right] \simeq 0.9159655942\cdots ,$$

$$\begin{aligned}
U_4' =& \int \frac{d^3 l d^3 k}{(2\pi)^6} \frac{e^{-\frac{\mathbf{k}^2}{\lambda^2}} e^{-\frac{(\mathbf{l}-\mathbf{p}')^2}{\lambda^2}}}{\mathbf{l}^2\left[(\mathbf{k}+\mathbf{l})^2 - p^2 - i\epsilon\right](\mathbf{k}^2 + m_\pi^2)} \\
=& \frac{e^{\frac{m_\pi^2}{\lambda^2}}}{(4\pi)^2}\left[-\log\left(\frac{m_\pi - ip}{\lambda}\right) - \frac{\gamma_E}{2} - \frac{2Catalan}{\pi} - \frac{2ip}{\lambda}\sqrt{\frac{2}{\pi}} + \frac{2m_\pi}{\sqrt{\pi}\lambda}\right],
\end{aligned}$$

$$\begin{aligned}
(H_0')^2 =& \int \frac{d^3 k d^3 l}{(2\pi)^6} \frac{e^{-\frac{\mathbf{l}^2}{\lambda^2}} e^{-\frac{\mathbf{k}^2}{\lambda^2}}}{\left[(\mathbf{l}+\mathbf{p}')^2 - p^2 - i\epsilon\right]\left[(\mathbf{k}+\mathbf{l}+\mathbf{p}')^2 - p^2 - i\epsilon\right]} \\
=& \frac{1}{(4\pi)^2}\left[\frac{\lambda^2}{4} + \frac{2+\sqrt{2}}{2}\frac{\lambda}{\sqrt{\pi}}ip - \frac{2(2+3\pi)}{3}\frac{p^2}{\pi} - \frac{28+17\sqrt{2}}{6}\frac{ip^3}{\sqrt{\pi}\lambda}\right],
\end{aligned}$$

$$\begin{aligned}
(H_0 X_1)' =& \int \frac{d^3 k d^3 l}{(2\pi)^6} \frac{e^{-\frac{\mathbf{l}^2}{\lambda^2}} e^{-\frac{\mathbf{k}^2}{\lambda^2}}}{\left[(\mathbf{l}+\mathbf{p}')^2 - p^2 - i\epsilon\right]\left[(\mathbf{k}+\mathbf{l}+\mathbf{p}')^2 - p^2 - i\epsilon\right]} \\
=& \frac{1}{(4\pi)^2}\left[\frac{\lambda^2}{4} - \frac{\lambda^2}{\pi} + \frac{\lambda m_\pi}{\sqrt{\pi}} + \frac{i\lambda p}{\sqrt{2\pi}} - \frac{2p^2}{3\pi} - 2p^2 + i m_\pi p - \frac{2m_\pi^2}{\pi}\right. \\
& \left. - \frac{17ip^3}{3\lambda\sqrt{2\pi}} - \frac{14ip^3}{3\lambda\sqrt{\pi}} - \frac{2m_\pi p^2}{3\lambda\sqrt{\pi}} - \frac{2im_\pi^2 p}{\lambda\sqrt{\pi}}\right],
\end{aligned}$$

$$\begin{aligned}
\xi X_1 H_0 =& \int \frac{d^3 k d^3 l}{(2\pi)^6}\left[\frac{1}{\mathbf{l}^2 - p^2 - i\epsilon} - \frac{1}{(\mathbf{l}-\mathbf{p}')^2 + m_\pi^2}\right]\frac{e^{-\frac{(\mathbf{l}-\mathbf{p}')^2}{\lambda^2}} e^{-\frac{\mathbf{k}^2}{\lambda^2}}}{(\mathbf{k}+\mathbf{l})^2 - p^2 - i\epsilon} \\
=& \frac{1}{(4\pi)^2}\left\{\frac{\lambda}{\sqrt{\pi}}(m_\pi + ip) - \frac{m_\pi^2}{4\pi}(4+\pi) + ipm_\pi - \frac{p^2}{3}\left(5 + \frac{2}{\pi}\right)\right. \\
& \left. + \frac{2}{\sqrt{\pi}\lambda}\left(\frac{m_\pi^3}{3} - \frac{3ipm_\pi^2}{2\sqrt{2}} - \frac{4p^2 m_\pi}{3} - \frac{7ip^3}{3} - ip^3\sqrt{2}\right)\right\}, \qquad \text{(A.42)}
\end{aligned}$$

$$
\begin{aligned}
(X_1)'^2 =& \int \frac{d^3k d^3l}{(2\pi)^6} \left[\frac{1}{\mathbf{l}^2 - p^2 - i\epsilon} - \frac{1}{(\mathbf{l}-\mathbf{p}')^2 + m_\pi^2}\right] \\
& \times \left[\frac{1}{(\mathbf{k}+\mathbf{l})^2 - p^2 - i\epsilon} - \frac{1}{\mathbf{k}^2 + m_\pi^2}\right] e^{-\frac{(\mathbf{l}-\mathbf{p}')^2}{\lambda^2}} e^{-\frac{\mathbf{k}^2}{\lambda^2}} \\
=& \frac{1}{(4\pi)^2} \left\{ \frac{m_\pi^2}{4\pi}(4+3\pi) + 2ipm_\pi - \frac{p^2}{3\pi}(5\pi - 4) \right. \\
& \left. - \frac{2}{\sqrt{\pi}\lambda}\left[\frac{5m_\pi^3}{3} + \frac{3ipm_\pi^2}{2\sqrt{2}} + ipm_\pi^2 + \frac{7p^2}{3}(m_\pi + ip) + ip^3\sqrt{2}\right]\right\},
\end{aligned}
$$

$$
(U_9 H_1)' = \int \frac{d^3k d^3l}{(2\pi)^6} \left(\frac{1}{\mathbf{l}^2 - p^2 - i\epsilon} - \frac{1}{\mathbf{l}^2}\right) \frac{e^{-\frac{(\mathbf{l}-\mathbf{p}')^2}{\lambda^2}} e^{-\frac{\mathbf{k}^2}{\lambda^2}}}{\mathbf{k}^2 + m_\pi^2} = \frac{H_1}{4\pi}\left[ip - \frac{2p^2}{\sqrt{\pi}\lambda} - \frac{2ip^3}{\lambda^2}\right],
$$

$$
\begin{aligned}
(H_0 U_9)' =& \int \frac{d^3k d^3l}{(2\pi)^6} \left(\frac{1}{\mathbf{l}^2 - p^2 - i\epsilon} - \frac{1}{\mathbf{l}^2}\right) \frac{e^{-\frac{(\mathbf{l}-\mathbf{p}')^2}{\lambda^2}} e^{-\frac{\mathbf{k}^2}{\lambda^2}}}{(\mathbf{k}+\mathbf{l}+\mathbf{p}')^2 - p^2 - i\epsilon} \\
=& \frac{1}{(4\pi)^2}\frac{\lambda}{\sqrt{\pi}}\left(ip - \frac{3\sqrt{\pi}}{2\lambda}p^2 - \frac{p^2}{\sqrt{\pi}\lambda} - \frac{2\sqrt{2}ip^3}{\lambda^2} - \frac{14ip^3}{3\lambda^2}\right),
\end{aligned}
$$

$$
\begin{aligned}
(U_9 X_1)' =& [(U_9 H_0)' - (U_9 H_1)'] \\
=& \frac{1}{(4\pi)^2}\left[im_\pi p - \frac{3p^2}{2} + \frac{p^2}{\pi} - \frac{2ip}{\sqrt{\pi}\lambda}\left(m_\pi^2 - im_\pi p + \frac{4p^2}{3} + \sqrt{2}p^2\right)\right],
\end{aligned}
\tag{A.43}
$$

$$
\begin{aligned}
\zeta_1(M) =& \int \frac{d^3\mathbf{k}d^3\mathbf{l}}{(2\pi)^6} \frac{1}{(\mathbf{l}+\mathbf{p}')^2+m_\pi^2} \frac{\mathbf{k}\cdot(\mathbf{l}+\mathbf{p}')}{(\mathbf{k}+\mathbf{l}+\mathbf{p}')^2-p^2} e^{-\frac{\mathbf{k}^2}{\lambda^2}} e^{-\frac{\mathbf{l}^2}{\lambda^2}} \\
=& \frac{1}{2}\left[\kappa_1\theta_1(M) - \theta_2 - \theta_4(M) + (p^2+m_\pi^2)\theta_3(M)\right], \\
\\
\zeta_2(M) =& \int \frac{d^3\mathbf{k}d^3\mathbf{l}}{(2\pi)^6} \frac{1}{(\mathbf{l}+\mathbf{p}')^2+m_\pi^2} \frac{1}{\mathbf{l}^2+m_\pi^2} \frac{\mathbf{k}\cdot(\mathbf{l}+\mathbf{p}')}{(\mathbf{k}+\mathbf{l}+\mathbf{p}')^2-p^2} e^{-\frac{\mathbf{k}^2}{\lambda^2}} e^{-\frac{\mathbf{l}^2}{\lambda^2}} \\
=& \frac{1}{2}\left[\kappa_1\theta_5(M) - \xi H_1 H_0 - \theta_7(M) + (p^2+m_\pi^2)\theta_6(M)\right], \\
\\
\zeta_3(M) =& \int \frac{d^3\mathbf{k}d^3\mathbf{l}}{(2\pi)^6} \frac{1}{(\mathbf{l}+\mathbf{p}')^2+m_\pi^2} \frac{(\mathbf{l}\cdot\mathbf{p}')+p^2}{(\mathbf{k}+\mathbf{l}+\mathbf{p}')^2-p^2} e^{-\frac{\mathbf{k}^2}{\lambda^2}} e^{-\frac{\mathbf{l}^2}{\lambda^2}} \\
=& \frac{1}{2}\left[\theta_2 - \theta_8(M) + (p^2-m_\pi^2)\theta_3(M)\right], \\
\\
\zeta_4(M) =& \int \frac{d^3\mathbf{k}d^3\mathbf{l}}{(2\pi)^6} \frac{1}{(\mathbf{l}+\mathbf{p}')^2+m_\pi^2} \frac{(\mathbf{l}\cdot\mathbf{p}')+p^2}{(\mathbf{k}+\mathbf{l}+\mathbf{p}')^2-p^2} \frac{1}{\mathbf{k}^2+m_\pi^2} e^{-\frac{\mathbf{k}^2}{\lambda^2}} e^{-\frac{\mathbf{l}^2}{\lambda^2}} \\
=& \frac{1}{2}\left[\theta_{14} - \theta_{10}(M) + (p^2-m_\pi^2)\theta_{11}(M)\right], \\
\\
\zeta_5(M) =& \int \frac{d^3\mathbf{k}d^3\mathbf{l}}{(2\pi)^6} \frac{1}{(\mathbf{l}+\mathbf{p}')^2+m_\pi^2} \frac{\left[(\mathbf{l}\cdot\mathbf{p}')+p^2\right]\left[\mathbf{k}\cdot(\mathbf{l}+\mathbf{p}')\right]}{(\mathbf{k}+\mathbf{l}+\mathbf{p}')^2-p^2} e^{-\frac{\mathbf{k}^2}{\lambda^2}} e^{-\frac{\mathbf{l}^2}{\lambda^2}}, \\
=& \frac{1}{2}\nu_1 - \frac{1}{4}\kappa_1\theta_{12}(M) + \frac{1}{4}\nu_2 + \frac{1}{4}\theta_{13}(M) - \frac{p^2+m_\pi^2}{4}\theta_8(M) + \frac{p^2-m_\pi^2}{2}\zeta_1(M) \\
\\
\zeta_6(M) =& \int \frac{d^3\mathbf{l}}{(2\pi)^3} \frac{(\mathbf{l}\cdot\mathbf{p}')+p^2}{(\mathbf{l}+\mathbf{p}')^2+m_\pi^2} e^{-\frac{\mathbf{l}^2}{\lambda^2}} \\
=& \frac{1}{2}\left[\kappa_1 - \theta_{12}(M) + (p^2-m_\pi^2)\theta_1(M)\right], \\
\\
\Delta\zeta_i(M) =& \zeta_i(M) - \zeta_i(0), \qquad i = 1 \sim 6, \qquad\qquad (A.44)
\end{aligned}
$$

$$
\begin{aligned}
\xi H_1 H_0 =& \int \frac{d^3\mathbf{k} d^3\mathbf{l}}{(2\pi)^6} \frac{1}{\mathbf{l}^2 + m_\pi^2} \frac{1}{\left(\mathbf{k}+\mathbf{l}+\mathbf{p}'\right)^2 - p^2} e^{-\frac{\mathbf{k}^2}{\lambda^2}} e^{-\frac{\mathbf{l}^2}{\lambda^2}}, \\
\theta_1(M) =& \int \frac{d^3\mathbf{l}}{(2\pi)^3} \frac{e^{-\frac{\mathbf{l}^2}{\lambda^2}}}{\left(\mathbf{l}+\mathbf{p}'\right)^2 + m_\pi^2} \\
=& \frac{2\sqrt{\pi}\lambda^2}{(4\pi)^2 ip} \int_0^\infty dx e^{-\frac{2M}{\lambda}x} \left(e^{\frac{2ip}{\lambda}x} - e^{-\frac{2ip}{\lambda}x}\right) e^{-x^2},
\end{aligned}
$$

$$
\begin{aligned}
\theta_2 =& \int \frac{d^3\mathbf{k} d^3\mathbf{l}}{(2\pi)^6} \frac{e^{-\frac{\mathbf{k}^2}{\lambda^2}} e^{-\frac{\mathbf{l}^2}{\lambda^2}}}{\left(\mathbf{l}+\mathbf{k}+\mathbf{p}'\right)^2 - p^2} \\
=& \frac{2\sqrt{2}\pi\lambda^5}{(4\pi)^4 ip} \int_0^\infty dx \left(e^{\frac{2\sqrt{2}ip}{\lambda}x} - 1\right) e^{-x^2},
\end{aligned}
$$

$$
\begin{aligned}
\theta_3 =& \int \frac{d^3k d^3l}{(2\pi)^6} \frac{e^{-\frac{\mathbf{l}^2}{\lambda^2}} e^{-\frac{\mathbf{k}^2}{\lambda^2}}}{\left[\left(\mathbf{l}+\mathbf{p}'\right)^2 + m_\pi^2\right] \left[\left(\mathbf{k}+\mathbf{l}+\mathbf{p}'\right)^2 - p^2\right]} \\
=& \frac{\lambda^4}{(4\pi)^3} \int_0^\infty dx \int_0^x dy \frac{e^{\frac{2ip}{\lambda}y}}{ipM} e^{-\frac{2M}{\lambda}x} \left(e^{\frac{2M}{\lambda}y} - e^{-\frac{2M}{\lambda}y}\right) \left(e^{\frac{2ip}{\lambda}x} - e^{-\frac{2ip}{\lambda}x}\right) e^{-x^2} e^{-y^2} \\
& + \frac{\lambda^4}{(4\pi)^3} \int_0^\infty dx \int_x^\infty dy \frac{e^{\frac{2ip}{\lambda}y}}{ipM} e^{-\frac{2M}{\lambda}y} \left(e^{\frac{2M}{\lambda}x} - e^{-\frac{2M}{\lambda}x}\right) \left(e^{\frac{2ip}{\lambda}x} - e^{-\frac{2ip}{\lambda}x}\right) e^{-x^2} e^{-y^2},
\end{aligned}
$$

$$
\begin{aligned}
\theta_4(M) =& \int \frac{d^3\mathbf{k} d^3\mathbf{l}}{(2\pi)^6} \frac{1}{\left(\mathbf{l}+\mathbf{p}'\right)^2 + m_\pi^2} \frac{\mathbf{k}^2}{\left(\mathbf{l}+\mathbf{k}+\mathbf{p}'\right)^2 - p^2} e^{-\frac{\mathbf{k}^2}{\lambda^2}} e^{-\frac{\mathbf{l}^2}{\lambda^2}} \\
=& \frac{\lambda^6}{2(4\pi)^3} \int_0^\infty dx \int_0^x dy \frac{e^{\frac{2ip}{\lambda}y}}{ipM} e^{-\frac{2M}{\lambda}x} \left(e^{\frac{2M}{\lambda}y} - e^{-\frac{2M}{\lambda}y}\right) \left(e^{\frac{2ip}{\lambda}x} - e^{-\frac{2ip}{\lambda}x}\right) \\
& \times \left(3 - 2y^2\right) e^{-x^2} e^{-y^2} \\
& + \frac{\lambda^6}{2(4\pi)^3} \int_0^\infty dx \int_x^\infty dy \frac{e^{\frac{2ip}{\lambda}y}}{ipM} e^{-\frac{2M}{\lambda}y} \left(e^{\frac{2M}{\lambda}x} - e^{-\frac{2M}{\lambda}x}\right) \left(e^{\frac{2ip}{\lambda}x} - e^{-\frac{2ip}{\lambda}x}\right) \\
& \times \left(3 - 2y^2\right) e^{-x^2} e^{-y^2},
\end{aligned}
\tag{A.45}
$$

$$
\begin{aligned}
\theta_5(M) =& \int \frac{d^3\mathbf{l}}{(2\pi)^3} \frac{1}{(\mathbf{l}+\mathbf{p}')^2 + m_\pi^2} \frac{1}{\mathbf{l}^2 + m_\pi^2} e^{-\frac{\mathbf{l}^2}{\lambda^2}} \\
=& \frac{2\sqrt{\pi}}{(4\pi)^2 ip} \int_0^\infty dx \frac{e^{-\frac{2M}{\lambda}x}}{x} \left(e^{\frac{2ip}{\lambda}x} - e^{-\frac{2ip}{\lambda}x}\right) \\
&\times \left[\sqrt{\pi} e^{-\frac{2m_\pi}{\lambda}x} - e^{-\frac{2m_\pi}{\lambda}x} \mathrm{Erfc}\left(x - \frac{m_\pi}{\lambda}\right) - e^{\frac{2m_\pi}{\lambda}x} \mathrm{Erfc}\left(x + \frac{m_\pi}{\lambda}\right)\right],
\end{aligned}
$$

$$
\begin{aligned}
\theta_6(M) =& \int \frac{d^3\mathbf{l} d^3\mathbf{k}}{(2\pi)^6} \frac{1}{(\mathbf{l}+\mathbf{p}')^2 + m_\pi^2} \frac{1}{\mathbf{l}^2 + m_\pi^2} \frac{1}{(\mathbf{k}+\mathbf{l}+\mathbf{p}')^2 - p^2} e^{-\frac{\mathbf{l}^2}{\lambda^2}} e^{-\frac{\mathbf{k}^2}{\lambda^2}} \\
=& \frac{\lambda^2}{(4\pi)^3 ipM} \int_0^\infty dx \int_0^x dz \frac{e^{\frac{2ip}{\lambda}z}}{x} e^{-\frac{2M}{\lambda}x} \left(e^{\frac{2M}{\lambda}z} - e^{-\frac{2M}{\lambda}z}\right) \left(e^{\frac{2ip}{\lambda}x} - e^{-\frac{2ip}{\lambda}x}\right) \\
&\times \left[\sqrt{\pi} e^{-\frac{2m_\pi}{\lambda}x} - e^{-\frac{2m_\pi}{\lambda}x} \mathrm{Erfc}\left(x - \frac{m_\pi}{\lambda}\right) - e^{\frac{2m_\pi}{\lambda}x} \mathrm{Erfc}\left(x + \frac{m_\pi}{\lambda}\right)\right] e^{-z^2} \\
&+ \frac{\lambda^2}{(4\pi)^3 ipM} \int_0^\infty dx \int_x^\infty dz \frac{e^{\frac{2ip}{\lambda}z}}{x} e^{-\frac{2M}{\lambda}z} \left(e^{\frac{2M}{\lambda}x} - e^{-\frac{2M}{\lambda}x}\right) \left(e^{\frac{2ip}{\lambda}x} - e^{-\frac{2ip}{\lambda}x}\right) \\
&\times \left[\sqrt{\pi} e^{-\frac{2m_\pi}{\lambda}x} - e^{-\frac{2m_\pi}{\lambda}x} \mathrm{Erfc}\left(x - \frac{m_\pi}{\lambda}\right) - e^{\frac{2m_\pi}{\lambda}x} \mathrm{Erfc}\left(x + \frac{m_\pi}{\lambda}\right)\right] e^{-z^2},
\end{aligned}
$$

$$
\begin{aligned}
\theta_7(M) =& \int \frac{d^3\mathbf{l} d^3\mathbf{k}}{(2\pi)^6} \frac{1}{(\mathbf{l}+\mathbf{p}')^2 + m_\pi^2} \frac{\mathbf{k}^2}{\mathbf{l}^2 + m_\pi^2} \frac{1}{(\mathbf{k}+\mathbf{l}+\mathbf{p}')^2 - p^2} e^{-\frac{\mathbf{l}^2}{\lambda^2}} e^{-\frac{\mathbf{k}^2}{\lambda^2}} \\
=& \frac{\lambda^4}{2(4\pi)^3 ipM} \int_0^\infty dx \int_0^x dz \frac{e^{\frac{2ip}{\lambda}z}}{x} e^{-\frac{2M}{\lambda}x} \left(e^{\frac{2M}{\lambda}z} - e^{-\frac{2M}{\lambda}z}\right) \left(e^{\frac{2ip}{\lambda}x} - e^{-\frac{2ip}{\lambda}x}\right) \\
&\times \left(3 - 2z^2\right) \left[\sqrt{\pi} e^{-\frac{2m_\pi}{\lambda}x} - e^{-\frac{2m_\pi}{\lambda}x} \mathrm{Erfc}\left(x - \frac{m_\pi}{\lambda}\right) - e^{\frac{2m_\pi}{\lambda}x} \mathrm{Erfc}\left(x + \frac{m_\pi}{\lambda}\right)\right] e^{-z^2} \\
&+ \frac{\lambda^4}{2(4\pi)^3 ipM} \int_0^\infty dx \int_x^\infty dz \frac{e^{\frac{2ip}{\lambda}z}}{x} e^{-\frac{2M}{\lambda}z} \left(e^{\frac{2M}{\lambda}x} - e^{-\frac{2M}{\lambda}x}\right) \left(e^{\frac{2ip}{\lambda}x} - e^{-\frac{2ip}{\lambda}x}\right) \\
&\times \left(3 - 2z^2\right) \left[\sqrt{\pi} e^{-\frac{2m_\pi}{\lambda}x} - e^{-\frac{2m_\pi}{\lambda}x} \mathrm{Erfc}\left(x - \frac{m_\pi}{\lambda}\right) - e^{\frac{2m_\pi}{\lambda}x} \mathrm{Erfc}\left(x + \frac{m_\pi}{\lambda}\right)\right] e^{-z^2},
\end{aligned}
\tag{A.46}
$$

$$\theta_8(M) = \int \frac{d^3\mathbf{l} d^3\mathbf{k}}{(2\pi)^6} \frac{1}{(\mathbf{l}+\mathbf{p}')^2 + m_\pi^2} \frac{\mathbf{l}^2}{(\mathbf{k}+\mathbf{l}+\mathbf{p}')^2 - p^2} e^{-\frac{\mathbf{l}^2}{\lambda^2}} e^{-\frac{\mathbf{k}^2}{\lambda^2}}$$
$$= \frac{\lambda^6}{2(4\pi)^3} \int_0^\infty dx \int_0^x dy \frac{e^{\frac{2ip}{\lambda}y}}{ipM} e^{-\frac{2M}{\lambda}x} \left(e^{\frac{2M}{\lambda}y} - e^{-\frac{2M}{\lambda}y}\right) \left(e^{\frac{2ip}{\lambda}x} - e^{-\frac{2ip}{\lambda}x}\right)$$
$$\times \left(3 - 2x^2\right) e^{-x^2} e^{-y^2}$$
$$+ \frac{\lambda^6}{2(4\pi)^3} \int_0^\infty dx \int_x^\infty dy \frac{e^{\frac{2ip}{\lambda}y}}{ipM} e^{-\frac{2M}{\lambda}y} \left(e^{\frac{2M}{\lambda}x} - e^{-\frac{2M}{\lambda}x}\right) \left(e^{\frac{2ip}{\lambda}x} - e^{-\frac{2ip}{\lambda}x}\right)$$
$$\times \left(3 - 2x^2\right) e^{-x^2} e^{-y^2},$$

$$\theta_{10}(M) = \int \frac{d^3\mathbf{l} d^3\mathbf{k}}{(2\pi)^6} \frac{1}{(\mathbf{l}+\mathbf{p}')^2 + m_\pi^2} \frac{\mathbf{l}^2}{(\mathbf{k}+\mathbf{l}+\mathbf{p}')^2 - p^2} \frac{1}{\mathbf{k}^2 + m_\pi^2} e^{-\frac{\mathbf{l}^2}{\lambda^2}} e^{-\frac{\mathbf{k}^2}{\lambda^2}}$$
$$= \frac{\lambda^4}{2(4\pi)^3} \int_0^\infty dx \int_0^x dy \frac{e^{\frac{2ip}{\lambda}y}}{y} \frac{1}{ipM} e^{-\frac{2M}{\lambda}x} \left(e^{\frac{2M}{\lambda}y} - e^{-\frac{2M}{\lambda}y}\right) \left(e^{\frac{2ip}{\lambda}x} - e^{-\frac{2ip}{\lambda}x}\right)$$
$$\times \left(3 - 2x^2\right) e^{-x^2} \left[\sqrt{\pi} e^{-\frac{2m_\pi}{\lambda}y} - e^{-\frac{2m_\pi}{\lambda}y} \mathrm{Erfc}\left(y - \frac{m_\pi}{\lambda}\right) - e^{\frac{2m_\pi}{\lambda}y} \mathrm{Erfc}\left(y + \frac{m_\pi}{\lambda}\right)\right]$$
$$+ \frac{\lambda^4}{2(4\pi)^3} \int_0^\infty dx \int_x^\infty dy \frac{e^{\frac{2ip}{\lambda}y}}{y} \frac{1}{ipM} e^{-\frac{2M}{\lambda}y} \left(e^{\frac{2M}{\lambda}x} - e^{-\frac{2M}{\lambda}x}\right) \left(e^{\frac{2ip}{\lambda}x} - e^{-\frac{2ip}{\lambda}x}\right)$$
$$\times \left(3 - 2x^2\right) e^{-x^2} \left[\sqrt{\pi} e^{-\frac{2m_\pi}{\lambda}y} - e^{-\frac{2m_\pi}{\lambda}y} \mathrm{Erfc}\left(y - \frac{m_\pi}{\lambda}\right) - e^{\frac{2m_\pi}{\lambda}y} \mathrm{Erfc}\left(y + \frac{m_\pi}{\lambda}\right)\right],$$

$$\theta_{11}(M) = \int \frac{d^3\mathbf{l} d^3\mathbf{k}}{(2\pi)^6} \frac{1}{(\mathbf{l}+\mathbf{p}')^2 + m_\pi^2} \frac{1}{(\mathbf{k}+\mathbf{l}+\mathbf{p}')^2 - p^2} \frac{1}{\mathbf{k}^2 + m_\pi^2} e^{-\frac{\mathbf{l}^2}{\lambda^2}} e^{-\frac{\mathbf{k}^2}{\lambda^2}}$$
$$= \frac{\lambda^2}{(4\pi)^3} \int_0^\infty dx \int_0^x dy \frac{e^{\frac{2ip}{\lambda}y}}{ipMy} e^{-\frac{2M}{\lambda}x} \left(e^{\frac{2M}{\lambda}y} - e^{-\frac{2M}{\lambda}y}\right) \left(e^{\frac{2ip}{\lambda}x} - e^{-\frac{2ip}{\lambda}x}\right)$$
$$\times e^{-x^2} \left[\sqrt{\pi} e^{-\frac{2m_\pi}{\lambda}y} - e^{-\frac{2m_\pi}{\lambda}y} \mathrm{Erfc}\left(y - \frac{m_\pi}{\lambda}\right) - e^{\frac{2m_\pi}{\lambda}y} \mathrm{Erfc}\left(y + \frac{m_\pi}{\lambda}\right)\right]$$
$$+ \frac{\lambda^2}{(4\pi)^3} \int_0^\infty dx \int_x^\infty dy \frac{e^{\frac{2ip}{\lambda}y}}{ipMy} e^{-\frac{2M}{\lambda}y} \left(e^{\frac{2M}{\lambda}x} - e^{-\frac{2M}{\lambda}x}\right) \left(e^{\frac{2ip}{\lambda}x} - e^{-\frac{2ip}{\lambda}x}\right)$$
$$\times e^{-x^2} \left[\sqrt{\pi} e^{-\frac{2m_\pi}{\lambda}y} - e^{-\frac{2m_\pi}{\lambda}y} \mathrm{Erfc}\left(y - \frac{m_\pi}{\lambda}\right) - e^{\frac{2m_\pi}{\lambda}y} \mathrm{Erfc}\left(y + \frac{m_\pi}{\lambda}\right)\right], \tag{A.47}$$

$$
\begin{aligned}
\theta_{12}(M) =& \int \frac{d^3\mathbf{l}}{(2\pi)^3} \frac{\mathbf{l}^2}{(\mathbf{l}+\mathbf{p}')^2 + m_\pi^2} e^{-\frac{\mathbf{l}^2}{\lambda^2}} \\
=& \frac{\sqrt{\pi}\lambda^4}{(4\pi)^2 ip} \int_0^\infty dx e^{-\frac{2M}{\lambda}x} \left(e^{\frac{2ip}{\lambda}x} - e^{-\frac{2ip}{\lambda}x} \right) \left(3 - 2x^2\right) e^{-x^2},
\end{aligned}
$$

$$
\begin{aligned}
\theta_{13}(M) =& \int \frac{d^3\mathbf{k} d^3\mathbf{l}}{(2\pi)^6} \frac{1}{(\mathbf{l}+\mathbf{p}')^2 + m_\pi^2} \frac{\mathbf{l}^2\mathbf{k}^2}{(\mathbf{l}+\mathbf{k}+\mathbf{p}')^2 - p^2} e^{-\frac{\mathbf{k}^2}{\lambda^2}} e^{-\frac{\mathbf{l}^2}{\lambda^2}} \\
=& \frac{\pi\lambda^8}{(4\pi)^4} \int_0^\infty dx \int_0^\infty dy \frac{e^{\frac{2ip}{\lambda}y}}{ipM} \left(e^{-\frac{2M}{\lambda}|x-y|} - e^{-\frac{2M}{\lambda}(x+y)} \right) \left(e^{\frac{2ip}{\lambda}x} - e^{-\frac{2ip}{\lambda}x} \right) \\
& \times \left(3 - 2x^2\right) \left(3 - 2y^2\right) e^{-x^2} e^{-y^2},
\end{aligned}
$$

$$
\begin{aligned}
\theta_{14}(M) =& \int \frac{d^3\mathbf{k} d^3\mathbf{l}}{(2\pi)^6} \frac{1}{(\mathbf{k}+\mathbf{l}+\mathbf{p}')^2 - p^2} \frac{1}{\mathbf{k}^2 + m_\pi^2} e^{-\frac{\mathbf{k}^2}{\lambda^2}} e^{-\frac{\mathbf{l}^2}{\lambda^2}} \\
=& \frac{\lambda^3}{(4\pi)^3} \int_0^\infty dx \frac{e^{\frac{2ip}{\lambda}x}}{ipx} \left(e^{\frac{2ip}{\lambda}x} - e^{-\frac{2ip}{\lambda}x} \right) \\
& \times \left[\sqrt{\pi} e^{-\frac{2m_\pi}{\lambda}x} - e^{-\frac{2m_\pi}{\lambda}x} \mathrm{Erfc}\left(x - \frac{m_\pi}{\lambda}\right) - e^{\frac{2m_\pi}{\lambda}x} \mathrm{Erfc}\left(x + \frac{m_\pi}{\lambda}\right) \right] e^{-x^2},
\end{aligned}
\tag{A.48}
$$

$$
\kappa_1 = \int \frac{d^3\mathbf{k}}{(2\pi)^3} e^{-\frac{\mathbf{k}^2}{\lambda^2}} = \frac{\sqrt{\pi}\lambda^3}{2(2\pi)^2},
$$

$$
\nu_1 = \int \frac{d^3l d^3k}{(2\pi)^6} \frac{\left[\mathbf{k}\cdot(\mathbf{l}+\mathbf{p})\right] e^{-\frac{\mathbf{l}^2}{\lambda^2}} e^{-\frac{\mathbf{k}^2}{\lambda^2}}}{(\mathbf{k}+\mathbf{l}+\mathbf{p}')^2 - p^2},
$$

$$
\nu_2 = \int \frac{d^3l d^3k}{(2\pi)^6} \frac{\mathbf{l}^2}{(\mathbf{k}+\mathbf{l}+\mathbf{p}')^2 - p^2} e^{-\frac{\mathbf{l}^2}{\lambda^2}} e^{-\frac{\mathbf{k}^2}{\lambda^2}}, \tag{A.49}
$$

$$
\begin{aligned}
H_1 \equiv & \int \frac{d^3\mathbf{k}}{(2\pi)^3} \frac{1}{\mathbf{k^2} + m_\pi^2} e^{-\frac{\mathbf{k^2}}{\lambda^2}} \\
= & \frac{1}{4\pi} \left[\frac{\lambda}{\sqrt{\pi}} - m_\pi + \frac{2}{\sqrt{\pi}} \frac{m_\pi^2}{\lambda} - \frac{m_\pi^3}{\lambda^2} + \frac{4}{3\sqrt{\pi}} \frac{m_\pi^4}{\lambda^3} - \frac{1}{2} \frac{m_\pi^5}{\lambda^4} \right] + O\left(\frac{1}{\lambda^5}\right).
\end{aligned}
$$

$$
H_3 \equiv \int \frac{d^3\mathbf{k}}{(2\pi)^3} e^{-\frac{\mathbf{k^2}}{\lambda^2}} = \frac{\lambda^3}{8\pi\sqrt{\pi}} = \left(\frac{\lambda^3}{4\pi}\right)\left(\frac{1}{2\sqrt{\pi}}\right),
$$

$$
H_4(M) \equiv \int \frac{d^n\mathbf{l}}{(2\pi)^n} \frac{1}{\mathbf{l^2} + m_\pi^2}, \quad (\ \textbf{without} \text{ exponential factor})
$$

$$
\begin{aligned}
H_5(M) \equiv & \int \frac{d^3\mathbf{k}}{(2\pi)^3} \int \frac{d^3\mathbf{l}}{(2\pi)^3} \frac{1}{\mathbf{k^2} - \mathbf{p^2} - i\epsilon} \frac{1}{(\mathbf{k} - \mathbf{l})^2 + m_\pi^2} \frac{1}{\mathbf{l^2} + m_\pi^2} e^{-\frac{(\mathbf{k}-\mathbf{l})^2}{\lambda^2}} \\
= & 4\sqrt{\pi} \left(\frac{1}{4\pi}\right)^3 \int_0^\infty dy \int_0^\infty \frac{dx}{x} e^{-x^2 - y^2 + 2(\beta - \tilde{M})x - 2\alpha y} \left(e^{2xy} - e^{-2xy}\right),
\end{aligned}
$$

$$
\begin{aligned}
H_6(M) \equiv & \int \frac{d^3\mathbf{k}}{(2\pi)^3} \int \frac{d^3\mathbf{l}}{(2\pi)^3} \frac{1}{\mathbf{l^2} + m_\pi^2} \frac{1}{(\mathbf{k} + \mathbf{l})^\mathbf{2} - \mathbf{p^2} - i\epsilon} e^{-\frac{\mathbf{k^2}}{\lambda^2}} \\
= & \lambda^2 \left(\frac{1}{4\pi}\right)^2 \left(\frac{1}{8\pi\sqrt{\pi}}\right) \int d^3\mathbf{x} \frac{1}{|\mathbf{x}|^2} e^{-\frac{\mathbf{x^2}}{4} - \tilde{M}|\mathbf{x}| + \beta|\mathbf{x}|},
\end{aligned}
$$

$$
\begin{aligned}
H_7(M) \equiv & \int \frac{d^3\mathbf{k}}{(2\pi)^3} \int \frac{d^3\mathbf{l}}{(2\pi)^3} \frac{1}{\mathbf{l^2} + m_\pi^2} \frac{\mathbf{k^2}}{(\mathbf{k} + \mathbf{l})^\mathbf{2} - \mathbf{p^2} - i\epsilon} e^{-\frac{\mathbf{k^2}}{\lambda^2}} \\
= & \lambda^4 \frac{\sqrt{\pi}}{2} \left(\frac{1}{4\pi}\right)^3 \int_0^\infty dx \left(6 - x^2\right) e^{-\frac{x^2}{4} - \tilde{M}x + \beta x},
\end{aligned}
\tag{A.50}
$$

$$
\begin{aligned}
R_1(M) \equiv & \int \frac{d^3\mathbf{k}d^3\mathbf{l}d^3\mathbf{q}}{(2\pi)^9} \frac{e^{-\frac{\mathbf{k^2}}{\lambda^2}}}{(\mathbf{k}+\mathbf{l})^\mathbf{2} - \mathbf{p^2} - i\epsilon} \frac{2(\mathbf{k}\cdot\mathbf{l})}{\mathbf{l^2}+m_\pi^2} \frac{e^{-\frac{\mathbf{q}^2}{\lambda^2}}}{(\mathbf{q}+\mathbf{l})^\mathbf{2} - \mathbf{p^2} - i\epsilon} \\
= & - W_4(M) - W_2 + H_3 H_6(M) + (p^2 + m_\pi^2) W_1(M),
\end{aligned}
$$

$$
\begin{aligned}
R_2(M) \equiv & \int \frac{d^3\mathbf{k}d^3\mathbf{l}d^3\mathbf{q}}{(2\pi)^9} \frac{1}{(\mathbf{k}+\mathbf{l})^\mathbf{2} - \mathbf{p^2} - i\epsilon} \frac{2(\mathbf{k}\cdot\mathbf{l})}{\mathbf{l^2}+m_\pi^2} \frac{1}{\mathbf{q^2}+m_\pi^2} e^{-\frac{\mathbf{k^2}}{\lambda^2}-\frac{\mathbf{q}^2}{\lambda^2}} \\
= & H_1 \Bigg[-H_7(M) + (p^2 + m_\pi^2) H_6(M) \\
& + \int \frac{d^3\mathbf{k}d^3\mathbf{l}}{(2\pi)^6} \bigg(\frac{1}{\mathbf{l^2}+m_\pi^2} - \frac{1}{(\mathbf{k}+\mathbf{l})^\mathbf{2} - \mathbf{p^2} - i\epsilon} \bigg) e^{-\frac{\mathbf{k^2}}{\lambda^2}} \Bigg],
\end{aligned}
$$

$$
\begin{aligned}
R_3(M) \equiv & \int \frac{d^3\mathbf{k}d^3\mathbf{l}d^3\mathbf{q}}{(2\pi)^9} \frac{e^{-\frac{\mathbf{k^2}}{\lambda^2}}}{(\mathbf{k}+\mathbf{l})^\mathbf{2} - \mathbf{p^2} - i\epsilon} \frac{2(\mathbf{k}\cdot\mathbf{l})}{\mathbf{l^2}+m_\pi^2} \frac{e^{-\frac{\mathbf{q}^2}{\lambda^2}}}{(\mathbf{q}+\mathbf{l})^\mathbf{2} - \mathbf{p^2} - i\epsilon} \frac{1}{\mathbf{q^2}+m_\pi^2} \\
= & - W_{12}(M) + H_3 H_5(M) - W_{10} + (p^2 + m_\pi^2) W_9(M),
\end{aligned}
$$

$$
\begin{aligned}
R_4(M) \equiv & \int \frac{d^3\mathbf{k}d^3\mathbf{l}d^3\mathbf{q}}{(2\pi)^9} \frac{e^{-\frac{\mathbf{k^2}}{\lambda^2}}}{(\mathbf{k}+\mathbf{l})^\mathbf{2} - \mathbf{p^2} - i\epsilon} \frac{4(\mathbf{k}\cdot\mathbf{l})(\mathbf{q}\cdot\mathbf{l})}{\mathbf{l^2}+m_\pi^2} \frac{e^{-\frac{\mathbf{q}^2}{\lambda^2}}}{(\mathbf{q}+\mathbf{l})^\mathbf{2} - \mathbf{p^2} - i\epsilon} \\
= & W_{20}(M) - 2(p^2 + m_\pi^2) W_{13}(M) + 2\left(W_{14} - W_{15}(M)\right) + W_{17} \\
& + (p^2 + m_\pi^2)^2 W_1(M) - (2p^2 + m_\pi^2) W_2 + 2(p^2 + m_\pi^2) H_3 H_6(M) \\
& + H_3^2 H_4(M) - 2H_3^2 H_4(-ip). \qquad \text{(A.51)}
\end{aligned}
$$

$$
\begin{aligned}
W_1(M) \equiv& \int \frac{d^3\mathbf{k}d^3\mathbf{l}d^3\mathbf{q}}{(2\pi)^9} \frac{e^{-\frac{\mathbf{k^2}}{\lambda^2}}}{(\mathbf{k}+\mathbf{l})^\mathbf{2} - \mathbf{p^2} - i\epsilon} \frac{1}{\mathbf{l^2} + m_\pi^2} \frac{e^{-\frac{\mathbf{q}^2}{\lambda^2}}}{(\mathbf{q}+\mathbf{l})^\mathbf{2} - \mathbf{p^2} - i\epsilon} \\
=& \frac{2\pi}{\tilde{M}} \lambda^3 \left(\frac{1}{4\pi}\right)^5 \int_0^\infty dx \int_0^\infty dz e^{-\frac{x^2}{4} - \frac{z^2}{4} + \beta(x+z)} \left(e^{-\tilde{M}|x-z|} - e^{-\tilde{M}(x+z)} \right),
\end{aligned}
$$

$$
\begin{aligned}
W_2 \equiv& \int \frac{d^3\mathbf{k}d^3\mathbf{l}d^3\mathbf{q}}{(2\pi)^9} \frac{e^{-\frac{\mathbf{k^2}}{\lambda^2}}}{(\mathbf{k}+\mathbf{l})^\mathbf{2} - \mathbf{p^2} - i\epsilon} \frac{e^{-\frac{\mathbf{q}^2}{\lambda^2}}}{(\mathbf{q}+\mathbf{l})^\mathbf{2} - \mathbf{p^2} - i\epsilon} \\
=& \lambda^5 \left(\frac{1}{4\pi}\right)^4 \int_0^\infty dx e^{-\frac{x^2}{2} + 2\beta x},
\end{aligned}
$$

$$
\begin{aligned}
W_3(M) \equiv& \int \frac{d^3\mathbf{k}d^3\mathbf{l}d^3\mathbf{q}}{(2\pi)^9} \frac{1}{\mathbf{l^2} + m_\pi^2} \frac{e^{-\frac{\mathbf{k^2}}{\lambda^2}} e^{-\frac{\mathbf{q}^2}{\lambda^2}}}{(\mathbf{q}+\mathbf{l})^\mathbf{2} - \mathbf{p^2} - i\epsilon} \\
=& \left[\int \frac{d^3\mathbf{k}}{(2\pi)^3} e^{-\frac{\mathbf{k^2}}{\lambda^2}} \right] \int \frac{d^3\mathbf{l}}{(2\pi)^3} \int \frac{d^3\mathbf{q}}{(2\pi)^3} \frac{1}{\mathbf{l^2} + m_\pi^2} \frac{1}{(\mathbf{q}+\mathbf{l})^\mathbf{2} - \mathbf{p^2} - i\epsilon} e^{-\frac{\mathbf{q}^2}{\lambda^2}} \\
=& H_3 H_6(M),
\end{aligned}
$$

$$
\begin{aligned}
W_4(M) \equiv& \int \frac{d^3\mathbf{k}d^3\mathbf{l}d^3\mathbf{q}}{(2\pi)^9} \frac{e^{-\frac{\mathbf{k^2}}{\lambda^2}}}{(\mathbf{k}+\mathbf{l})^\mathbf{2} - \mathbf{p^2} - i\epsilon} \frac{\mathbf{k^2}}{\mathbf{l^2} + m_\pi^2} \frac{e^{-\frac{\mathbf{q}^2}{\lambda^2}}}{(\mathbf{q}+\mathbf{l})^\mathbf{2} - \mathbf{p^2} - i\epsilon} \\
=& \frac{\lambda^5}{8} \left(\frac{1}{4\pi}\right)^5 \frac{1}{\tilde{M}} \int d^3\mathbf{x} \int_0^\infty dz \frac{1}{|\mathbf{x}|^2} \left(6 - \mathbf{x^2}\right) e^{-\frac{\mathbf{x^2}}{4} - \frac{z^2}{4}} e^{\beta(|\mathbf{x}|+z)} \\
& \times \left(e^{-\tilde{M}||\mathbf{x}|-z|} - e^{-\tilde{M}(|\mathbf{x}|+z)} \right),
\end{aligned}
$$

$$
\begin{aligned}
W_5(M) \equiv& \int \frac{d^3\mathbf{k}d^3\mathbf{l}d^3\mathbf{q}}{(2\pi)^9} \frac{1}{(\mathbf{k}+\mathbf{l})^\mathbf{2} - \mathbf{p^2} - i\epsilon} \frac{1}{\mathbf{l^2} + m_\pi^2} \frac{1}{\mathbf{q^2} + m_\pi^2} e^{-\frac{\mathbf{k^2}}{\lambda^2} - \frac{\mathbf{q}^2}{\lambda^2}} \\
=& \int \frac{d^3\mathbf{k}d^3\mathbf{l}}{(2\pi)^6} \frac{e^{-\frac{\mathbf{k^2}}{\lambda^2}}}{(\mathbf{k}+\mathbf{l})^\mathbf{2} - \mathbf{p^2} - i\epsilon} \frac{1}{\mathbf{l^2} + m_\pi^2} \left[\int \frac{d^3\mathbf{q}}{(2\pi)^3} \frac{e^{-\frac{\mathbf{q}^2}{\lambda^2}}}{\mathbf{q^2} + m_\pi^2} \right] \\
=& H_1 H_6(M), \qquad \text{(A.52)}
\end{aligned}
$$

$$
\begin{aligned}
W_6 \equiv& \int \frac{d^3\mathbf{k} d^3\mathbf{l} d^3\mathbf{q}}{(2\pi)^9} \frac{1}{(\mathbf{k}+\mathbf{l})^\mathbf{2} - \mathbf{p}^\mathbf{2} - i\epsilon} \frac{1}{\mathbf{q}^\mathbf{2} + m_\pi^2} e^{-\frac{\mathbf{k}^\mathbf{2}}{\lambda^2} - \frac{\mathbf{q}^2}{\lambda^2}} \\
=& \left[\int \frac{d^3\mathbf{k}}{(2\pi)^3} e^{-\frac{\mathbf{k}^\mathbf{2}}{\lambda^2}} \right] \left[\int \frac{d^3\mathbf{l}}{(2\pi)^3} \frac{1}{\mathbf{l}^\mathbf{2} - \mathbf{p}^\mathbf{2} - i\epsilon} \right] \left[\int \frac{d^3\mathbf{q}}{(2\pi)^3} \frac{1}{\mathbf{q}^\mathbf{2} + m_\pi^2} e^{-\frac{\mathbf{q}^2}{\lambda^2}} \right] \\
=& W_7(-ip),
\end{aligned}
$$

$$
\begin{aligned}
W_7(M) \equiv& \int \frac{d^3\mathbf{k} d^3\mathbf{l} d^3\mathbf{q}}{(2\pi)^9} \frac{1}{\mathbf{l}^\mathbf{2} + m_\pi^2} \frac{1}{\mathbf{q}^\mathbf{2} + m_\pi^2} e^{-\frac{\mathbf{k}^\mathbf{2}}{\lambda^2} - \frac{\mathbf{q}^2}{\lambda^2}} \\
=& \left[\int \frac{d^3\mathbf{k}}{(2\pi)^3} e^{-\frac{\mathbf{k}^\mathbf{2}}{\lambda^2}} \right] \left[\int \frac{d^3\mathbf{l}}{(2\pi)^3} \frac{1}{\mathbf{l}^\mathbf{2} + m_\pi^2} \right] \left[\int \frac{d^3\mathbf{q}}{(2\pi)^3} \frac{1}{\mathbf{q}^\mathbf{2} + m_\pi^2} e^{-\frac{\mathbf{q}^2}{\lambda^2}} \right] \\
=& H_1 H_3 H_4(M),
\end{aligned}
$$

$$
\begin{aligned}
W_8(M) \equiv& \int \frac{d^3\mathbf{k} d^3\mathbf{l} d^3\mathbf{q}}{(2\pi)^9} \frac{e^{-\frac{\mathbf{k}^\mathbf{2}}{\lambda^2}}}{(\mathbf{k}+\mathbf{l})^\mathbf{2} - \mathbf{p}^\mathbf{2} - i\epsilon} \frac{\mathbf{k}^\mathbf{2}}{\mathbf{l}^\mathbf{2} + m_\pi^2} \frac{e^{-\frac{\mathbf{q}^2}{\lambda^2}}}{\mathbf{q}^\mathbf{2} + m_\pi^2} \\
=& H_3 H_7(M),
\end{aligned}
$$

$$
\begin{aligned}
W_9(M) \equiv& \int \frac{d^3\mathbf{k} d^3\mathbf{l} d^3\mathbf{q}}{(2\pi)^9} \frac{e^{-\frac{\mathbf{k}^\mathbf{2}}{\lambda^2}}}{(\mathbf{k}+\mathbf{l})^\mathbf{2} - \mathbf{p}^\mathbf{2} - i\epsilon} \frac{1}{\mathbf{l}^\mathbf{2} + m_\pi^2} \frac{e^{-\frac{\mathbf{q}^2}{\lambda^2}}}{(\mathbf{q}+\mathbf{l})^\mathbf{2} - \mathbf{p}^\mathbf{2} - i\epsilon} \frac{1}{\mathbf{q}^\mathbf{2} + m_\pi^2} \\
=& \frac{2\lambda}{\tilde{M}} \left(\frac{1}{4\pi} \right)^4 \int_0^\infty dx \int_0^\infty dw \int_0^\infty \frac{dz}{z} e^{-x^2 - z^2 - w^2 + 2\beta(x+z) - 2\alpha w} \\
& \times \left(e^{-2\tilde{M}|x-z|} - e^{-2\tilde{M}(x+z)} \right) \left(e^{2zw} - e^{-2zw} \right),
\end{aligned}
$$

$$
\begin{aligned}
W_{10} \equiv& \int \frac{d^3\mathbf{k} d^3\mathbf{l} d^3\mathbf{q}}{(2\pi)^9} \frac{e^{-\frac{\mathbf{k}^\mathbf{2}}{\lambda^2}}}{(\mathbf{k}+\mathbf{l})^\mathbf{2} - \mathbf{p}^\mathbf{2} - i\epsilon} \frac{e^{-\frac{\mathbf{q}^2}{\lambda^2}}}{(\mathbf{q}+\mathbf{l})^\mathbf{2} - \mathbf{p}^\mathbf{2} - i\epsilon} \frac{1}{\mathbf{q}^\mathbf{2} + m_\pi^2} \\
=& 2\lambda^3 \left(\frac{1}{4\pi} \right)^4 \int_0^\infty \frac{dx}{x} e^{-2x^2 + 4\beta x} \int_0^\infty dz e^{-z^2 - 2\alpha z} \left(e^{2xz} - e^{-2xz} \right),
\end{aligned} \tag{A.53}
$$

$$
\begin{aligned}
W_{11}(M) \equiv & \int \frac{d^3\mathbf{k}d^3\mathbf{l}d^3\mathbf{q}}{(2\pi)^9} \frac{1}{\mathbf{l^2}+m_\pi^2} \frac{1}{(\mathbf{q}+\mathbf{l})^\mathbf{2}-\mathbf{p^2}-i\epsilon} \frac{1}{\mathbf{q^2}+m_\pi^2} e^{-\frac{\mathbf{k^2}}{\lambda^2}-\frac{\mathbf{q}^2}{\lambda^2}} \\
= & \left[\int \frac{d^3\mathbf{k}}{(2\pi)^3} e^{-\frac{\mathbf{k^2}}{\lambda^2}}\right] \int \frac{d^3\mathbf{l}d^3\mathbf{q}}{(2\pi)^6} \frac{1}{\mathbf{l^2}-\mathbf{p^2}-i\epsilon} \frac{1}{(\mathbf{l}-\mathbf{q})^\mathbf{2}+m_\pi^2} \frac{e^{-\frac{\mathbf{q}^2}{\lambda^2}}}{\mathbf{q^2}+m_\pi^2} \\
= & H_3 H_5(M),
\end{aligned}
$$

$$
\begin{aligned}
W_{12}(M) \equiv & \int \frac{d^3\mathbf{k}d^3\mathbf{l}d^3\mathbf{q}}{(2\pi)^9} \frac{\mathbf{k^2} e^{-\frac{\mathbf{k^2}}{\lambda^2}}}{(\mathbf{k}+\mathbf{l})^\mathbf{2}-\mathbf{p^2}-i\epsilon} \frac{1}{\mathbf{l^2}+m_\pi^2} \frac{1}{(\mathbf{q}+\mathbf{l})^\mathbf{2}-\mathbf{p^2}-i\epsilon} \frac{e^{-\frac{\mathbf{q}^2}{\lambda^2}}}{\mathbf{q^2}+m_\pi^2} \\
= & \frac{\lambda^3}{\tilde{M}} \left(\frac{1}{4\pi}\right)^4 \int_0^\infty dx \int_0^\infty \frac{dz}{z} \left(3-2x^2\right) e^{-(x^2+z^2)} e^{2\beta(x+z)} \\
& \times \left(e^{-2\tilde{M}|x-z|} - e^{-2\tilde{M}(x+z)}\right) \\
& \times \left[e^{(\alpha-z)^2} Er\left(\alpha-z\right) - e^{(\alpha+z)^2} Er\left(\alpha+z\right)\right],
\end{aligned}
$$

$$
\begin{aligned}
W_{13}(M) \equiv & \int \frac{d^3\mathbf{k}d^3\mathbf{l}d^3\mathbf{q}}{(2\pi)^9} \frac{e^{-\frac{\mathbf{k^2}}{\lambda^2}}}{(\mathbf{k}+\mathbf{l})^\mathbf{2}-\mathbf{p^2}-i\epsilon} \frac{\mathbf{k^2}}{\mathbf{l^2}+m_\pi^2} \frac{e^{-\frac{\mathbf{q}^2}{\lambda^2}}}{(\mathbf{q}+\mathbf{l})^\mathbf{2}-\mathbf{p^2}-i\epsilon} \\
= & \frac{2\pi}{\tilde{M}} \lambda^5 \pi \left(\frac{1}{4\pi}\right)^7 \int_0^\infty dz \int d^3\mathbf{x}(6-\mathbf{x^2}) \frac{1}{|\mathbf{x}|^2} e^{-\frac{\mathbf{x^2}}{4}-\frac{z^2}{4}+\beta(|\mathbf{x}|+z)} \\
& \times \left(e^{-\tilde{M}|x-z|} - e^{-\tilde{M}(x+z)}\right),
\end{aligned}
$$

$$
\begin{aligned}
W_{14} \equiv & \int \frac{d^3\mathbf{k}d^3\mathbf{l}d^3\mathbf{q}}{(2\pi)^9} \frac{\mathbf{k^2}}{(\mathbf{k}+\mathbf{l})^\mathbf{2}-\mathbf{p^2}-i\epsilon} \frac{1}{(\mathbf{q}+\mathbf{l})^\mathbf{2}-\mathbf{p^2}-i\epsilon} e^{-\frac{\mathbf{k^2}}{\lambda^2}-\frac{\mathbf{q}^2}{\lambda^2}} \\
= & \lambda^7 \pi \left(\frac{1}{4\pi}\right)^5 \int_0^\infty dx (6-x^2) e^{-\frac{x^2}{2}+2\beta x},
\end{aligned}
$$

$$
\begin{aligned}
W_{15}(M) \equiv & \int \frac{d^3\mathbf{k}d^3\mathbf{l}d^3\mathbf{q}}{(2\pi)^9} \frac{\mathbf{k^2}}{(\mathbf{k}+\mathbf{l})^\mathbf{2}-\mathbf{p^2}-i\epsilon} \frac{1}{\mathbf{l^2}+m_\pi^2} e^{-\frac{\mathbf{k^2}}{\lambda^2}-\frac{\mathbf{q}^2}{\lambda^2}} \\
= & H_3 H_7(M), \qquad \text{(A.54)}
\end{aligned}
$$

$$
\begin{aligned}
W_{19} \equiv& \int \frac{d^3\mathbf{k}d^3\mathbf{l}d^3\mathbf{q}}{(2\pi)^9} \frac{1}{(\mathbf{k}+\mathbf{l})^\mathbf{2} - \mathbf{p}^\mathbf{2} - i\epsilon} e^{-\frac{\mathbf{k}^\mathbf{2}}{\lambda^2} - \frac{\mathbf{q}^2}{\lambda^2}} \\
=& H_3^2 H_4(M = -ip),
\end{aligned}
$$

$$
\begin{aligned}
W_{20}(M) \equiv& \int \frac{d^3\mathbf{k}d^3\mathbf{l}d^3\mathbf{q}}{(2\pi)^9} \frac{e^{-\frac{\mathbf{k}^\mathbf{2}}{\lambda^2}}}{(\mathbf{k}+\mathbf{l})^\mathbf{2} - \mathbf{p}^\mathbf{2} - i\epsilon} \frac{\mathbf{k}^\mathbf{2}\mathbf{q}^\mathbf{2}}{\mathbf{l}^\mathbf{2} + m_\pi^2} \frac{e^{-\frac{\mathbf{q}^2}{\lambda^2}}}{(\mathbf{q}+\mathbf{l})^\mathbf{2} - \mathbf{p}^\mathbf{2} - i\epsilon} \\
=& \frac{\lambda^7}{2} \frac{1}{\tilde{M}} \left(\frac{1}{4\pi}\right)^4 \int_0^\infty dx \int_0^\infty dz \left(3 - 2x^2\right) \left(3 - 2z^2\right) e^{-x^2 - z^2 + 2\beta(x+z)} \\
& \times \left(e^{-2\tilde{M}|x-z|} - e^{-2\tilde{M}(x+z)}\right),
\end{aligned} \tag{A.55}
$$

$$
\begin{aligned}
[U_9 H_0 X_1] \equiv& \int \frac{d^3\mathbf{k}d^3\mathbf{l}d^3\mathbf{q}}{(2\pi)^9} \left[\frac{1}{\mathbf{l}^\mathbf{2} - \mathbf{p}^\mathbf{2} - i\epsilon} - \frac{1}{\mathbf{l}^\mathbf{2}}\right] \\
& \times \frac{1}{(\mathbf{k}+\mathbf{l})^\mathbf{2} - \mathbf{p}^\mathbf{2} - i\epsilon} \left[\frac{1}{(\mathbf{q}+\mathbf{l})^\mathbf{2} - \mathbf{p}^\mathbf{2} - i\epsilon} - \frac{1}{\mathbf{q}^\mathbf{2} + m_\pi^2}\right] e^{-\frac{\mathbf{k}^\mathbf{2}}{\lambda^2} - \frac{\mathbf{q}^\mathbf{2}}{\lambda^2}} \\
=& \Delta W_1(-ip) - \Delta W_5(-ip),
\end{aligned}
$$

$$
\begin{aligned}
\left[H_0 X_1^2\right] \equiv& \int \frac{d^3\mathbf{k}d^3\mathbf{l}d^3\mathbf{q}}{(2\pi)^9} \frac{1}{\mathbf{l}^\mathbf{2} - \mathbf{p}^\mathbf{2} - i\epsilon} \left[\frac{1}{(\mathbf{k}+\mathbf{l})^\mathbf{2} - \mathbf{p}^\mathbf{2} - i\epsilon} - \frac{1}{\mathbf{k}^\mathbf{2} + m_\pi^2}\right] \\
& \times \left[\frac{1}{(\mathbf{q}+\mathbf{l})^\mathbf{2} - \mathbf{p}^\mathbf{2} - i\epsilon} - \frac{1}{\mathbf{q}^\mathbf{2} + m_\pi^2}\right] e^{-\frac{\mathbf{k}^\mathbf{2}}{\lambda^2} - \frac{\mathbf{q}^\mathbf{2}}{\lambda^2}}. \\
=& W_1(-ip) - 2H_1 H_6(-ip) + H_1^2 H_4(-ip),
\end{aligned}
$$

$$
\begin{aligned}
\left[U_9 X_1^2\right] \equiv& \int \frac{d^3\mathbf{k}d^3\mathbf{l}d^3\mathbf{q}}{(2\pi)^9} \left[\frac{1}{\mathbf{l}^\mathbf{2} - \mathbf{p}^\mathbf{2} - i\epsilon} - \frac{1}{\mathbf{l}^\mathbf{2}}\right] \left[\frac{1}{(\mathbf{k}+\mathbf{l})^\mathbf{2} - \mathbf{p}^\mathbf{2} - i\epsilon} - \frac{1}{\mathbf{k}^\mathbf{2} + m_\pi^2}\right] \\
& \times \left(\frac{1}{(\mathbf{q}+\mathbf{l})^\mathbf{2} - \mathbf{p}^\mathbf{2} - i\epsilon} - \frac{1}{\mathbf{q}^\mathbf{2} + m_\pi^2}\right) e^{-\frac{\mathbf{k}^\mathbf{2}}{\lambda^2} - \frac{\mathbf{q}^\mathbf{2}}{\lambda^2}} \\
=& \Delta W_1(-ip) - 2\Delta W_5(-ip) + H_1^2 \Delta H_4(-ip).
\end{aligned} \tag{A.56}
$$

$$
\begin{aligned}
[H_0 J_4] \equiv & \int \frac{d^3\mathbf{k} d^3\mathbf{l} d^3\mathbf{q}}{(2\pi)^9} \frac{e^{-\frac{(\mathbf{l}-\mathbf{q})^2}{\lambda^2}}}{\mathbf{q^2}-\mathbf{p^2}-i\epsilon} \frac{e^{-\frac{(\mathbf{k}-\mathbf{l})^2}{\lambda^2}}}{\mathbf{k^2}-\mathbf{p^2}-i\epsilon} \frac{1}{\mathbf{l^2}} \frac{1}{(\mathbf{k}-\mathbf{l})^2+m_\pi^2} \\
=& W_9(M \to 0) \\
=& \left(\frac{1}{4\pi}\right)^3 e^{\alpha^2} \Bigg[- \left(\frac{\lambda}{\sqrt{\pi}} + ip - \frac{2p^2}{\sqrt{\pi}\lambda}\right) \log\left(\frac{m_\pi - ip}{\lambda}\right) \\
& + \frac{\lambda}{\sqrt{\pi}} \left(-1 + \sqrt{2} - \frac{\gamma_E}{2} - \sinh^{-1}(1)\right) + \frac{m_\pi}{2} \\
& - ip \left\{ \frac{1 + 2Catalan}{\pi} + \frac{1}{2}(1+\gamma_E) \right\} + i\frac{8 m_\pi p}{3\sqrt{\pi}\lambda} + \left(\frac{5-4\sqrt{2}}{6}\right) \frac{m_\pi^2}{\sqrt{\pi}\lambda} \\
& + \frac{p^2}{6\sqrt{\pi}\lambda} \left(13 + 4\sqrt{2} + 6\gamma_E + 12\sinh^{-1}(1)\right) \Bigg] + O\left(\frac{1}{\lambda^2}\right).
\end{aligned}
\tag{A.57}
$$

$$
\begin{aligned}
[H_0 V_2] \equiv & \int \frac{d^3\mathbf{k} d^3\mathbf{l} d^3\mathbf{q}}{(2\pi)^9} \frac{e^{-\frac{(\mathbf{l}-\mathbf{q})^2}{\lambda^2}}}{\mathbf{q^2}-\mathbf{p^2}-i\epsilon} \frac{e^{-\frac{(\mathbf{k}-\mathbf{l})^2}{\lambda^2}}}{\mathbf{k^2}-\mathbf{p^2}-i\epsilon} \frac{1}{\mathbf{l^2}-\mathbf{p^2}-i\epsilon} \frac{1}{(\mathbf{k}-\mathbf{l})^2+m_\pi^2} \\
=& W_9(M = -ip) \\
=& \left(\frac{1}{4\pi}\right)^3 e^{\alpha^2} \Bigg[- \left(\frac{\lambda}{\sqrt{\pi}} + ip - \frac{8p^2}{3\sqrt{\pi}\lambda}\right) \log\left(\frac{m_\pi - 2ip}{\lambda}\right) \\
& + \frac{\lambda}{\sqrt{\pi}} \left(-1 + \sqrt{2} - \frac{\gamma_E}{2} - \sinh^{-1}(1)\right) + \frac{m_\pi}{2} \\
& - ip \left\{ \frac{3 + 2Catalan}{\pi} + \frac{1+\gamma_E}{2} \right\} + i\frac{8 m_\pi p}{3\sqrt{\pi}\lambda} + \left(\frac{5-4\sqrt{2}}{6}\right) \frac{m_\pi^2}{\sqrt{\pi}\lambda} \\
& + \frac{2p^2}{9\sqrt{\pi}\lambda} \left\{31 - 2\sqrt{2} + 6\gamma_E + 12\sinh^{-1}(1)\right\} \Bigg] + O\left(\frac{1}{\lambda^2}\right),
\end{aligned}
\tag{A.58}
$$

$$
\begin{aligned}
V_8 =& \int \frac{d^3k}{(2\pi)^3} \int \frac{d^3l}{(2\pi)^3} \int \frac{d^3q}{(2\pi)^3} \frac{1}{\mathbf{k}^2 - p^2 - i\epsilon} \frac{1}{\mathbf{l}^2 - p^2 - i\epsilon} \frac{1}{\mathbf{q}^2 - p^2 - i\epsilon} \\
& \qquad \times \frac{1}{(\mathbf{k}-\mathbf{l})^2 + m_\pi^2} \frac{1}{(\mathbf{l}-\mathbf{q})^2 + m_\pi^2} e^{-\frac{(\mathbf{k}-\mathbf{l})^2}{\lambda^2}} e^{-\frac{(\mathbf{l}-\mathbf{q})^2}{\lambda^2}} \\
=& -\left(\frac{1}{4\pi}\right)^3 \frac{i}{p} e^{\frac{2m_\pi^2}{\lambda^2}} \left\{ -\mathrm{Li}_2\left(\frac{m_\pi}{2ip - m_\pi}\right) - \frac{\pi^2}{12} \right. \\
& \left. + \frac{4p}{i\sqrt{\pi}\lambda}\left[\sqrt{2} - \log\left(\frac{m_\pi - 2ip}{\lambda}\right) - \sinh^{-1}(1) - \frac{\gamma_E}{2}\right]\right\} + \mathcal{O}(\lambda^{-2}),
\end{aligned}
\tag{A.59}
$$

$$
\begin{aligned}
J_2 =& \int \frac{d^3k}{(2\pi)^3} \int \frac{d^3l}{(2\pi)^3} \int \frac{d^3q}{(2\pi)^3} \frac{1}{\mathbf{l}^2} \frac{1}{\mathbf{k}^2 - p^2 - i\epsilon} \frac{1}{\mathbf{q}^2 - p^2 - i\epsilon} \\
& \qquad \times \frac{1}{(\mathbf{k}-\mathbf{l})^2 + m_\pi^2} \frac{1}{(\mathbf{l}-\mathbf{q})^2 + m_\pi^2} e^{-\frac{(\mathbf{k}-\mathbf{l})^2}{\lambda^2}} e^{-\frac{(\mathbf{l}-\mathbf{q})^2}{\lambda^2}} \\
=& \left(\frac{1}{4\pi}\right)^3 e^{\frac{2m_\pi^2}{\lambda^2}} \left\{ \frac{\log(4)}{m_\pi - ip} \right. \\
& \left. + \frac{4}{\sqrt{\pi}\lambda}\left[\log\left(\frac{m_\pi - ip}{\lambda}\right) + \sinh^{-1}(1) + \frac{\gamma}{2} - \sqrt{2}\right]\right\} + \mathcal{O}(\lambda^{-2}),
\end{aligned}
\tag{A.60}
$$

$$
\begin{aligned}
J_3 =& \int \frac{d^3k}{(2\pi)^3} \int \frac{d^3l}{(2\pi)^3} \int \frac{d^3q}{(2\pi)^3} \frac{1}{\mathbf{k}^2 - p^2 - i\epsilon} \frac{1}{\mathbf{q}^2 - p^2 - i\epsilon} \\
& \qquad \times \frac{1}{(\mathbf{k}-\mathbf{l})^2 + m_\pi^2} \frac{1}{(\mathbf{l}-\mathbf{q})^2 + m_\pi^2} e^{-\frac{(\mathbf{k}-\mathbf{l})^2}{\lambda^2}} e^{-\frac{(\mathbf{l}-\mathbf{q})^2}{\lambda^2}} \\
=& 2\lambda \left(\frac{1}{4\pi}\right)^4 e^{\frac{2m_\pi^2}{\lambda^2}} \left\{ 4\sqrt{\pi}\sinh^{-1}(1) \right. \\
& - \frac{2m_\pi \pi}{\lambda}\left[1 - \gamma_E - \log(4)\right] + 4\pi \frac{m_\pi - ip}{\lambda} \log\left(\frac{m_\pi - ip}{\lambda}\right) \\
& + \frac{4ip}{\lambda}\left[-2Catalan + \gamma\sqrt{\pi} + \pi\left(1 - \frac{3}{2}\gamma - 3\log(2)\right)\right] \\
& \left. + \frac{16ipm_\pi\sqrt{\pi}}{\lambda^2} + \frac{4\sqrt{\pi}m_\pi^2}{\lambda^2}\left[-\sqrt{2} + \sinh^{-1}(1)\right]\right\} + \mathcal{O}(\lambda^{-2}),
\end{aligned}
\tag{A.61}
$$

$$
\begin{aligned}
J_5 =& \frac{1}{\omega^2}\int\frac{d^3k}{(2\pi)^3}\int\frac{d^3l}{(2\pi)^3}\int\frac{d^3q}{(2\pi)^3}\left(\frac{1}{\mathbf{l}^2+\omega^2}-\frac{1}{\mathbf{l}^2}\right)\frac{1}{\mathbf{k}^2-p^2-i\epsilon}\frac{1}{\mathbf{q}^2-p^2-i\epsilon}\\
&\times\frac{e^{-\frac{(\mathbf{k}-\mathbf{l})^2}{\lambda^2}}}{(\mathbf{k}-\mathbf{l})^2+m_\pi^2}\frac{e^{-\frac{(\mathbf{l}-\mathbf{q})^2}{\lambda^2}}}{(\mathbf{l}-\mathbf{q})^2+m_\pi^2}\\
=&\left(\frac{1}{4\pi}\right)^3 e^{\frac{2m_\pi^2}{\lambda^2}}\left\{\frac{1}{\omega}\left[-\frac{1}{(m_\pi-ip)^2}+\frac{4}{\sqrt{\pi}\lambda(m_\pi-ip)}\right]+\frac{1+\log(4)}{3(m_\pi-ip)^3}\right.\\
&\left.-\frac{2}{\sqrt{\pi}\lambda(m_\pi-ip)^2}\right\}+\mathcal{O}\left(\lambda^{-2},\omega\right), \qquad \text{(A.62)}
\end{aligned}
$$

$$
\begin{aligned}
J_6 =& \frac{1}{\omega^2}\int\frac{d^3l}{(2\pi)^3}\int\frac{d^3k}{(2\pi)^3}\left(\frac{1}{\mathbf{l}^2+\omega^2}-\frac{1}{\mathbf{l}^2}\right)\frac{1}{\mathbf{k}^2-p^2-i\epsilon}\frac{e^{-\frac{(\mathbf{k}-\mathbf{l})^2}{\lambda^2}}}{(\mathbf{k}-\mathbf{l})^2+m_\pi^2}\\
=&\left(\frac{1}{4\pi}\right)^2 e^{\frac{m_\pi^2}{\lambda^2}}\left[\frac{1}{\omega}\left(-\frac{1}{m_\pi-ip}+\frac{2}{\sqrt{\pi}\lambda}\right)+\frac{1}{2(m_\pi-ip)^2}\right]+\mathcal{O}\left(\lambda^{-2},\omega\right), \qquad \text{(A.63)}
\end{aligned}
$$

$$
J_8 = \frac{1}{\omega^2}\int\frac{d^3l}{(2\pi)^3}\left(\frac{1}{\mathbf{l}^2+\omega^2}-\frac{1}{\mathbf{l}^2}\right) = -\frac{1}{4\pi}\frac{1}{\omega}, \qquad \text{(A.64)}
$$

$$
\begin{aligned}
\mathrm{Box}_0 =& \int_{-1}^{1} d\cos\theta \int \frac{d^3k}{(2\pi)^3} \frac{1}{(k^2+2\mathbf{k}\cdot\mathbf{p})\,(\mathbf{k}^2+m_\pi^2)\,((\mathbf{k}-\mathbf{q})^2+m_\pi^2)} \\
=&\frac{1}{8p^3\pi}\left[\frac{i}{4}\log^2\left(1+\frac{4p^2}{m_\pi^2}\right)\right. \\
&\left.+\mathrm{ImLi}_2\left(\frac{im_\pi p-2p^2}{m_\pi^2}\right)+\mathrm{ImLi}_2\left(\frac{2p^2-im_\pi p}{m_\pi^2+4p^2}\right)\right], \qquad \text{(A.65)}
\end{aligned}
$$

$$
\begin{aligned}
\mathrm{Box}_1 =& \int_{-1}^{1} d\cos\theta \int \frac{d^3k}{(2\pi)^3} \frac{(1-\cos\theta)}{(k^2+2\mathbf{k}\cdot\mathbf{p})\,(\mathbf{k}^2+m_\pi^2)\,((\mathbf{k}-\mathbf{q})^2+m_\pi^2)} \\
=&\frac{1}{8p^3\pi}\left\{-i-\frac{m_\pi^3}{2p^3}\log\left(1+\frac{p^2}{m_\pi^2}\right)-\frac{i}{4}\left(\frac{m_\pi^4}{4p^4}+\frac{m_\pi^2}{p^2}\right)\log^2\left(\frac{4p^2}{m_\pi^2}+1\right)\right. \\
&+\frac{(m_\pi^2+2p^2)}{p^2}\tan^{-1}\left(\frac{m_\pi p}{m_\pi^2+2p^2}\right)+i\left(\frac{m_\pi^2}{2p^2}+1\right)\log\left(\frac{4p^2}{m_\pi^2}+1\right) \\
&\left.-\left(\frac{m_\pi^4}{4p^4}+\frac{m_\pi^2}{p^2}\right)\left[\mathrm{ImLi}_2\left(\frac{im_\pi p-2p^2}{m_\pi^2}\right)+\mathrm{ImLi}_2\left(\frac{2p^2-im_\pi p}{m_\pi^2+4p^2}\right)\right]\right\}, \\
&\qquad \text{(A.66)}
\end{aligned}
$$

$$
\begin{aligned}
\mathrm{Box}_2 =& \int_{-1}^{1} d\cos\theta \int \frac{d^3k}{(2\pi)^3} \frac{(1-\cos\theta)^2}{(k^2+2\mathbf{k}\cdot\mathbf{p})\,(\mathbf{k}^2+m_\pi^2)\,((\mathbf{k}-\mathbf{q})^2+m_\pi^2)} \\
=&\frac{1}{6p^3\pi}\left\{-\frac{3m_\pi^3}{8p^3}+\left(\frac{9m_\pi^7}{64p^7}+\frac{15m_\pi^5}{16p^5}\right)\log\left(\frac{p^2}{m_\pi^2}+1\right)\right. \\
&-\frac{3}{4}\left(\frac{m_\pi^2}{2p^2}+1\right)\left(\frac{3m_\pi^4}{4p^4}+\frac{3m_\pi^2}{p^2}-2\right)\tan^{-1}\left(\frac{m_\pi p}{m_\pi^2+2p^2}\right) \\
&+\frac{3}{8}i\left[\frac{3m_\pi^4}{4p^4}+\frac{3m_\pi^2}{p^2}+\frac{3}{4}\left(\frac{m_\pi^4}{4p^4}+\frac{m_\pi^2}{p^2}\right)^2\log^2\left(\frac{4p^2}{m_\pi^2}+1\right)\right. \\
&\left.+\left(-\frac{m_\pi^2}{2p^2}-1\right)\left(\frac{3m_\pi^4}{4p^4}+\frac{3m_\pi^2}{p^2}-2\right)\log\left(\frac{4p^2}{m_\pi^2}+1\right)-1\right] \\
&\left.+\frac{9}{8}\left(\frac{m_\pi^4}{4p^4}+\frac{m_\pi^2}{p^2}\right)^2\left[\mathrm{ImLi}_2\left(\frac{im_\pi p-2p^2}{m_\pi^2}\right)+\mathrm{ImLi}_2\left(\frac{2p^2-im_\pi p}{m_\pi^2+4p^2}\right)\right]\right\}. \\
&\qquad \text{(A.67)}
\end{aligned}
$$

A.4 Table of Integral formulae

We show the table of integrals appear in loop integral. Intervals of integration of all integrals are $(0, \infty)$

Integrand	Value
$e^{-x^2}\log(x)$	$-\frac{\sqrt{\pi}}{4}\left[\gamma_E + 2\log(2)\right]$
$xe^{-x^2}\log(x)$	$-\frac{\gamma_E}{4}$
$e^{-x^2}\mathrm{Erfc}(x)$	$\frac{\pi}{8}$
$xe^{-x^2}\mathrm{Erfc}(x)$	$\frac{\sqrt{\pi}}{8}\left(2-\sqrt{\pi}\right)$
$\mathrm{Erfc}(x)\log(x)$	$\frac{\sqrt{\pi}}{8}\left(2-\sqrt{\pi}\right)$
$e^{-x^2}\mathrm{Erfc}(x)\log(x)$	$-\frac{\pi\gamma_E}{16}+\frac{1}{8}\left(-2Catalan - \pi\log(2)\right)$
$xe^{-x^2}\mathrm{Erfc}(x)\log(x)$	$\frac{\sqrt{\pi}}{16}\left[\left(\sqrt{2}-2\right)\gamma_E - 4\sinh^{-1}(1) + \sqrt{2}\log(8)\right]$
$[\mathrm{Erfc}(x)]^2$	$\frac{\sqrt{\pi}}{4}\left(2-\sqrt{2}\right)$

Appendix B

Wilsonian RG analysis for the P waves

In this section, we show the results of Wilsonian RG analysis for the P-wave nucleon-nucleon scattering including pions. The phase shift calculation for P-wave has to be based on this analysis [21].

B.1 The RGEs for the P waves in the NEFT without pions

The RGEs for the P waves in the NEFT without pions to the next-to-leading order are obtained in [22] . With suitable redefinitions of dimensionless coupling constants, they take the same form in all the channels:

$$\frac{dx}{dt} = -3x - (x+y+z)^2, \tag{B.1}$$

$$\frac{dy}{dt} = -5y - \left(\frac{1}{2}x^2 + 2xy + \frac{3}{2}y^2 + yz - \frac{1}{2}z^2\right), \tag{B.2}$$

$$\frac{dz}{dt} = -5z + \left(\frac{1}{2}x^2 + xy - xz + \frac{1}{2}y^2 - yz - \frac{3}{2}z^2\right), \tag{B.3}$$

where x, y, z are dimensionless coupling constants for the leading-order, the next-to-leading-order, and the redundant operators. The parameter t is defines as $t = \ln(\Lambda_0/\Lambda)$. See Ref. [22] for details. Even though there is a nontrivial fixed point, it does not seem to be important for the realistic two-nucleon systems in the P waves.

B.2 Pion exchange in the P waves

In the (naive) KSW power counting [11], the leading-order (Q^0) contribution consists solely of the single-pion exchange. The order Q contribution comes from the potential-box diagram, and the four nucleon operators contribute only in higher orders in Q. This is a very strange situation however. The cutoff dependence of the potential-box diagram should be absorbed by contact terms, but there seem no such terms at the order. Is the power counting inconsistent?

The crucial observation is that the one-pion exchange in the P waves is different from that in the S waves. Actually, the momentum-dependence of the one-pion exchange in the P waves are

$$F_{\gamma S} = \left(\frac{2\pi^2}{M\Lambda}\right)\left(\frac{3m_\pi^2}{2}\right)\left[\frac{1}{r_{13}+m_\pi^2} - \frac{1}{r_{14}+m_\pi^2}\right], \tag{B.4}$$

$$F_{\gamma T}^{kj} = \left(\frac{2\pi^2}{M\Lambda}\right)\left\{\delta^{kj}\left(\frac{m_\pi^2}{2}\right)\left[\frac{1}{r_{13}+m_\pi^2} - \frac{1}{r_{14}+m_\pi^2}\right] + \left[\frac{p_{13}^k p_{13}^j}{r_{13}+m_\pi^2} - \frac{p_{14}^k p_{14}^j}{r_{14}+m_\pi^2}\right]\right\}, \tag{B.5}$$

where $\vec{p}_{ij} \equiv \vec{p}_i - \vec{p}_j$, $r_{ij} \equiv |\vec{p}_{ij}|^2$ with $\vec{p}_i$ being an external momentum, M and Λ are the nucleon mass and the floating cutoff respectively. Note that there is a minus sign between the t- and u-channel contributions. Because of this sign, the leading-order terms with large momentum transfer cancel. It effectively demotes the pion exchange to the order of the leading contact interaction.

B.3 RGEs

In this section, we present sets of RGEs for the case including pions for all the channels in the P waves up to the next-to-leading order. The contributions from the contact interactions are the same as in Eqs. (B.1) – (B.3), so that we show them as “(pionless).” The dimensionless coupling constant γ denotes the strength of the pion exchange, and satisfies

$$\frac{d}{dt}\gamma = -\gamma. \tag{B.6}$$

An additional contact operator which is proportional to m_π^2 appears to this order. The corresponding dimensionless coupling constant is denoted by

u. The contribution from the contact terms to the RGE for u is given by

$$\frac{du}{dt} = -3u - 2(x+y+z)u. \tag{B.7}$$

$^1P_1$ channel:

In this channel, there is no tensor force. Only the coupling u receives the contribution from the pion exchange.

$$\frac{du}{dt} = \text{(pionless)} + 4(x+y+z)\gamma. \tag{B.8}$$

$^3P_0$ channel:

In this channel, the tensor force is attractive.

$$\frac{dx}{dt} = \text{(pionless)} - \frac{8}{3}(x+y+z)\gamma - \frac{16}{9}\gamma^2, \tag{B.9}$$
$$\frac{dy}{dt} = \text{(pionless)} - \frac{4}{15}(4x+9y-z)\gamma - \frac{8}{15}\gamma^2, \tag{B.10}$$
$$\frac{dz}{dt} = \text{(pionless)} + \frac{4}{3}(x+y-z)\gamma + \frac{8}{9}\gamma^2, \tag{B.11}$$
$$\frac{du}{dt} = \text{(pionless)} + \frac{4}{3}(x+y+z-2u)\gamma + \frac{16}{9}\gamma^2. \tag{B.12}$$

$^3P_1$ channel:

In this channel, the tensor force is repulsive.

$$\frac{dx}{dt} = \text{(pionless)} + \frac{4}{3}(x+y+z)\gamma - \frac{4}{9}\gamma^2, \tag{B.13}$$
$$\frac{dy}{dt} = \text{(pionless)} + \frac{2}{15}(4x+9y-z)\gamma - \frac{2}{15}\gamma^2, \tag{B.14}$$
$$\frac{dz}{dt} = \text{(pionless)} - \frac{2}{3}(x+y-z)\gamma + \frac{2}{9}\gamma^2, \tag{B.15}$$
$$\frac{du}{dt} = \text{(pionless)} + \frac{4}{3}u\gamma. \tag{B.16}$$

$^3P_2$ channel:

In this channel, the tensor force is attractive.

$$\frac{dx}{dt} = (\text{pionless}) - \frac{4}{15}(x+y+z)\gamma - \frac{4}{9}\gamma^2, \tag{B.17}$$

$$\frac{dy}{dt} = (\text{pionless}) - \frac{2}{75}(4x+9y-z)\gamma + \frac{22}{75}\gamma^2, \tag{B.18}$$

$$\frac{dz}{dt} = (\text{pionless}) + \frac{2}{15}(x+y-z)\gamma + \frac{2}{9}\gamma^2, \tag{B.19}$$

$$\frac{du}{dt} = (\text{pionless}) + \frac{8}{15}\left(x+y+z-\frac{1}{2}u\right)\gamma + \frac{16}{9}\gamma^2. \tag{B.20}$$

Bibliography

[1] R. Machleidt, F. Sammarruca, and Y. Song. The Nonlocal nature of the nuclear force and its impact on nuclear structure. *Phys.Rev.*, Vol. C53, pp. 1483–1487, 1996.

[2] R. Machleidt. The High precision, charge dependent Bonn nucleon-nucleon potential (CD-Bonn). *Phys.Rev.*, Vol. C63, p. 024001, 2001.

[3] Robert B. Wiringa, V.G.J. Stoks, and R. Schiavilla. An Accurate nucleon-nucleon potential with charge independence breaking. *Phys.Rev.*, Vol. C51, pp. 38–51, 1995.

[4] V.G.J. Stoks, R.A.M. Klomp, C.P.F. Terheggen, and J.J. de Swart. Construction of high quality N N potential models. *Phys.Rev.*, Vol. C49, pp. 2950–2962, 1994.

[5] Steven Weinberg. Phenomenological Lagrangians. *Physica*, Vol. A96, p. 327, 1979.

[6] Steven Weinberg. Nuclear forces from chiral Lagrangians. *Phys.Lett.*, Vol. B251, pp. 288–292, 1990.

[7] Steven Weinberg. Effective chiral Lagrangians for nucleon - pion interactions and nuclear forces. *Nucl.Phys.*, Vol. B363, pp. 3–18, 1991.

[8] David B. Kaplan, Martin J. Savage, and Mark B. Wise. Nucleon - nucleon scattering from effective field theory. *Nucl.Phys.*, Vol. B478, pp. 629–659, 1996.

[9] David B. Kaplan, Martin J. Savage, and Mark B. Wise. A New expansion for nucleon-nucleon interactions. *Phys.Lett.*, Vol. B424, pp. 390–396, 1998.

[10] U. van Kolck. Effective field theory of short range forces. *Nucl.Phys.*, Vol. A645, pp. 273–302, 1999.

[11] Sean Fleming, Thomas Mehen, and Iain W. Stewart. NNLO corrections to nucleon-nucleon scattering and perturbative pions. *Nucl.Phys.*, Vol. A677, pp. 313–366, 2000.

[12] Koji Harada, Hirofumi Kubo, and Yuki Yamamoto. Pions in nuclear effective field theory: How they behave differently at different scales and how they decouple at very low energies. *Few Body Syst.*, Vol. 54, pp. 239–243, 2013.

[13] Silas R. Beane, David B. Kaplan, and Aleksi Vuorinen. Perturbative nuclear physics. *Phys.Rev.*, Vol. C80, p. 011001, 2009.

[14] Sean Fleming, Thomas Mehen, and Iain W. Stewart. The N N scattering 3S1 - 3D1 mixing angle at NNLO. *Phys.Rev.*, Vol. C61, p. 044005, 2000.

[15] E. Epelbaum, W. Glockle, and Ulf-G. Meissner. The Two-nucleon system at next-to-next-to-next-to-leading order. *Nucl.Phys.*, Vol. A747, pp. 362–424, 2005.

[16] David B. Kaplan, Martin J. Savage, and Mark B. Wise. Two nucleon systems from effective field theory. *Nucl.Phys.*, Vol. B534, pp. 329–355, 1998.

[17] Thomas Mehen and Iain W. Stewart. Renormalization schemes and the range of two nucleon effective field theory. *Phys.Rev.*, Vol. C59, pp. 2365–2383, 1999.

[18] V.G.J. Stoks, R.A.M. Kompl, M.C.M. Rentmeester, and J.J. de Swart. Partial wave analaysis of all nucleon-nucleon scattering data below 350-MeV. *Phys.Rev.*, Vol. C48, pp. 792–815, 1993.

[19] Koji Harada, Hirofumi Kubo, and Yuki Yamamoto. Pions are neither perturbative nor nonperturbative: Wilsonian renormalization group analysis of nuclear effective field theory including pions. *Phys.Rev.*, Vol. C83, p. 034002, 2011.

[20] Koji Harada and Hirofumi Kubo. Anomalous dimensions determine the power counting: Wilsonian RG analysis of nuclear EFT. *Nucl.Phys.*, Vol. B758, pp. 304–329, 2006.

[21] H. Kubo, K. Harada, T. Sakaeda, and Y. Yamamoto. Wilsonian RG Analysis of the P-wave Nucleon-Nucleon Scattering Including Pions. *Few Body Syst.*, Vol. Published online, , 2013.

[22] Koji Harada, Hirofumi Kubo, and Atsushi Ninomiya. More about the Wilsonian analysis on the pionless NEFT. *Int.J.Mod.Phys.*, Vol. A24, pp. 3191–3225, 2009.